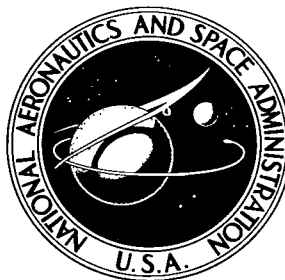


NASA TECHNICAL NOTE



NASA TN D-8065 *cl*

NASA TN D-8065

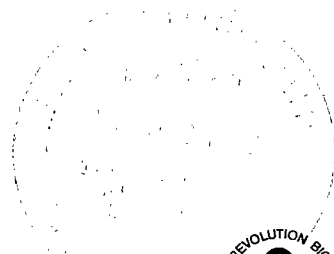


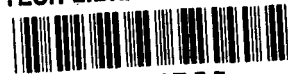
AERODYNAMIC CHARACTERISTICS
OF A HYPERSONIC RESEARCH
AIRPLANE CONCEPT HAVING
A 70° SWEPT DOUBLE-DELTA WING
AT MACH NUMBERS FROM 1.50 TO 2.86

LOAN COPY: RETURN TO
AFWL TECHNICAL LIBRARY
KIRTLAND AFB, N. M.

*Jim A. Penland, Roger H. Fournier,
and Don C. Marcum, Jr.*

*Langley Research Center
Hampton, Va. 23665*





0133755

1. Report No. NASA TN D-8065		2. Government Accession No.		3. Recipient's Catalog No.	
4. Title and Subtitle AERODYNAMIC CHARACTERISTICS OF A HYPERSONIC RESEARCH AIRPLANE CONCEPT HAVING A 70° SWEEPED DOUBLE-DELTA WING AT MACH NUMBERS FROM 1.50 TO 2.86		5. Report Date December 1975		6. Performing Organization Code	
7. Author(s) Jim A. Penland, Roger H. Fournier, and Don C. Marcum, Jr.		8. Performing Organization Report No. L-10305		10. Work Unit No. 505-11-31-02	
9. Performing Organization Name and Address NASA Langley Research Center Hampton, Va. 23665		11. Contract or Grant No.		13. Type of Report and Period Covered Technical Note	
12. Sponsoring Agency Name and Address National Aeronautics and Space Administration Washington, D.C. 20546		14. Sponsoring Agency Code		15. Supplementary Notes	
16. Abstract <p>An experimental investigation of the static longitudinal, lateral, and directional stability characteristics of a hypersonic research airplane concept having a 70° swept double-delta wing was conducted in the Langley Unitary Plan wind tunnel. The configuration variables included wing planform, tip fins, center fin, and scramjet engine modules. The investigation was conducted at Mach numbers from 1.50 to 2.86 and at a constant Reynolds number, based on fuselage length, of 3.33×10^6. Tests were conducted through an angle-of-attack range from about -4° to 24° with angles of sideslip of 0° and 3° and at elevon deflections of 0°, -10°, and -20°.</p> <p>The complete configuration was trimmable up to angles of attack of about 22° with the exception of regions at low angles of attack where positive elevon deflections should provide trim capability. The angle-of-attack range for which static longitudinal stability also exists was reduced at the higher Mach numbers due to the tendency of the complete configuration to pitch up at the higher angles of attack. The complete configuration was statically stable directionally up to trimmed angles of attack of at least 20° for all Mach numbers M with the exception of a region near 4° at $M = 2.86$ and exhibited positive effective dihedral at all positive trimmed angles of attack.</p>					
17. Key Words (Suggested by Author(s)) Hypersonic aircraft Supersonic stability and control Lift Aerodynamics		18. Distribution Statement Unclassified - Unlimited Subject Category 09			
19. Security Classif. (of this report) Unclassified	20. Security Classif. (of this page) Unclassified	21. No. of Pages 81	22. Price* \$4.75		

AERODYNAMIC CHARACTERISTICS OF A HYPERSONIC RESEARCH
AIRPLANE CONCEPT HAVING A 70° SWEPT DOUBLE-DELTA
WING AT MACH NUMBERS FROM 1.50 TO 2.86

Jim A. Penland, Roger H. Fournier, and Don C. Marcum, Jr.
Langley Research Center

SUMMARY

An experimental investigation of the static longitudinal, lateral, and directional stability characteristics of a hypersonic research airplane concept having a 70° swept double-delta wing was conducted in the Langley Unitary Plan wind tunnel. The configuration variables included wing planform, tip fins, center fin, and scramjet engine modules. The investigation was conducted at Mach numbers from 1.50 to 2.86 and at a constant Reynolds number, based on fuselage length, of 3.33×10^6 . Tests were conducted through an angle-of-attack range from about -4° to 24° with angles of sideslip of 0° and 3° and at elevon deflections of 0° , -10° , and -20° .

The complete configuration was trimmable up to angles of attack of about 22° with the exception of regions at low angles of attack where positive elevon deflections should provide trim capability. The angle-of-attack range for which static longitudinal stability also exists was reduced at the higher Mach numbers due to the tendency of the complete configuration to pitch up at the higher angles of attack. The complete configuration was statically stable directionally up to trimmed angles of attack of at least 20° for all Mach numbers M with the exception of a region near 4° at $M = 2.86$ and exhibited positive effective dihedral at all positive trimmed angles of attack.

INTRODUCTION

A need exists for comprehensive flight research in the range of Mach number M from 3 to 5 and for detailed exploration to $M \approx 8$. Present jet-fueled airplanes are cruising at speeds of $M \approx 2$ for ranges greater than 4827 km (3000 miles) and at $M \approx 3$ for ranges up to 8045 km (5000 miles) with in-flight refueling (refs. 1, 2, and 3), and it appears that the Mach number limit for aircraft utilizing conventional petroleum-based fuels is about $M \approx 5$ (ref. 4). Some unique problems associated with these higher Mach numbers include the development of new propulsion systems, which use nonpetroleum-derived fuels such as liquid hydrogen (ref. 5): for example, turbojets for low speeds, ramjets for moderate supersonic speeds, and scramjets (supersonic combustion ramjets) for high supersonic

speeds and hypersonic speeds. New structural concepts must be developed which can provide cooled airframes and engine surfaces for protection from high aerodynamic heating and insulated tankage for cryogenic fuels such as liquid hydrogen.

One industry study (refs. 6 to 9) concluded that only through the use of both ground facilities and flight vehicles could these major required advancements in technology be made. These findings were in accord with previous NACA-NASA experience with the various research airplane projects from the X-1 through the X-15, each of which resulted in extensive technology advancement at a minimum expenditure of cost and time.

The present configuration is one of several research airplane concepts under experimental study at the Langley Research Center (refs. 10 to 12) that meet the requirements envisioned as necessary to provide a technology base for future high-speed aircraft. Such a research airplane would be air launched from a B-52 or C-5, have a length of 15.24 to 24.38 meters (50 to 80 feet), a flight time of up to 800 seconds with a nominal 40-seconds cruise at a Mach number of about 7 on the scramjet engine, and return to base for a dead-stick landing.

The purpose of the present study was to investigate experimentally the longitudinal, lateral, and directional stability and control of this large-fuselage, double-delta wing design at supersonic speeds. A study has also been completed at subsonic speeds (ref. 13). Tests were parametric in nature and included configuration buildup, variations in wing planform, and longitudinal control. This study was conducted at Mach numbers from 1.50 to 2.86 at a constant Reynolds number, based on fuselage length, of 3.33×10^6 . The angle-of-attack range was from about -4° to 24° with angles of sideslip of 0° and 3° .

SYMBOLS

The longitudinal characteristics are presented about the stability axes, and the lateral-directional characteristics are presented about the body axes. The body- and stability-axis systems are illustrated in figure 1. The moment reference point was at the design center-of-gravity location which was at a longitudinal station 64.5 percent of the fuselage length and a vertical station 1.3 percent of the fuselage length below the vehicle reference line. Values are given in SI Units and, where useful, also in U.S. Units. Measurements and calculations were made in U.S. Customary Units.

A_r reference area, area of 70° delta wing including fuselage intercept

b wing span

C_D drag coefficient, $D/q_\infty A_r$

$C_{D,b}$	base-drag coefficient, $\text{Base drag}/q_{\infty} A_r$
C_L	lift coefficient, $L/q_{\infty} A_r$
$C_{L\alpha}$	rate of change of C_L with angle of attack per degree
C_l	rolling-moment coefficient, $M_X/q_{\infty} A_r b$
$C_{l\beta}$	rate of change of C_l with angle of sideslip per degree
C_m	pitching-moment coefficient, $M_Y/q_{\infty} A_r \ell$
$C_{m\alpha}$	rate of change of C_m with angle of attack per degree
$\partial C_m / \partial C_L$	rate of change of C_m with lift coefficient, longitudinal stability parameter
C_n	yawing-moment coefficient, $M_Z/q_{\infty} A_r b$
$C_{n\beta}$	rate of change of C_n with angle of sideslip per degree
C_Y	side-force coefficient, $F_Y/q_{\infty} A_r$
$C_{Y\beta}$	rate of change of C_Y with angle of sideslip per degree
c.g.	design center of gravity, moment reference point
D	drag, $F_N \sin \alpha + F_A \cos \alpha$
F_A	axial force along X-axis; positive direction, $-X$
F_N	normal force along Z-axis; positive direction, $-Z$
F_Y	side force along Y-axis; positive direction, $+Y$
L	lift, $F_N \cos \alpha - F_A \sin \alpha$
L/D	lift-drag ratio
ℓ	length of model fuselage

M	Mach number
M_X, M_Y, M_Z	moments about X-, Y-, and Z-axes, respectively
q_∞	free-stream dynamic pressure
X, Y, Z	reference axes
α	angle of attack, degrees
β	angle of sideslip, degrees
δ_e	elevon-deflection angle, positive when trailing edge is down, degrees

Subscripts:

s	stability-axis system
t	trim condition, $C_m = 0$

Model nomenclature:

B	body
E	scramjet engine
F_D	forward delta wing
V_C	center fin, vertical
V_T	tip fins, vertical
W	wing

MODEL

A photograph of a model of the winged hypersonic research airplane configuration is shown in figure 2. The 0.021-scale test model was of modular design, as shown in figure 3,

to allow the buildup of variations of the basic model (fig. 4(a)) from components consisting of the body, forward delta wing, 70° swept delta wing with positive camber, tip fins, and center fin. The model design rationale was primarily based on the stability and control requirements at the design hypersonic cruise Mach number range from 8 to 10. The forward delta wing was included in the design to help decrease the rearward shift of the aerodynamic center with Mach number. The tip fins were designed with 7.5° of toe-in and located outboard of the fuselage wake to assure directional stability at hypersonic speeds and were interchanged with a center fin having the same planform area. The wedge-shaped center fin (fig. 4(b)) was tested to assess the difference in directional stability as compared with the tip fins. Elevons could be deflected from 5° to -20°. A model scramjet engine was also used to complete the configuration buildup (fig. 4(c)). This test engine consisted of six clustered modules of the concept described in reference 14, having scale outside dimensions, angles, and areas but without scale inside fuel struts and contraction ratios. The design internal contraction ratio of the model scramjet was approximately 2 compared to about 4 for the flight engine to take partly into account the relatively low Reynolds number of the tests and the resulting thick turbulent boundary layer. The body, 70° swept delta wing, and model scramjet engine were constructed of stainless steel, and the forward delta wing, tip fins, and center fin were constructed of aluminum alloy. The geometric details of the models are shown in figure 4 and are given in table I.

APPARATUS AND TESTS

Tunnel

The investigation was conducted in the low Mach number test section of the Langley Unitary Plan wind tunnel, which is a continuous-flow variable-pressure tunnel. The test sections are 1.22 meters square and 2.13 meters long. The nozzle leading to the test section consists of asymmetric sliding blocks which permit variations of Mach numbers from about 1.5 to 2.9.

Test Conditions

Tests were made at Mach numbers of 1.50, 2.00, 2.36, and 2.86 with a constant Reynolds number, based on fuselage length, of 3.33×10^6 . The dewpoint was maintained sufficiently low to assure negligible condensation effects in the test section. The angle-of-attack range was from about -4° to 24° for angles of sideslip of 0° and 3°. A limited number of tests were also conducted over an angle-of-sideslip range from about -4° to 8° at an angle of attack of 0°. Transition strips, 0.159 cm wide composed of No. 50 grit, were placed 3.05 cm downstream of the apex of the model nose and 1.02 cm inside the leading edges of the model scramjet engine. Transition strips were also placed at the following

locations (measured normal to the leading edge): 0.18 cm for the forward delta wing, 0.35 cm for the 70° swept delta wing and the bottom leading edge of the tip fins, and 0.58 cm for the top leading edge of the tip fins and the center fin.

Measurements and Corrections

The aerodynamic forces and moments were measured by means of a six-component strain-gage balance which was housed within the body. Balance-chamber pressure was measured with pressure tubes located in the vicinity of the balance.

Angles of attack and sideslip have been corrected for the deflection of the balance and sting due to aerodynamic loads. The angle of attack was also corrected for tunnel-flow angularity. The drag coefficients have been corrected to the condition of free-stream static pressure on the model base. Typical base-drag coefficients are presented in figure 5. No correction was made to the drag data for flow through the model scramjet engine.

RESULTS AND DISCUSSION

Static Longitudinal Characteristics

Configuration buildup.- The untrimmed longitudinal aerodynamic characteristics of the body-wing configuration alone and with various forward-delta, tip-fin, center-fin, and engine components are presented in figures 6 and 7. A comparison of the longitudinal aerodynamic characteristics of various tip-fin and center-fin configurations is presented in figure 8. The primary effect of the addition of the forward delta wing on the longitudinal characteristics of the configurations was a decrease in the longitudinal stability due to the added area ahead of the center of gravity (figs. 6 to 8). There was also a slight increase in lift at the lower Mach numbers that became more pronounced as the Mach number increased. The addition of the tip fins to the body-wing configuration slightly increased the lift and the nose-down pitching moment (fig. 6), whereas the addition of the center fin to the body-wing configuration slightly decreased the nose-down pitching moment (fig. 7). The addition of either the tip fins or the center fin resulted in about the same increase in drag and, therefore, about the same loss in L/D (figs. 6 and 7). In regard to performance and longitudinal stability, it may be concluded that there is essentially little difference between the tip or center vertical fins in this Mach number range. In general, the addition of the engine modules increased the drag, increased the lift, and decreased the longitudinal stability.

Trim characteristics.- The effect of elevon deflection on the longitudinal aerodynamic characteristics of the complete configuration ($BWV_T F_D E$) is presented in figure 9: Elevon deflections of 0°, -10°, and -20° are presented at all Mach numbers, and the additional elevon deflections (dashed lines) were obtained from cross plots and interpolations of the data.

The elevon-deflection data were used to determine the longitudinal aerodynamic characteristics at trim (fig. 10) of the BWV_TF_DE configuration. Trim data were not obtained at the lower lift coefficients because of lack of test data with positive elevon deflections which would be required to trim the model in that region. The maximum trimmed lift coefficient decreased from 0.67 at $M = 1.50$ to 0.50 at $M = 2.86$, and the maximum trimmed angle of attack ranged from 23.4° at $M = 1.50$ to 22.6° at $M = 2.86$. The maximum trimmed lift-drag ratio was 2.76 at $M = 1.50$ and 2.98 at $M = 2.86$. The complete configuration (BWV_TF_DE) was statically stable longitudinally at the lower trimmed lift coefficients; however, at the higher Mach numbers, the stability decreased to zero because of the tendency of the configuration to pitch up at the higher lift coefficients and corresponding angles of attack.

Static Lateral-Directional Characteristics

Basic lateral aerodynamic characteristics of the BWV_TF_DE configuration are presented in figure 11 for an angle of attack of 0° . These data were obtained to determine the linearity of the lateral aerodynamic characteristics. In general, the data are linear and the lateral-directional stability characteristics presented in figures 12 to 15 were evaluated at $\beta = 0^\circ$ and $\beta = 3^\circ$.

The body-wing and body-wing forward-delta configurations were directionally unstable at all Mach numbers (fig. 12) but did have positive effective dihedral ($-C_{l\beta}$) above $\alpha = 2^\circ$ for all Mach numbers. In general, the addition of the forward delta wing to the body-wing configuration (BWF_D) provided a small positive increment in $C_{n\beta}$ and improved the positive effective dihedral. The addition of the tip fins to the body-wing configuration (BWV_T) provided a relatively constant positive increment in $C_{n\beta}$ and did not significantly change the positive effective dihedral. The BWV_T configuration was directionally stable at $M = 1.50$ and $M = 2.00$ for all angles of attack and at $M = 2.36$ and $M = 2.86$ for angles of attack near 0° . In figure 13 the center-fin configuration (BWV_C), which has the same total planform area as the tip-fin configuration (BWV_T), was about twice as effective in increasing $C_{n\beta}$ at low angles of attack, probably due to a better flow field and less tip losses, and significantly increased the positive effective dihedral due to its location above the center of gravity. The $C_{n\beta}$ provided by the center fin deteriorated with angle of attack and was less than the $C_{n\beta}$ provided by the tip fins at high angles of attack (from about 13° to 17°), due in part to shielding of the fin by the fuselage. The BWV_C configuration became directionally unstable at angles of attack from about 12° to 19° , and the decrease in $C_{n\beta}$ continued over the remaining angle-of-attack range. This is a typical deterioration in $C_{n\beta}$ with α for center-fin configurations at supersonic speeds. (See ref. 15.) In general, the addition of the forward delta wing to the body-wing-fin configurations (BWV_TF_D and BWV_CF_D) provided a positive increment in $C_{n\beta}$ and improved the positive effective dihedral. The forward delta wing increased the angle-of-attack range for which the

body-wing-fin configurations were directionally stable and was particularly effective for the center-fin configuration (BWV_{cFD}) at $M = 1.5$, indicating that there was a favorable interaction of the vortex from the forward delta wing and the center fin. The addition of the engine modules had little effect on the directional stability or effective dihedral. The complete configuration (BWV_{TFDE}) was directionally stable up to angles of attack of at least 20° for all Mach numbers, with the exception of a region near 4° at $M = 2.86$, and exhibited positive effective dihedral at all positive angles of attack.

As expected, the effect of elevon deflection on the lateral-directional stability characteristics of the BWV_{TFDE} configuration was small (fig. 15), and the trimmed lateral-directional stability characteristics would be approximately the same as those of the complete configuration with undeflected elevons.

CONCLUSIONS

An analysis of the experimental aerodynamic data for a hypersonic research airplane configuration with various component arrangements at Mach numbers from 1.50 to 2.86 and at a constant Reynolds number, based on model fuselage length, of 3.33×10^6 leads to the following conclusions:

1. The addition of the forward delta wing increased the lift as expected, decreased the longitudinal stability due to its location ahead of the center of gravity, provided a small positive increment in the directional-stability parameter $C_{n\beta}$, and improved the positive effective dihedral.
2. The longitudinal characteristics of the tip fins and the center fin were essentially similar, whereas the center fin which had the same total planform area as the tip fins was about twice as effective in increasing $C_{n\beta}$ at low angles of attack and significantly increased the positive effective dihedral. The $C_{n\beta}$ provided by the center fin deteriorated with angle of attack and was less than the $C_{n\beta}$ provided by the tip fins at high angles of attack.
3. In general, the addition of the engine modules increased the drag, increased the lift, decreased the longitudinal stability, and had a negligible effect on directional stability and positive effective dihedral.
4. The complete configuration was trimmable up to angles of attack of about 22° with the exception of regions at low angles of attack where positive elevon deflections should provide trim capability. The angle-of-attack range for which static longitudinal stability also exists was reduced at the higher Mach numbers due to the tendency of the complete configuration to pitch up at the higher angles of attack.

5. The complete configuration was statically stable directionally up to trimmed angles of attack of at least 20° for all Mach numbers M , with the exception of a region near 4° at $M = 2.86$, and exhibited positive effective dihedral at all positive trimmed angles of attack.

Langley Research Center
National Aeronautics and Space Administration
Hampton, Va. 23665
September 16, 1975

REFERENCES

1. Wetmore, Warren C.: Concorde Impressive in Flights. *Aviat. Week & Space Technol.*, vol. 100, no. 25, June 24, 1974, pp. 25-28.
2. SR-71 Sets Record. *Aviat. Week & Space Technol.*, vol. 101, no. 10, Sept. 9, 1974, p. 17.
3. SR-71 Sets Mark in New Speed Category: London-Los Angeles. *Aviat. Week & Space Technol.*, vol. 101, no. 12, Sept. 23, 1974, p. 28.
4. Kirkham, Frank S.; Jackson, L. Robert; and Weidner, John P.: The Case for a High-Speed Research Airplane — Results From an In-House Study. AIAA Paper No. 74-988, Aug. 1974.
5. Small, W. J.; Fetterman, D. E.; and Bonner, T. F., Jr.: Potential of Hydrogen Fuel for Future Air Transportation Systems. [Preprint] 73-ICT-104, American Soc. Mech. Eng., Sept. 1973.
6. Hypersonic Research Facilities Study. Phase I — Preliminary Studies. Volume II, Part 1 — Research Requirements and Ground Facility Synthesis. NASA CR-114323, 1970.
7. Hypersonic Research Facilities Study. Phase I — Preliminary Studies. Volume II, Part 2 — Flight Vehicle Synthesis. NASA CR-114324, 1970.
8. Hypersonic Research Facilities Study. Phase II — Parametric Studies. Volume III, Part 2 — Flight Vehicle Synthesis. NASA CR-114326, 1970.
9. Hypersonic Research Facilities Study. Phase III — Final Studies. Volume IV, Part 1 — Flight Research Facilities. NASA CR-114327, 1970.
10. Clark, Louis E.: Hypersonic Aerodynamic Characteristics of an All-Body Research Aircraft Configuration. NASA TN D-7358, 1973.
11. Penland, Jim A.; Creel, Theodore R., Jr.; and Howard, Floyd G.: Experimental Low-Speed and Calculated High-Speed Aerodynamic Characteristics of a Hypersonic Research Airplane Concept Having a 65° Swept Delta Wing. NASA TN D-7633, 1974.
12. Penland, Jim A.; and Creel, Theodore R., Jr.: Low-Speed Aerodynamic Characteristics of a Lifting-Body Hypersonic Research Aircraft Configuration. NASA TN D-7851, 1975.
13. Creel, Theodore R., Jr.; and Penland, Jim A.: Low-Speed Aerodynamic Characteristics of a Hypersonic Research Airplane Concept Having a 70° Swept Delta Wing. NASA TM X-71974, 1974.
14. Henry, John R.; and Anderson, Griffin Y.: Design Considerations for the Airframe-Integrated Scramjet. NASA TM X-2895, 1973.

15. Spencer, Bernard, Jr.; and Fournier, Roger H.: Supersonic Aerodynamic Characteristics of Hypersonic Low-Wave-Drag Elliptical-Body-Tail Combinations as Affected by Changes in Stabilizer Configuration. NASA TM X-2747, 1973.

TABLE I.- GEOMETRIC CHARACTERISTICS OF MODEL

Wing:

Area, reference (includes fuselage intercept), m ² (in ²)	0.043	(67.200)
Area, exposed, m ² (in ²)	0.023	(36.121)
Area, wetted, m ² (in ²)	0.047	(72.242)
Span, m (in.)	0.217	(8.542)
Aspect ratio	1.086	
Root chord, at fuselage center line, m (in.)	0.353	(13.896)
Tip chord, m (in.)	0.085	(3.355)
Taper ratio	0.241	
Mean aerodynamic chord, m (in.)	0.248	(9.779)

Sweepback angles:

Leading edge, deg	70
25-percent-chord line, deg	64
Trailing edge, deg	0
Dihedral angle, at airfoil mean line, deg	-3.64
Incidence angle, deg	0
Airfoil section	(See fig. 4(a))

Airfoil thickness ratio:

Exposed root	0.05
Tip	0.06

Leading-edge radius at —

Fuselage-line chord, m (in.)	5.08×10^{-4}	(0.020)
Tip, m (in.)	5.08×10^{-4}	(0.020)
Area of both elevons, m ² (in ²)	0.005	(7.161)

Forward delta wing:

Area exposed, outside of fuselage, forward of wing

leading edge, m ² (in ²)	0.002	(3.394)
Leading-edge sweep, deg	80	

TABLE I.- Continued

Tip fin:

Area, each, m ² (in ²)	0.004	(5.848)
Span, m (in.)	0.069	(2.730)
Aspect ratio	1.274	
Root chord, m (in.)	0.086	(3.383)
Tip chord, m (in.)	0.029	(1.135)
Taper ratio	0.336	
Mean aerodynamic chord, m (in.)	0.062	(2.445)

Sweepback angles:

Leading edge, top, deg	55.0	
Leading edge, bottom, deg	70.1	
Trailing edge, top, deg	21.3	
Toe-in angle, deg	7.5	

Airfoil section:

Leading-edge radius, m (in.)	5.08×10^{-4}	(0.020)
--	-----------------------	---------

Center fin:

Area, exposed, m ² (in ²)	0.007	(11.492)
Span, exposed, m (in.)	0.086	(3.380)
Aspect ratio of exposed area	0.994	
Root chord, at fuselage surface line, m (in.)	0.128	(5.040)
Tip chord, m (in.)	0.045	(1.760)
Taper ratio	0.349	
Mean aerodynamic chord of exposed area, m (in.)	0.093	(3.664)

Sweepback angles:

Leading edge, deg	55.0	
Trailing edge, deg	24.6	

Airfoil section:

Thickness ratio at —

Tip	0.106	
Root	0.106	
Leading-edge radius, m (in.)	5.08×10^{-4}	(0.020)

TABLE I.- Concluded

Fuselage:

Length, m (in.)	0.508 (20.000)
Maximum height, m (in.)	0.071 (2.782)
Maximum width, m (in.)	0.073 (2.866)
Fineness ratio of equivalent round body	6.822
Planform area, m ² (in ²)	0.026 (40.445)
Wetted area, m ² (in ²)	0.083 (128.460)
Wetted area, with wing on, m ² (in ²)	0.078 (120.695)
Wetted area, with both delta wings on, m ² (in ²)	0.077 (118.747)
Base area, m ² (in ²)	0.002 (3.726)

Complete model, with both delta wings:

Planform area, m ² (in ²)	0.052 (79.960)
Aspect ratio of planform	0.913

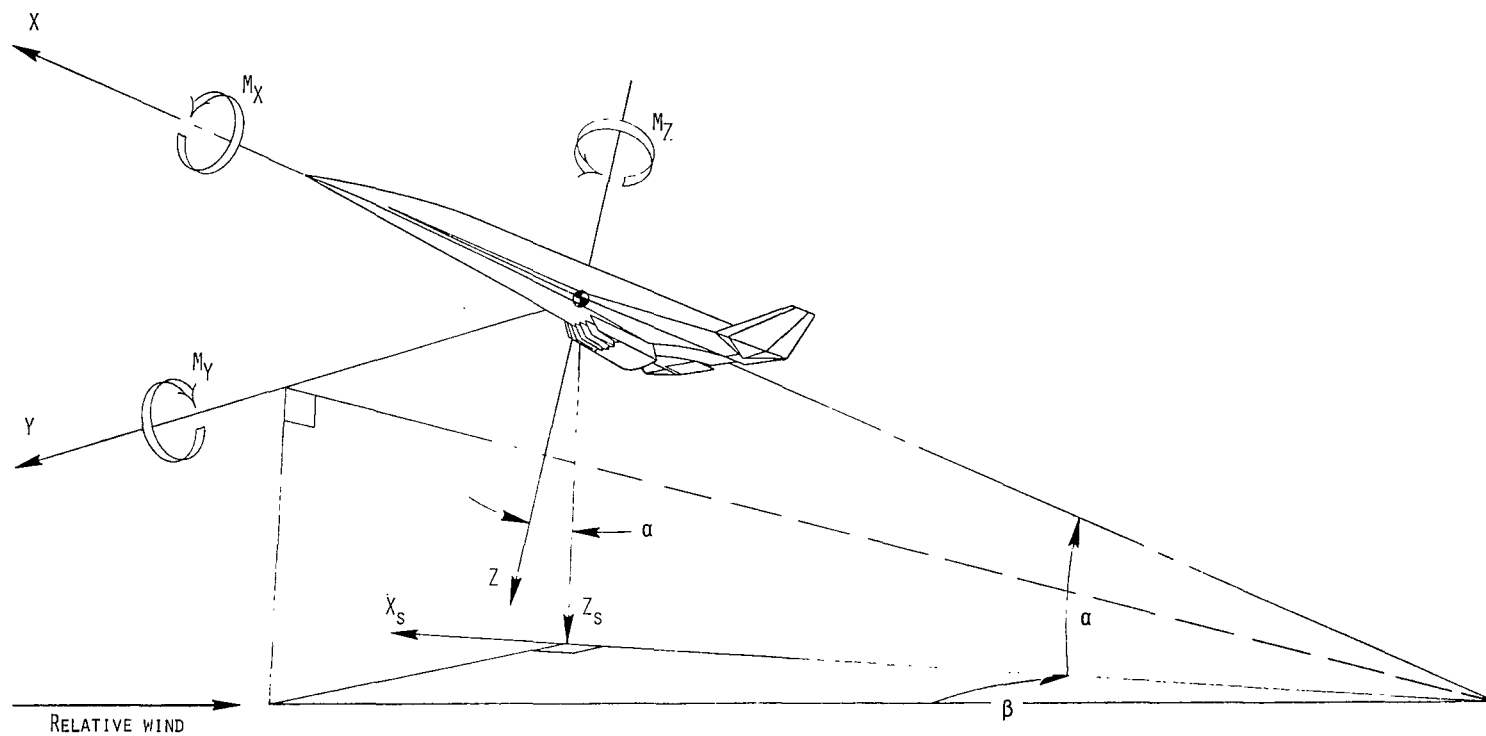
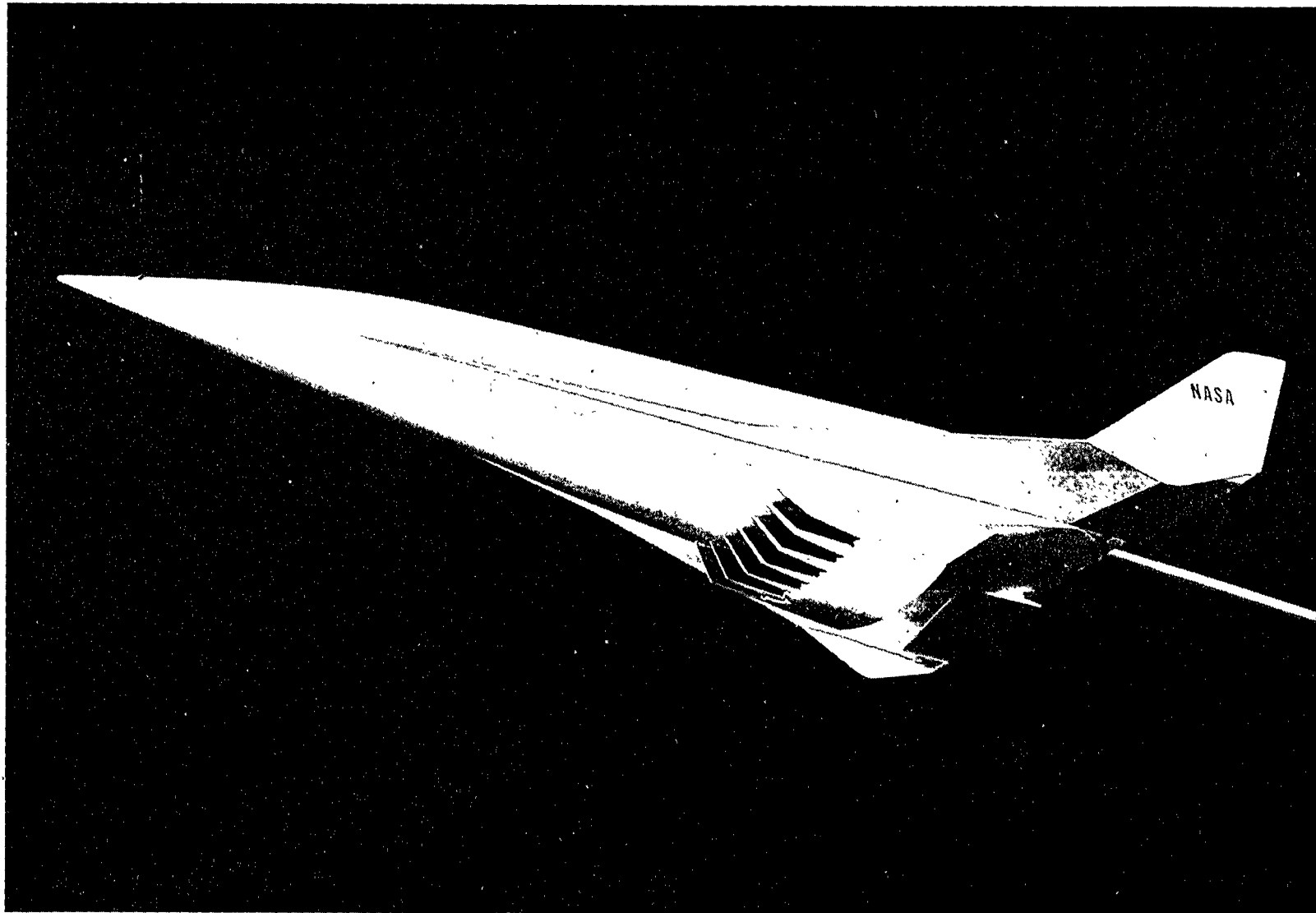


Figure 1.- Systems of reference axes. Arrows indicate positive directions.



L-72-9146

Figure 2.- Photograph of a model of the winged hypersonic research airplane.

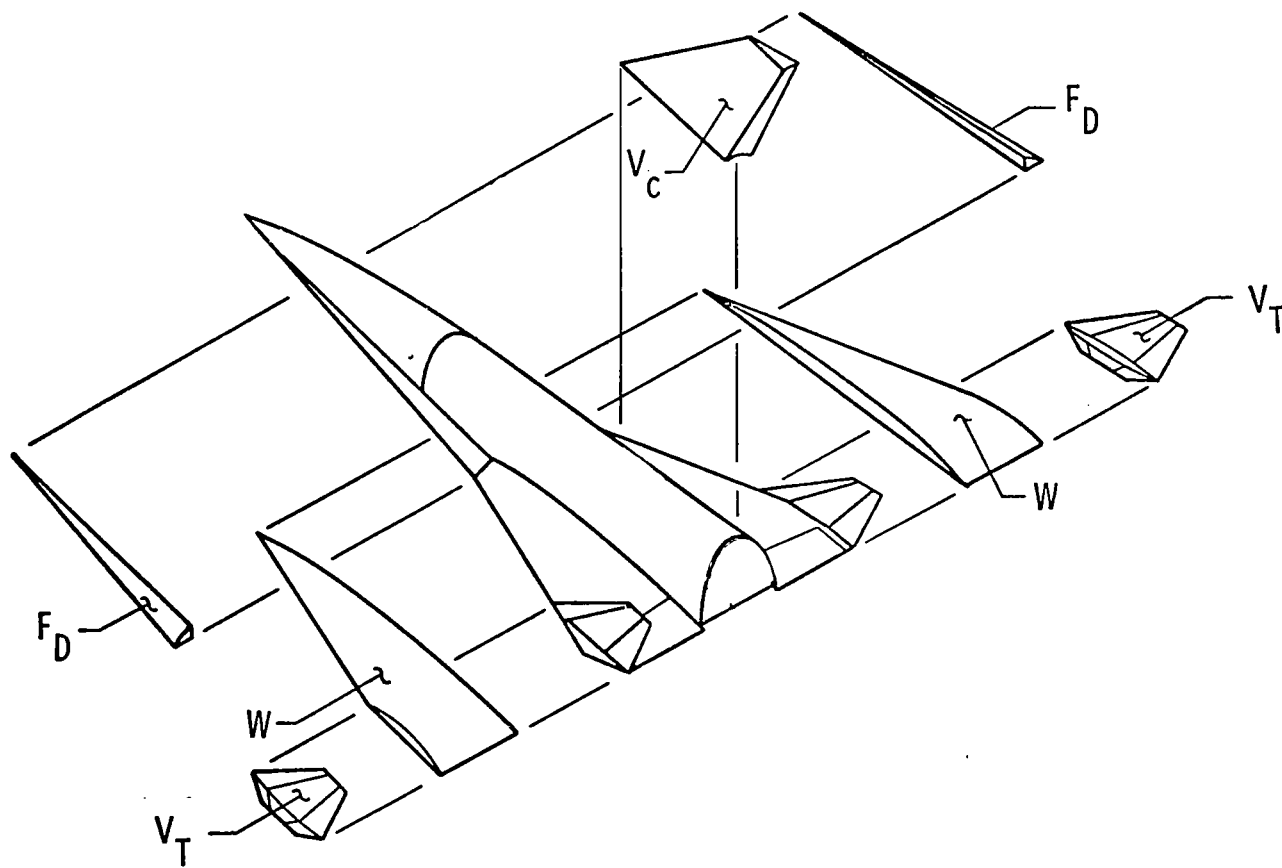
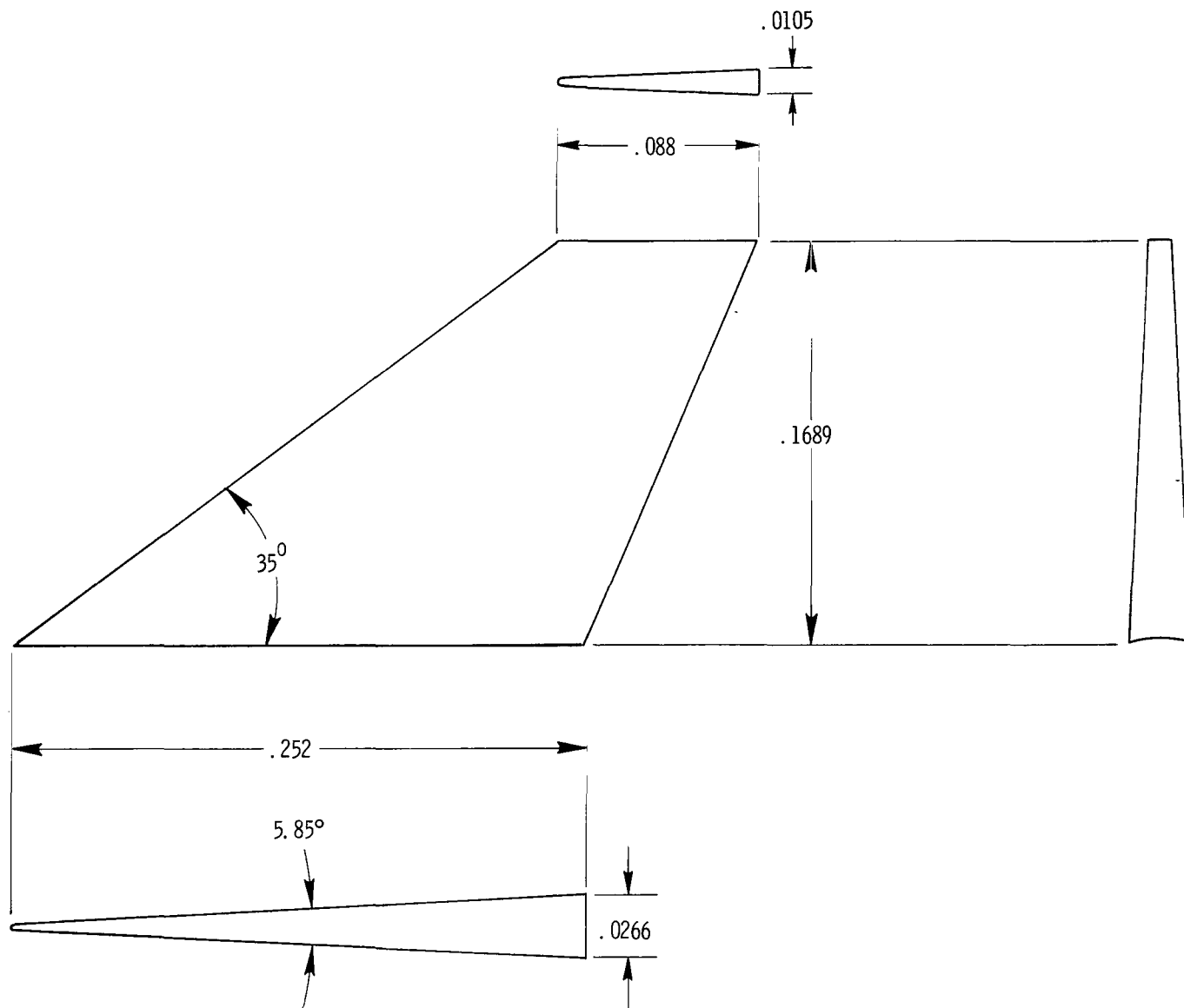


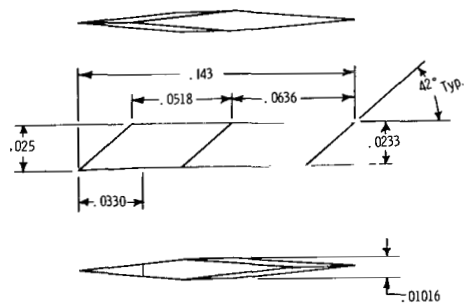
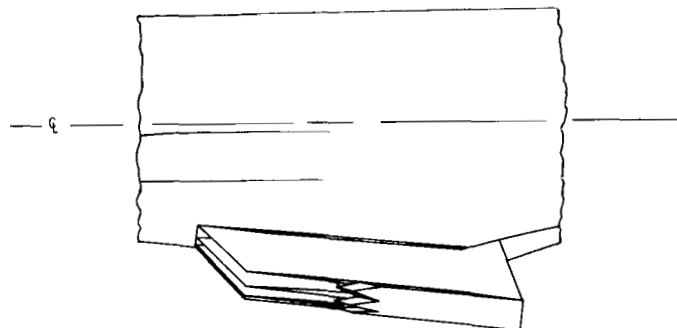
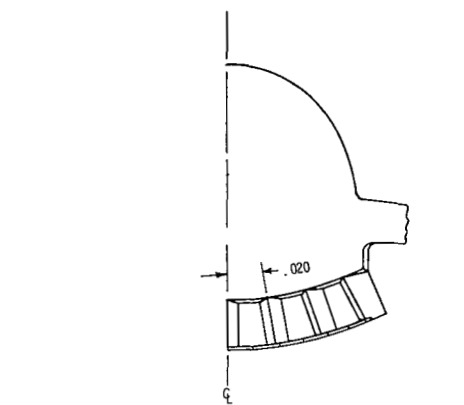
Figure 3.- Sketch of model used showing interchangeable parts.

Figure 4.- Model general dimensions. All dimensions have been normalized by the body length ($\ell = 50.8$ cm).

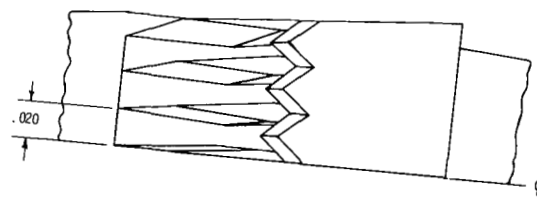


(b) Center vertical fin.

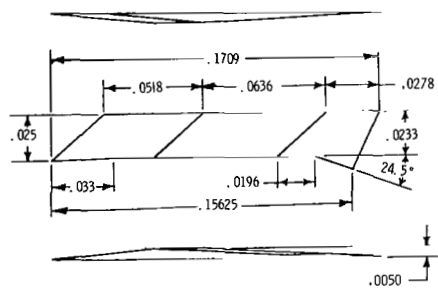
Figure 4.- Continued.



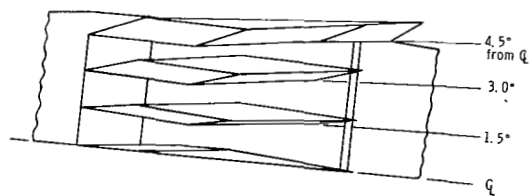
Inside splitter plate



Bottom view of scramjet engine with cowl on



left outside plate



Bottom view of scramjet engine with cowl removed

(c) Scramjet engine.

Figure 4.- Concluded.

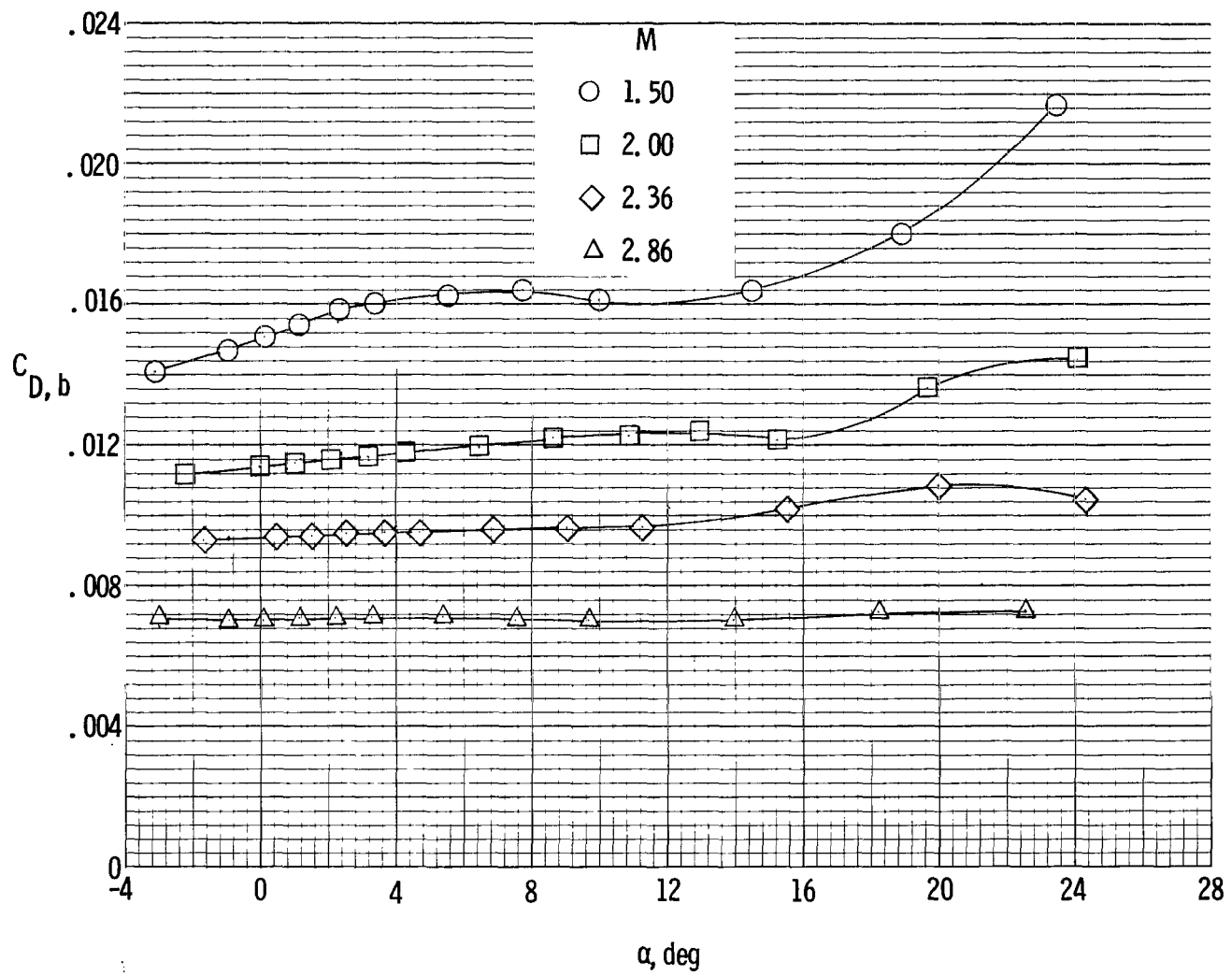
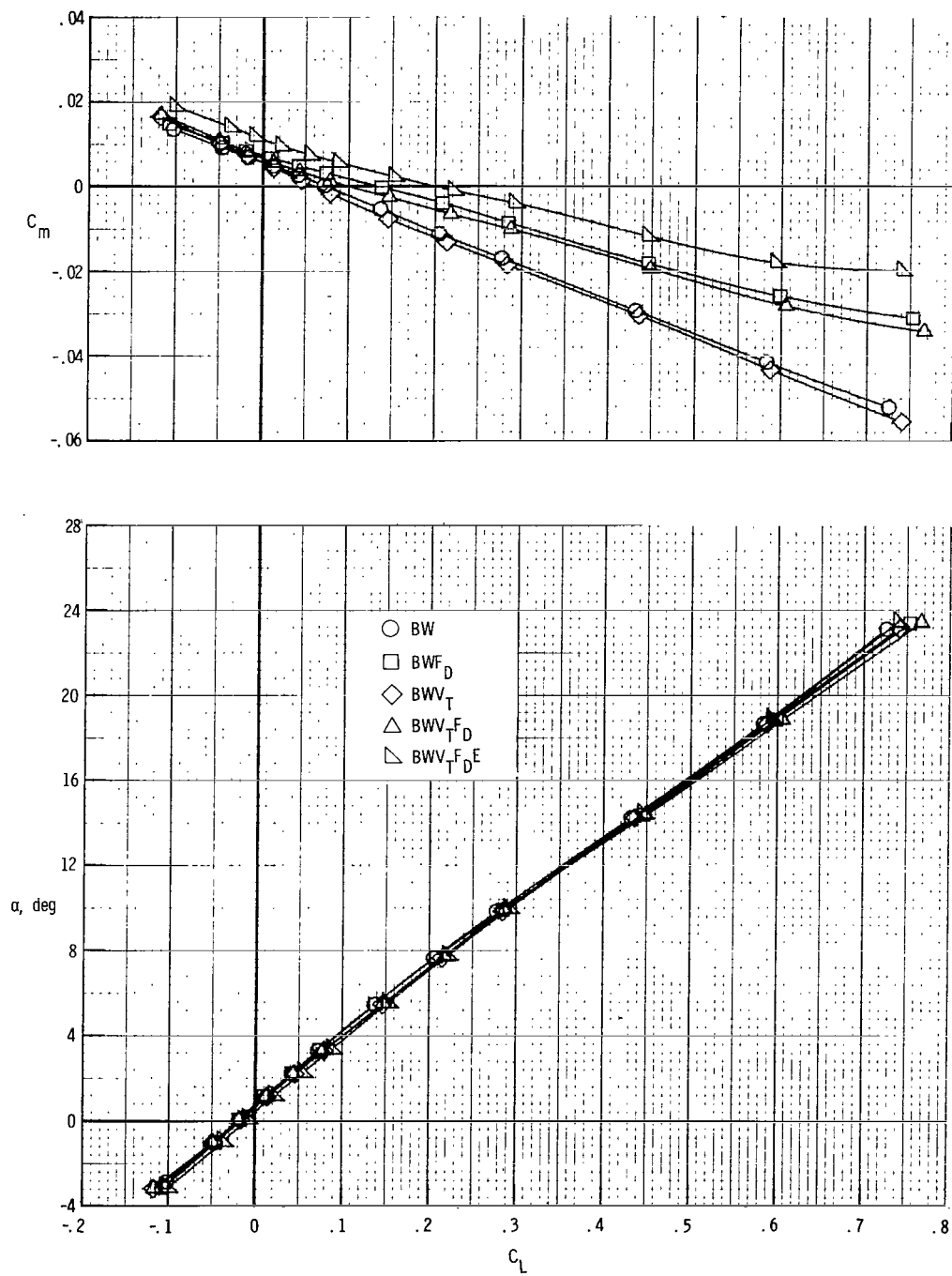
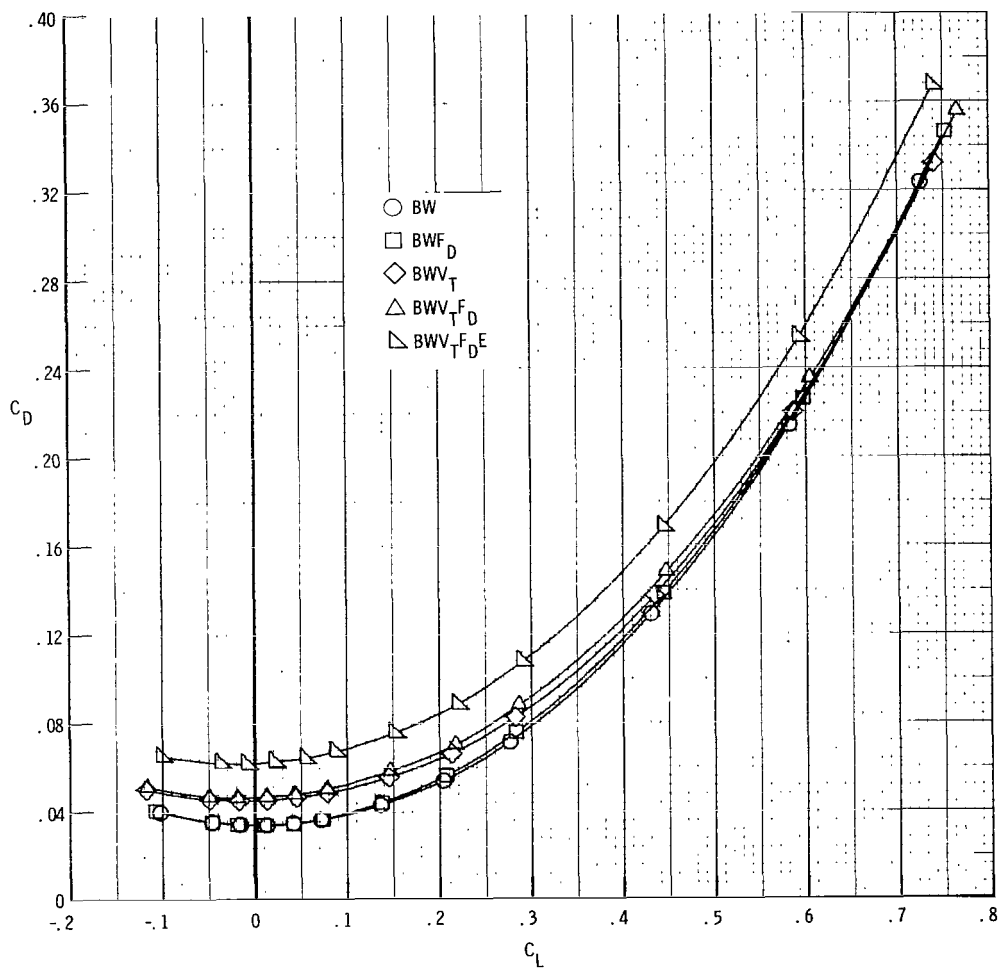
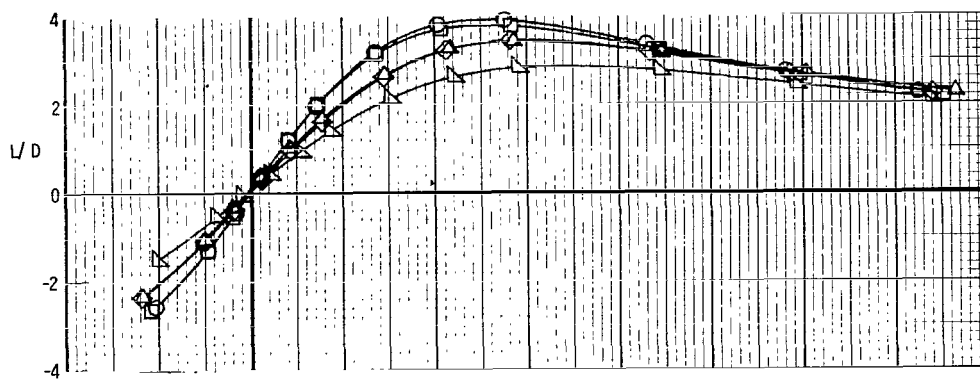


Figure 5.- Variation of base-drag coefficient with angle of attack. $BWV_T F_D^E$; $\delta_e = 0^\circ$.



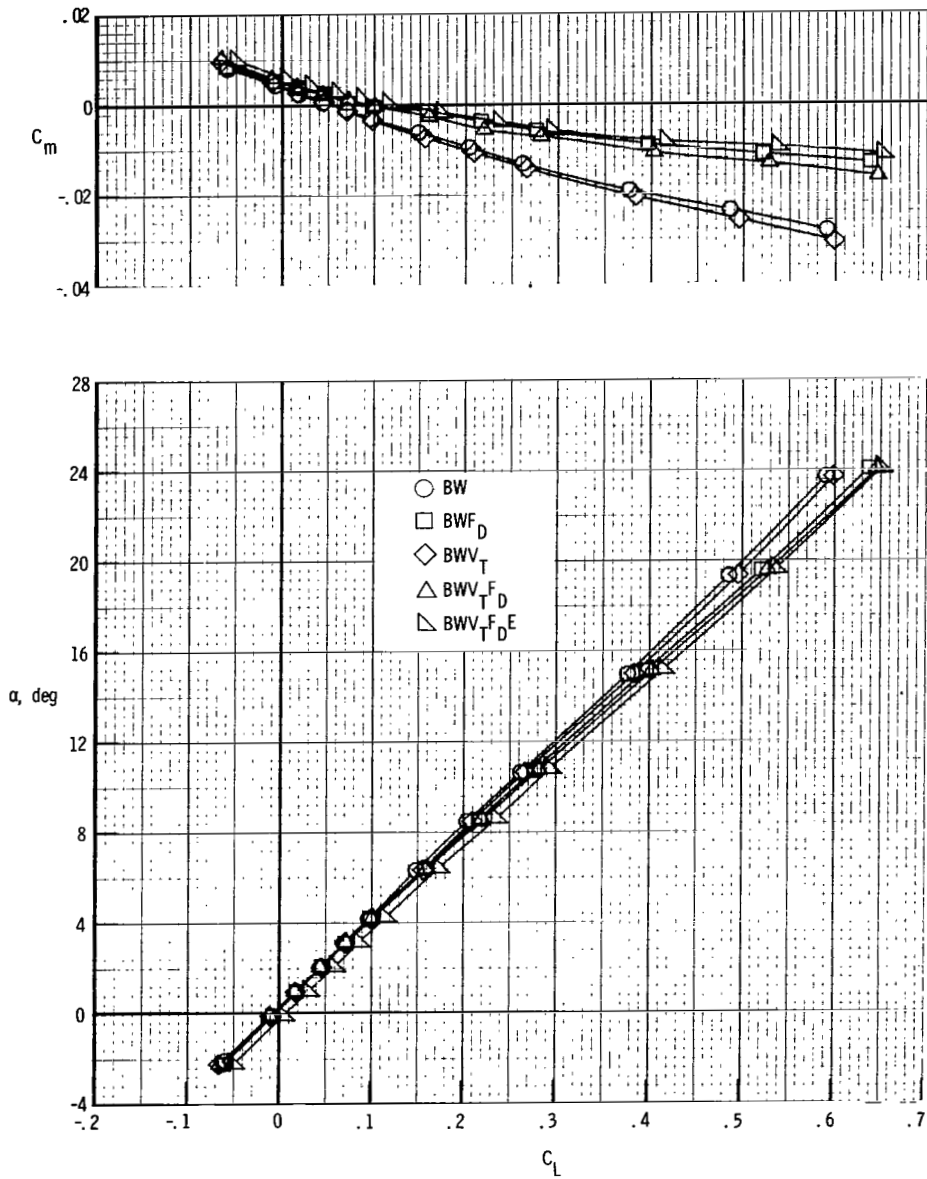
(a) $M = 1.50$.

Figure 6.- Longitudinal aerodynamic characteristics of the body-wing configuration alone and with various forward-delta, tip-fin, and engine components.



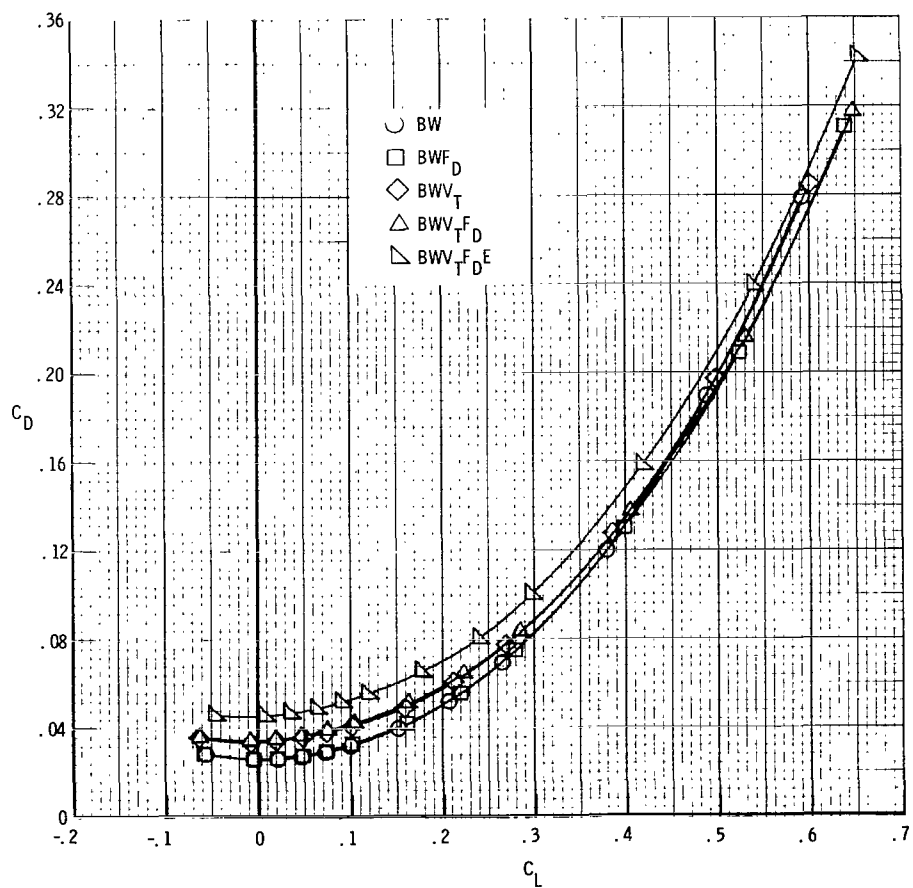
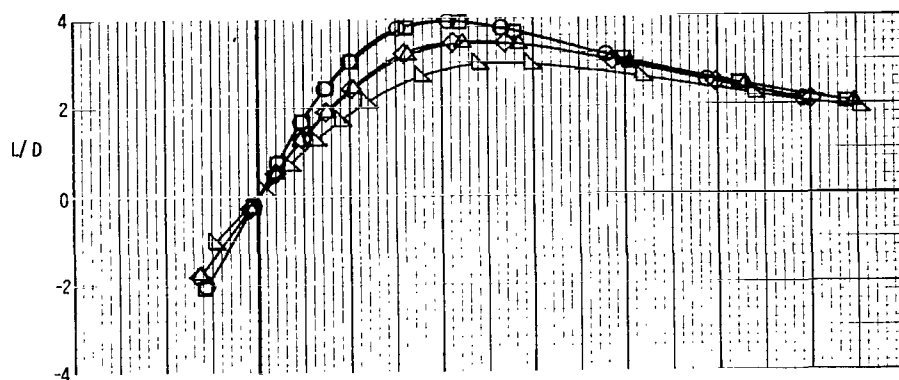
(a) $M = 1.50$. Concluded.

Figure 6.- Continued.



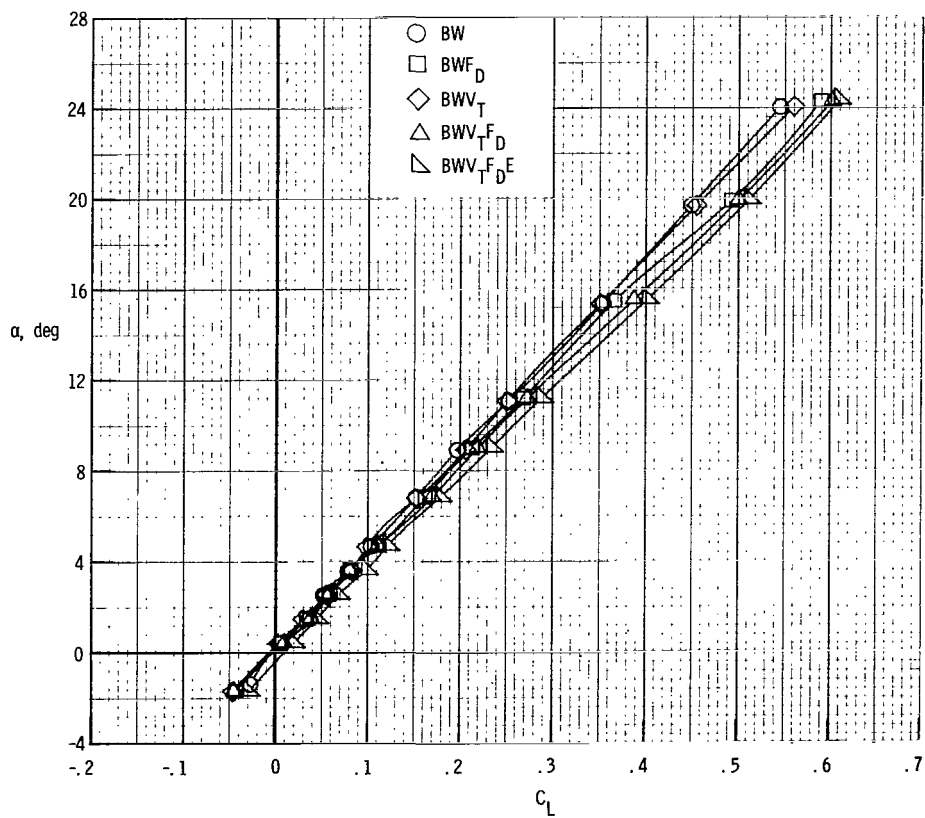
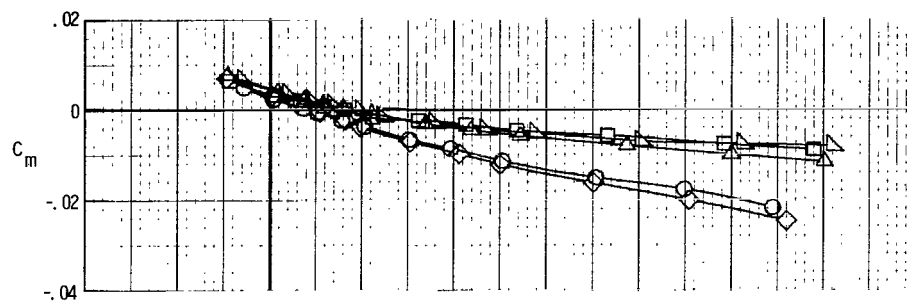
(b) $M = 2.00$.

Figure 6.- Continued.



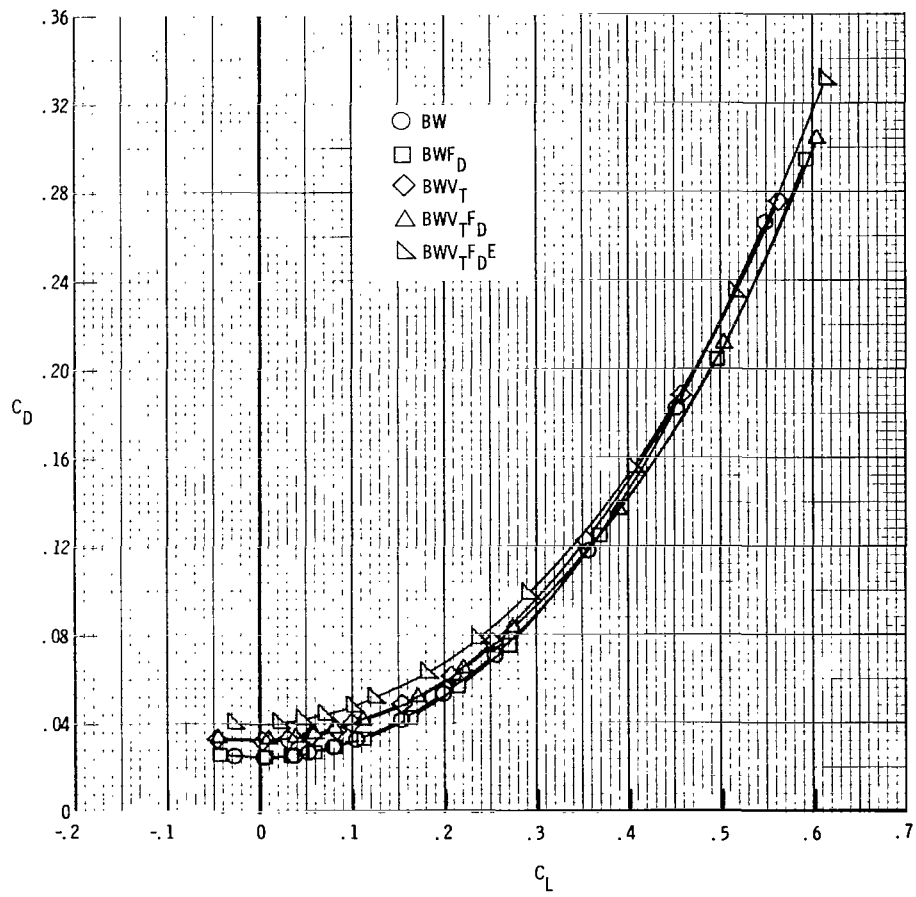
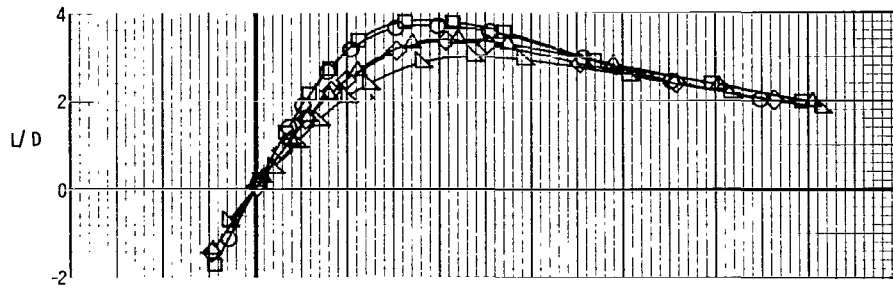
(b) $M = 2.00$. Concluded.

Figure 6.- Continued.



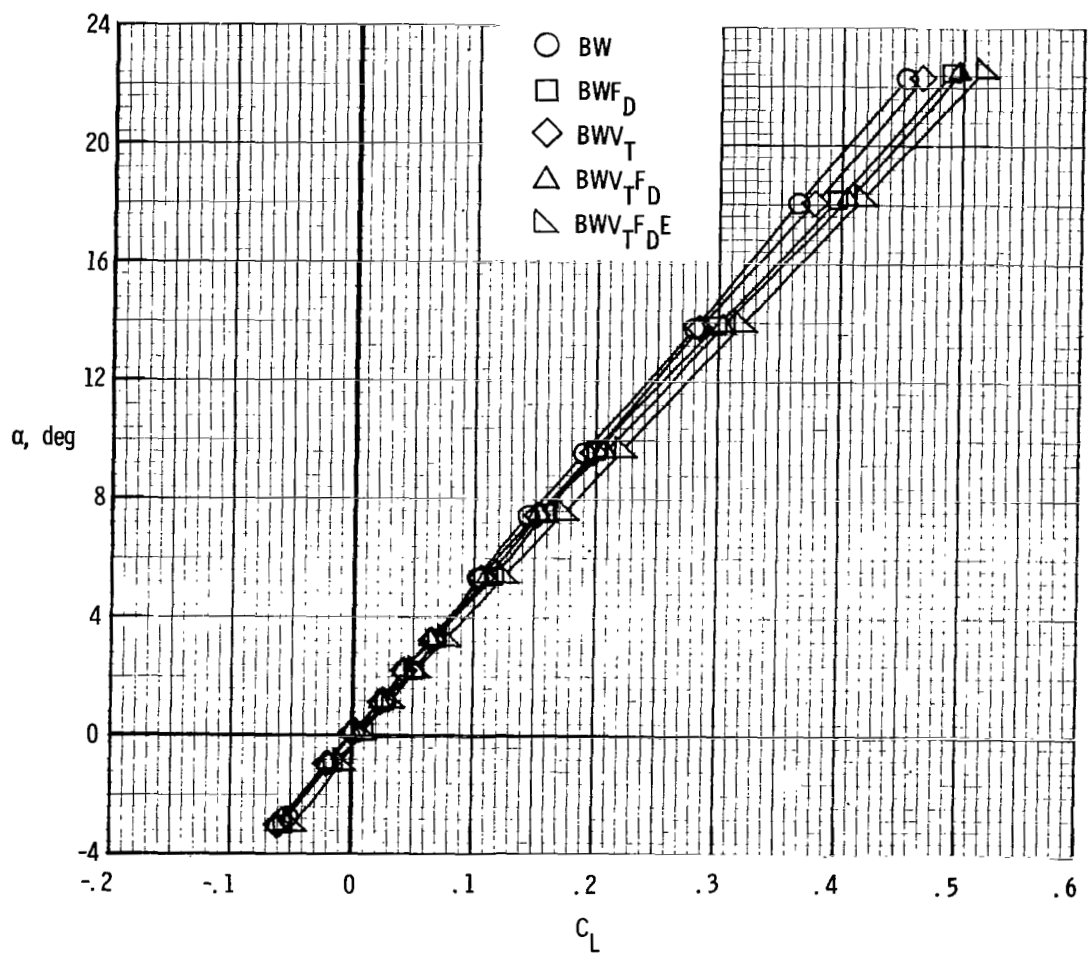
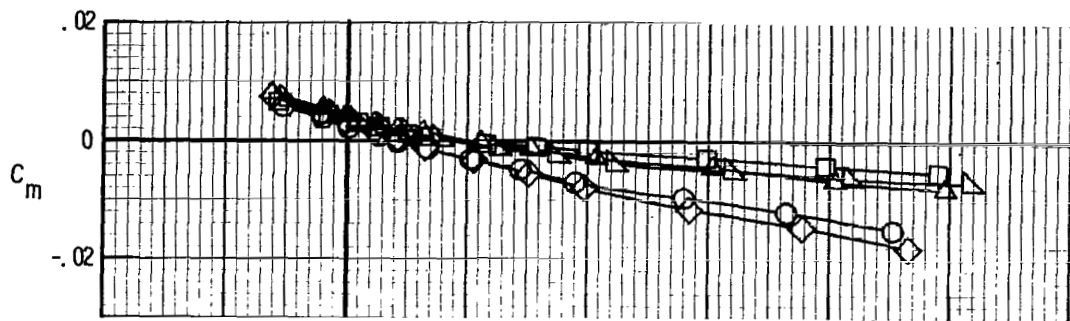
(c) $M = 2.36$.

Figure 6.- Continued.



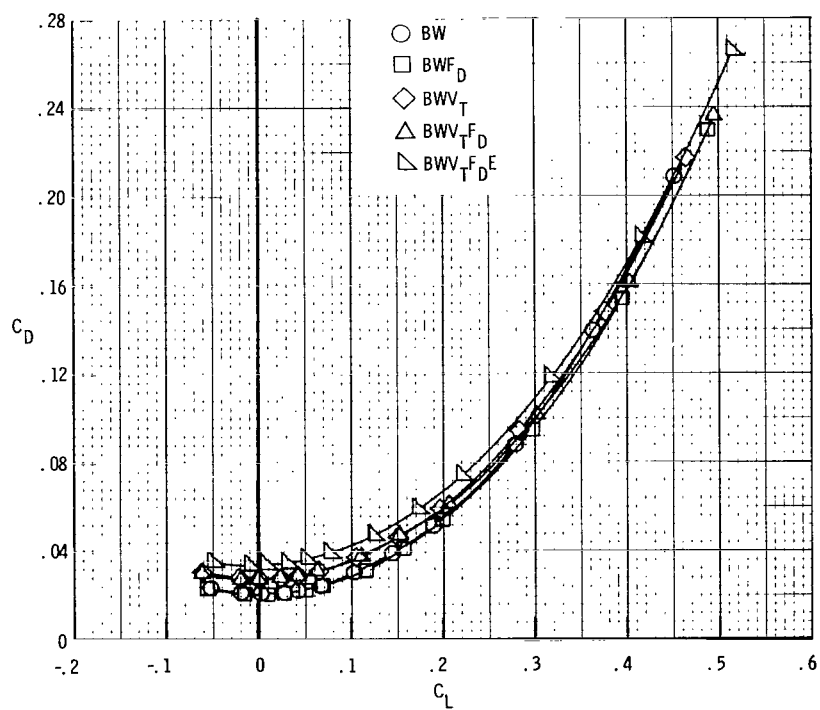
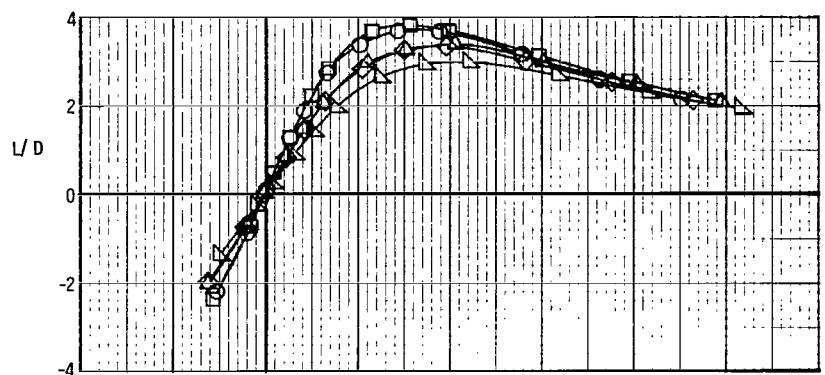
(c) $M = 2.36$. Concluded.

Figure 6.- Continued.



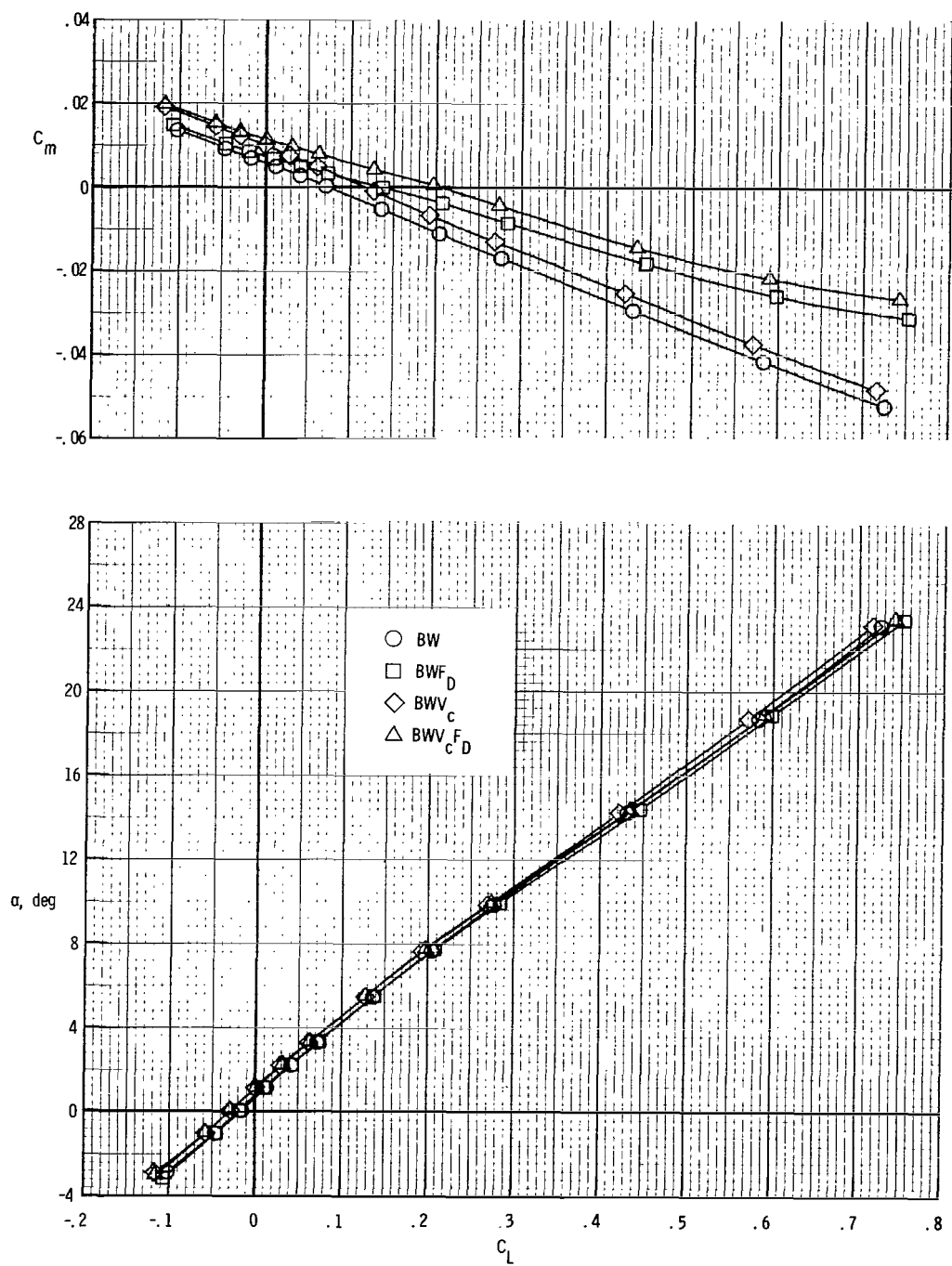
(d) $M = 2.86$.

Figure 6.- Continued.



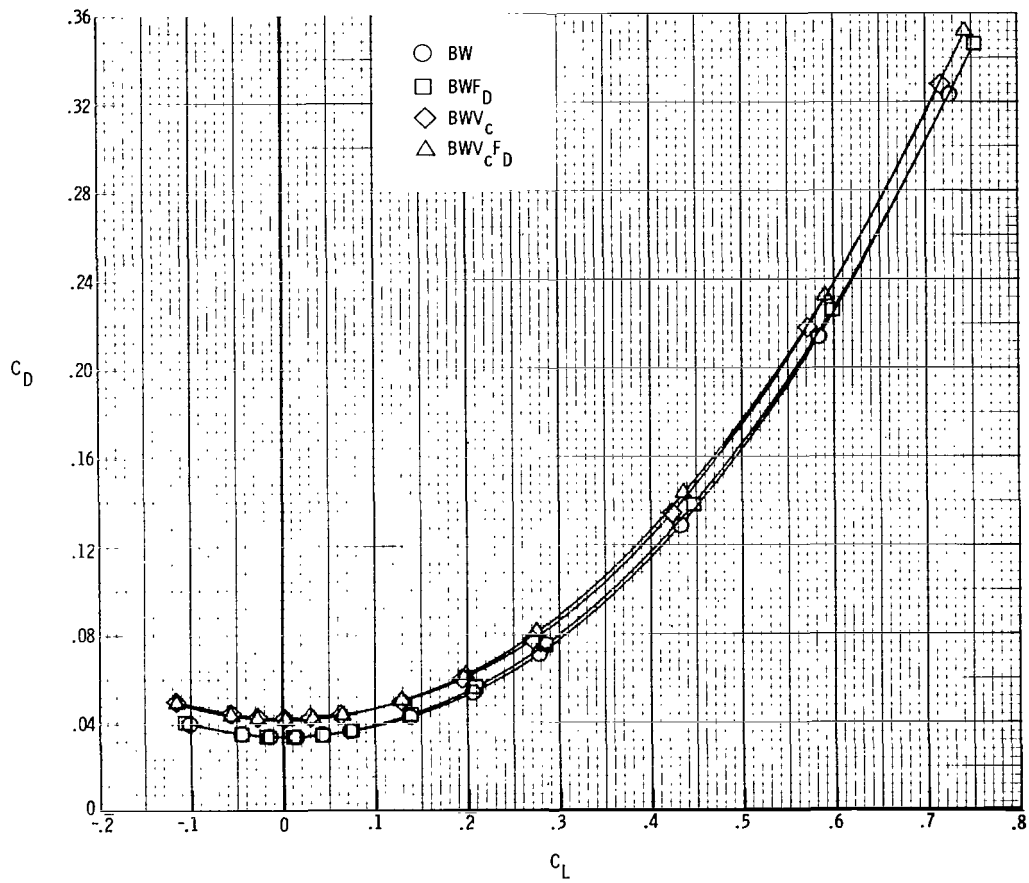
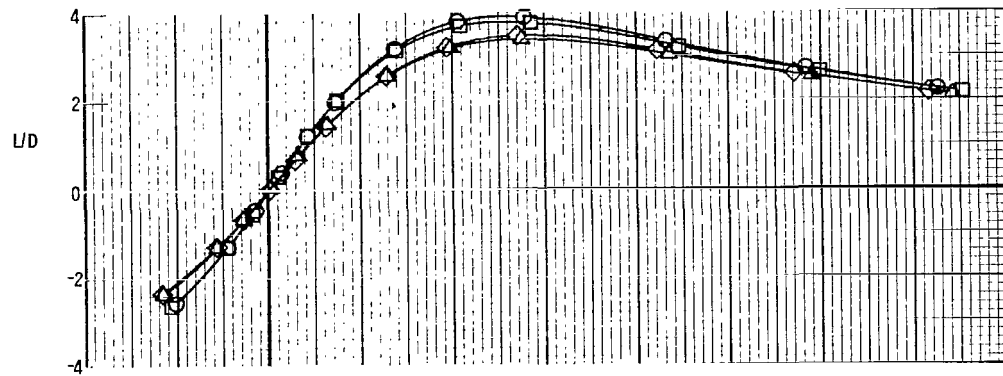
(d) $M = 2.86$. Concluded.

Figure 6.- Concluded.



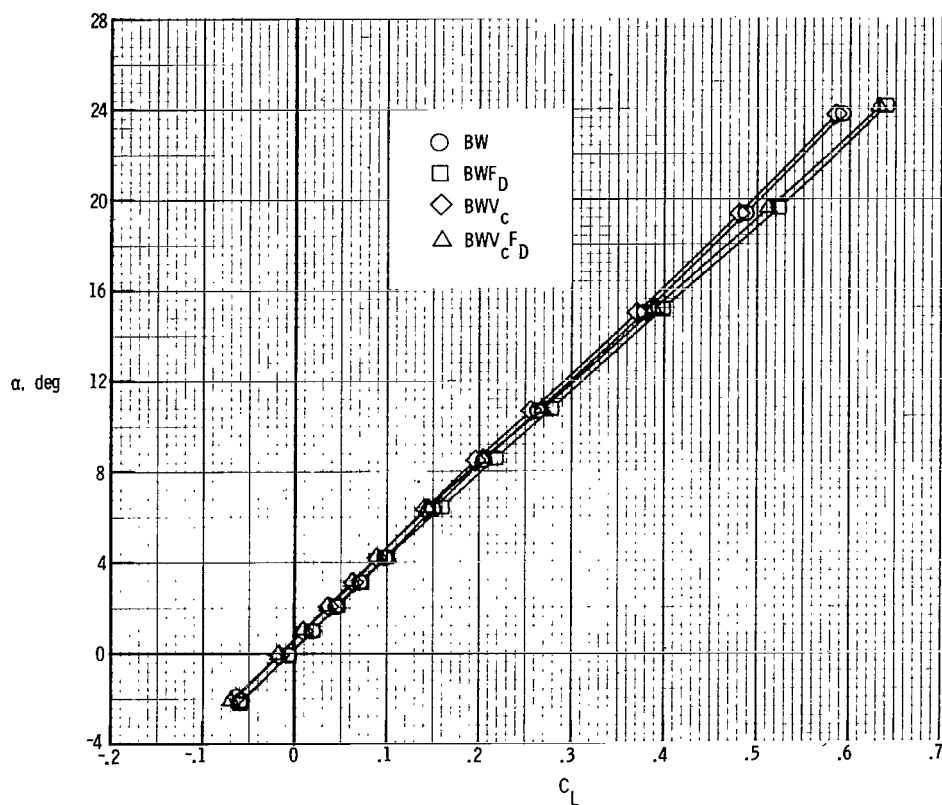
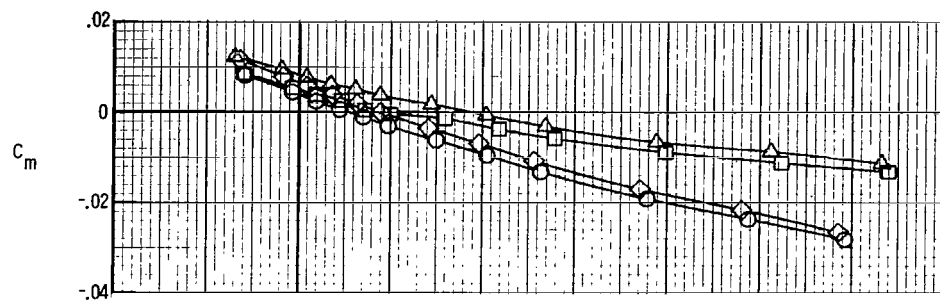
(a) $M = 1.50$.

Figure 7.- Longitudinal aerodynamic characteristics of the body-wing configuration alone and with various forward-delta and center-fin components.



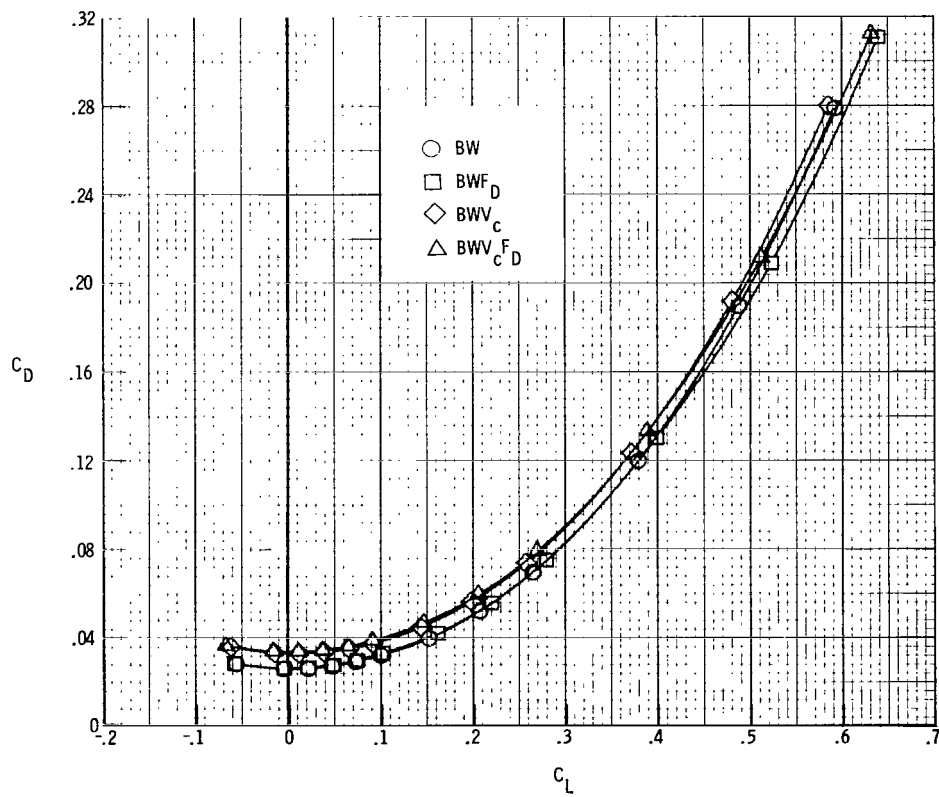
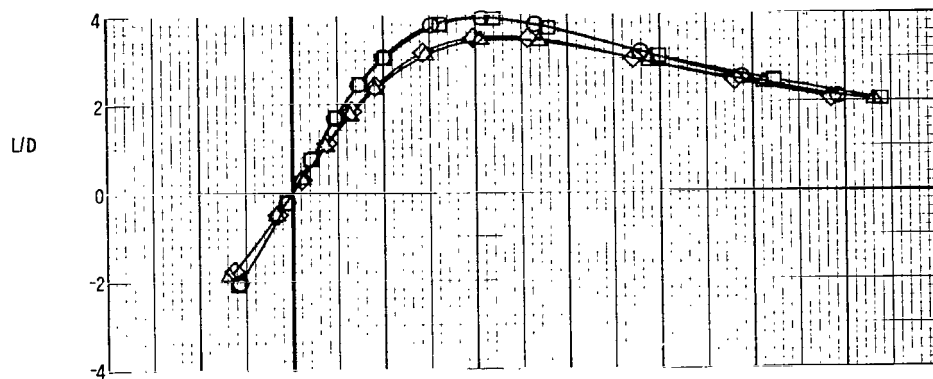
(a) $M = 1.50$. Concluded.

Figure 7.- Continued.



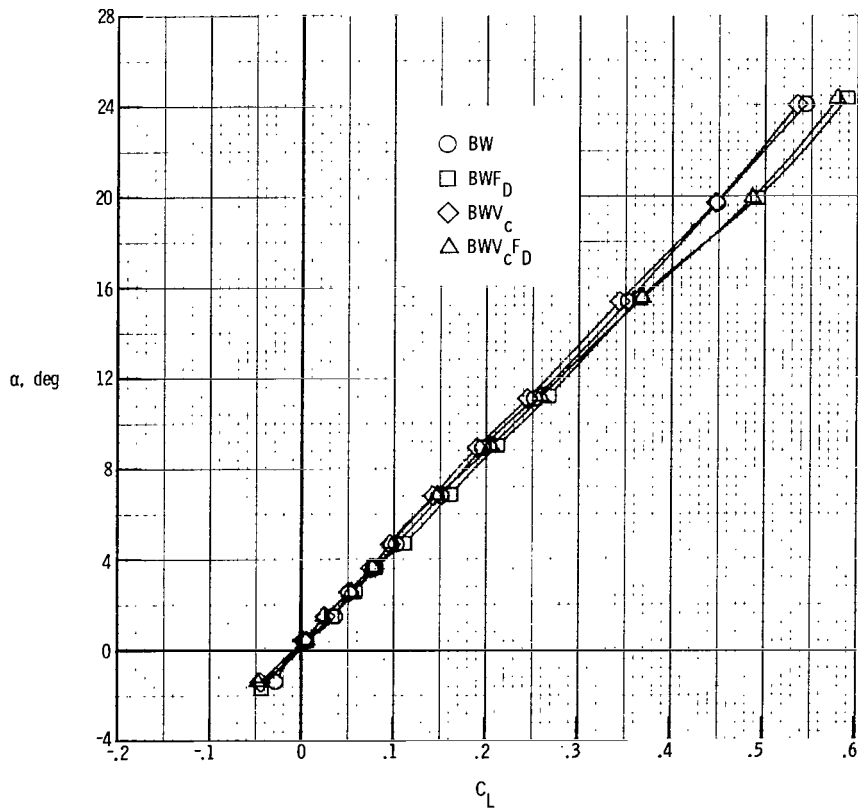
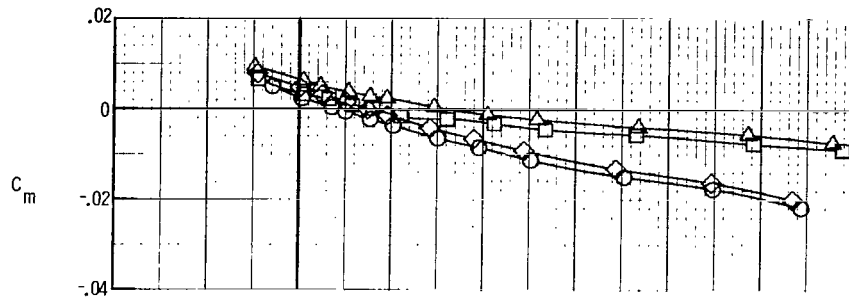
(b) $M = 2.00$.

Figure 7.- Continued.



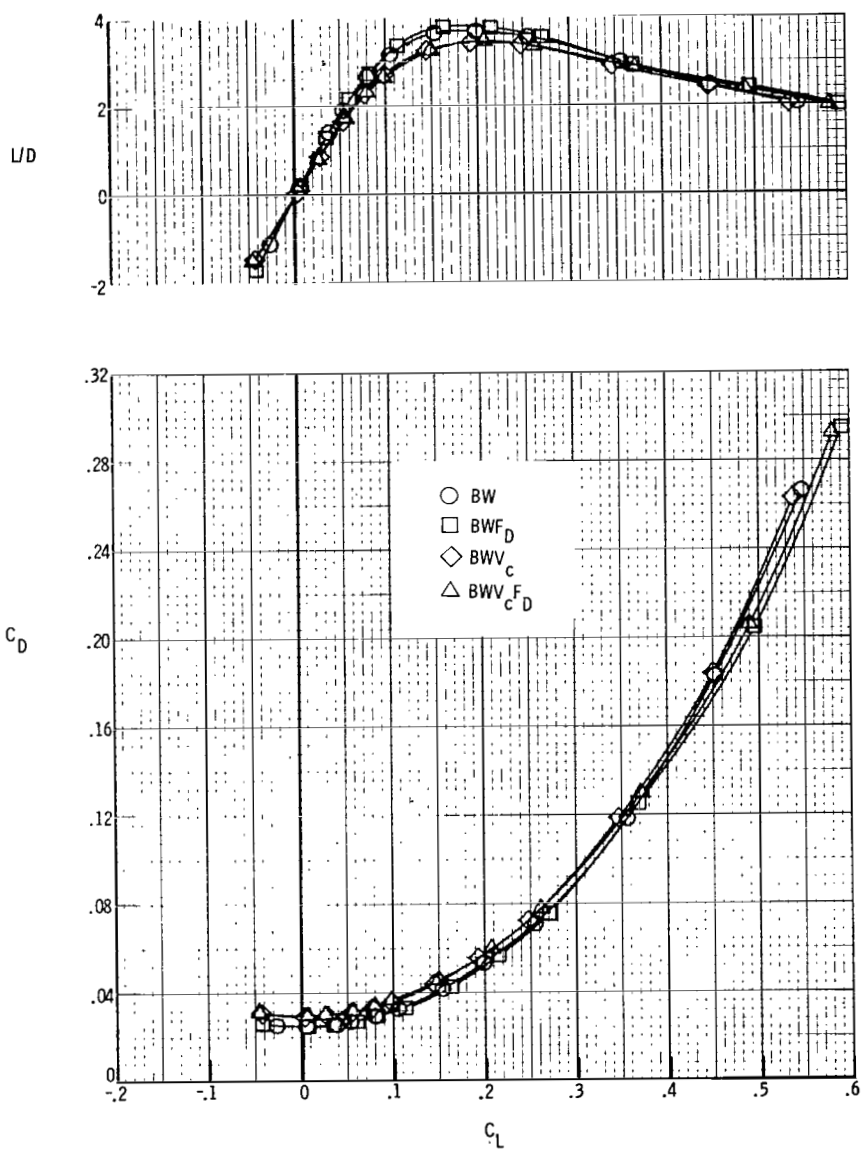
(b) $M = 2.00$. Concluded.

Figure 7.- Continued.



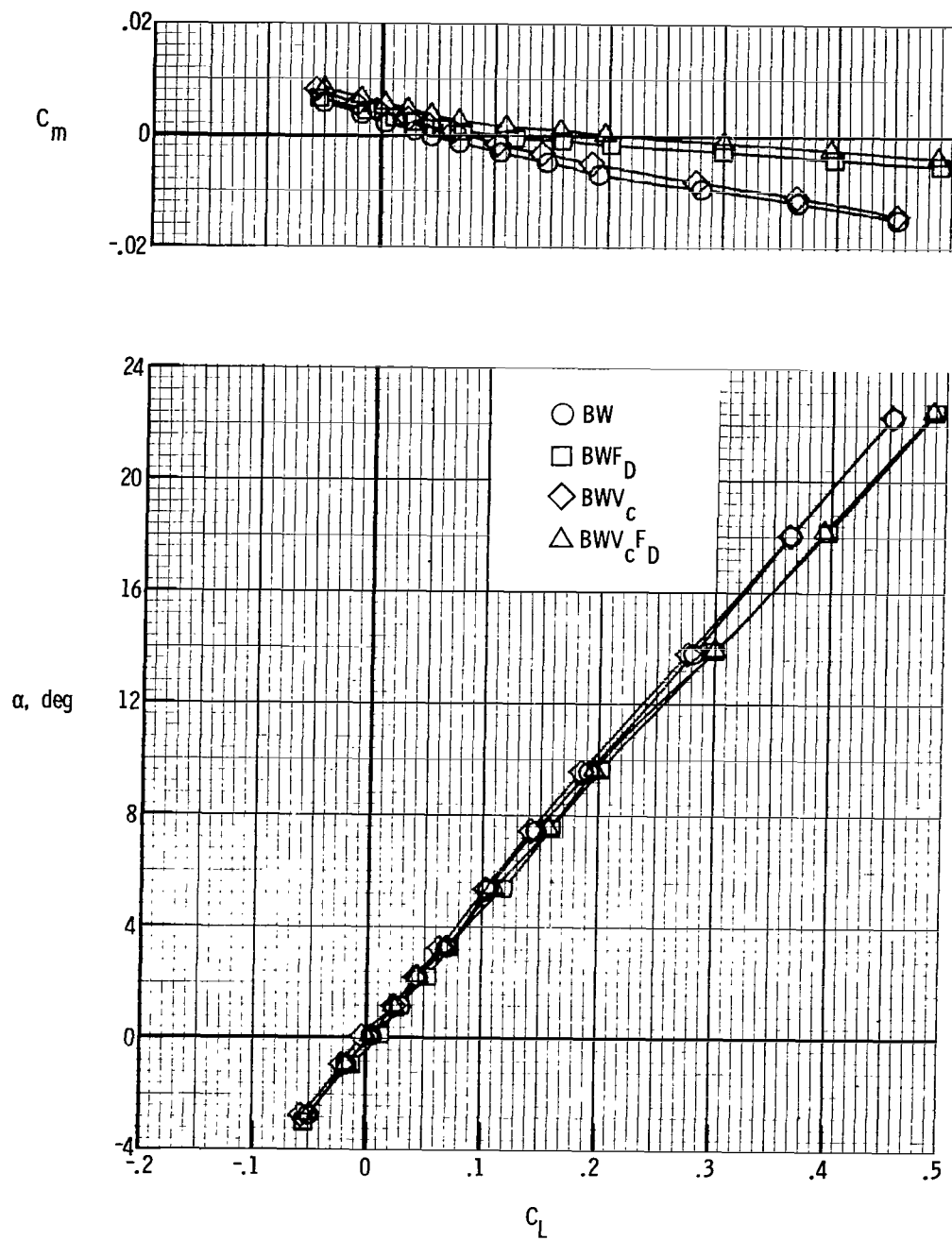
(c) $M = 2.36$.

Figure 7.- Continued.



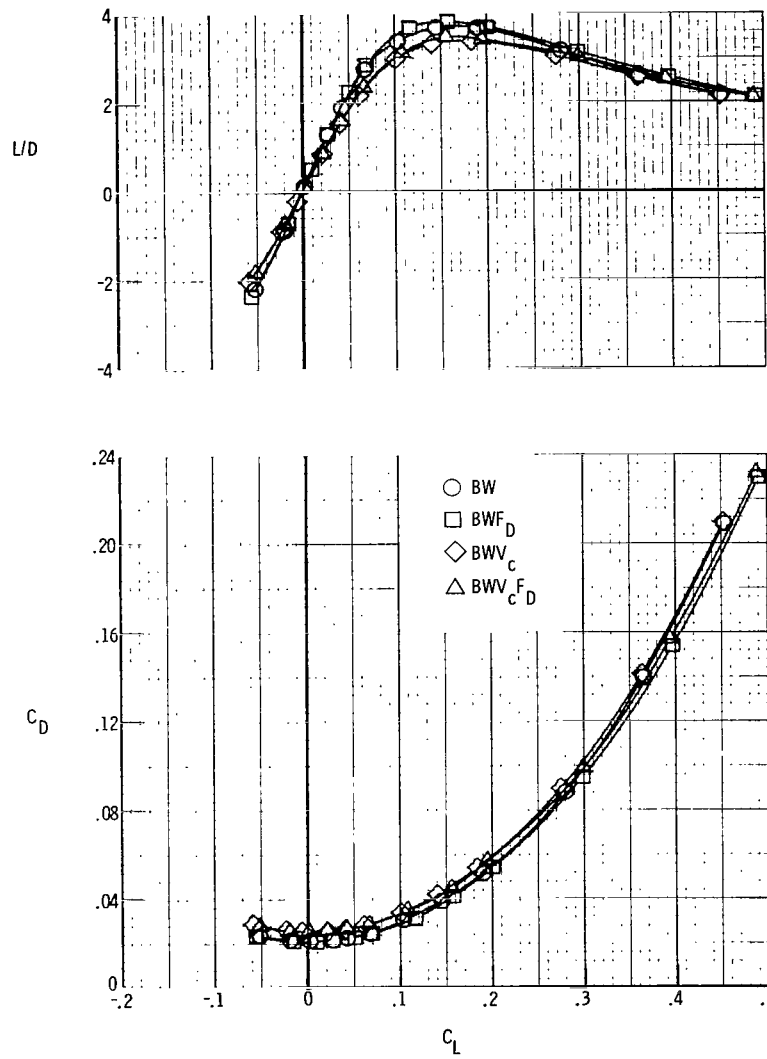
(c) $M = 2.36$. Concluded.

Figure 7.- Continued.



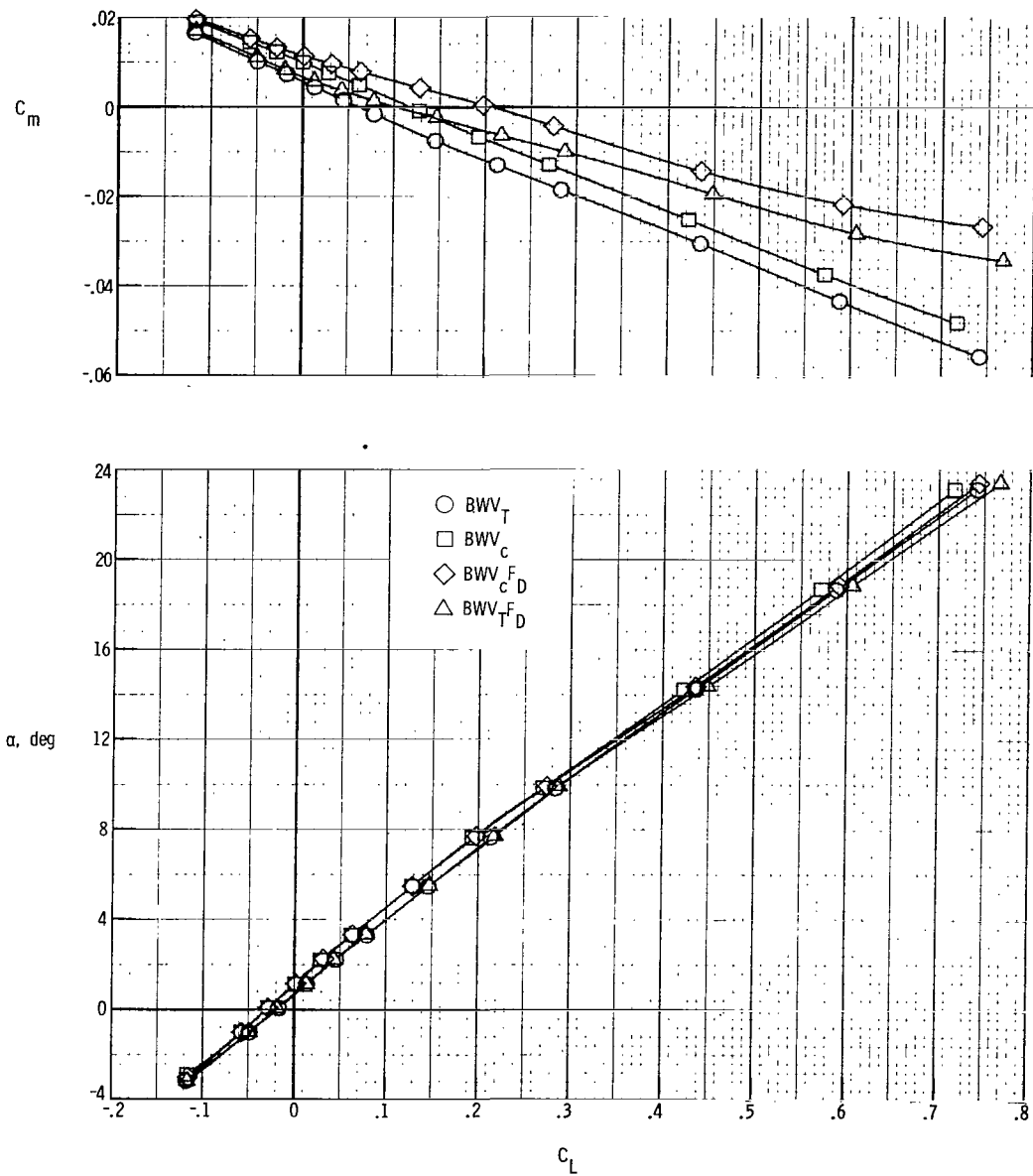
(d) $M = 2.86$.

Figure 7.- Continued.



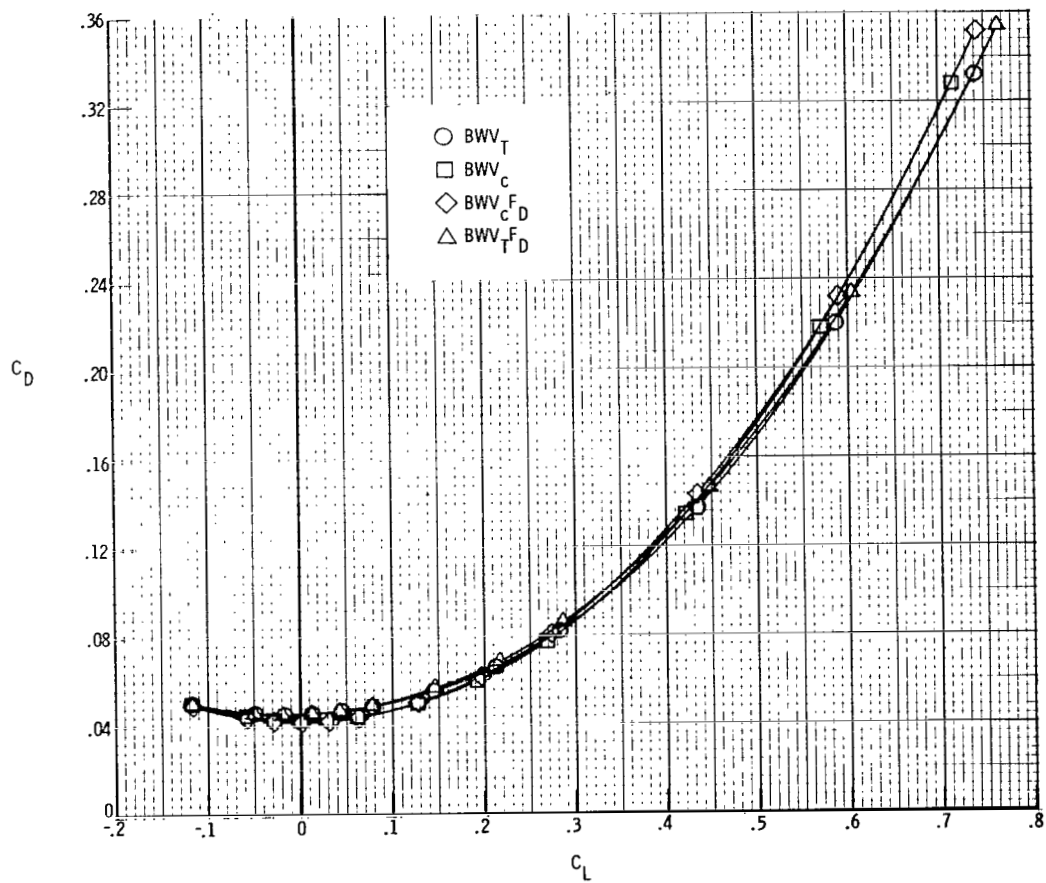
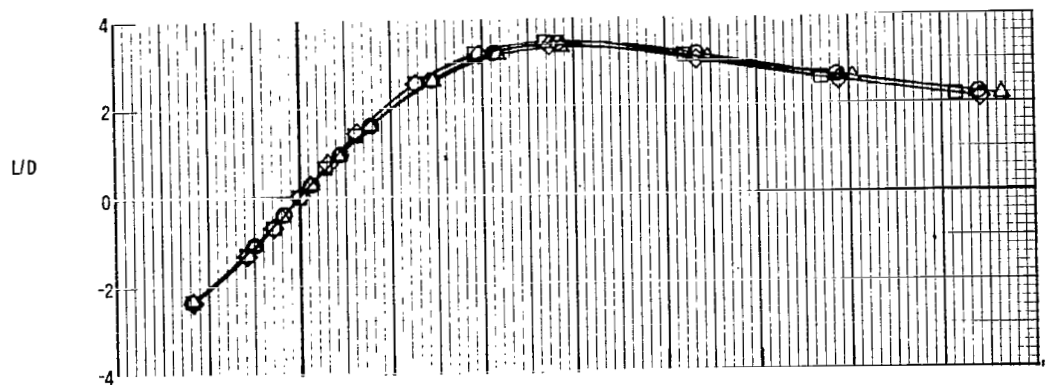
(d) $M = 2.86$. Concluded.

Figure 7.- Concluded.



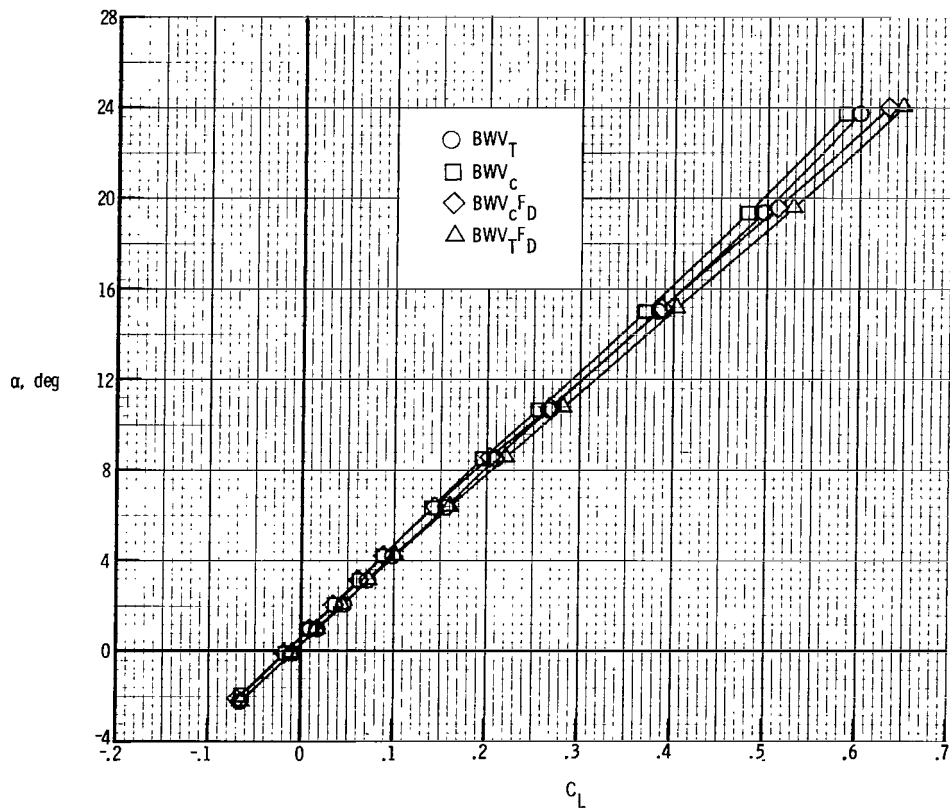
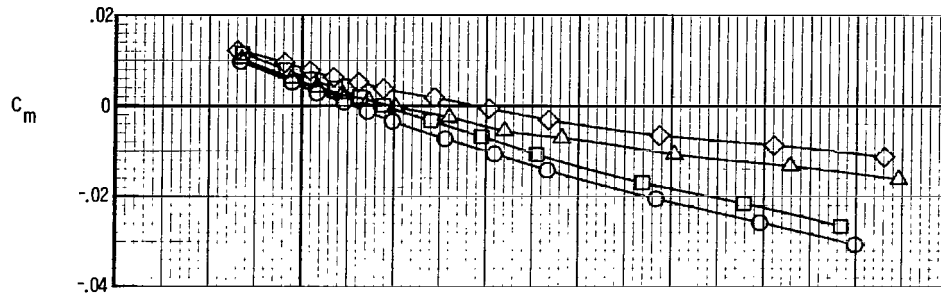
(a) $M = 1.50$.

Figure 8.- Comparison of the longitudinal aerodynamic characteristics of tip-fin and center-fin configurations.



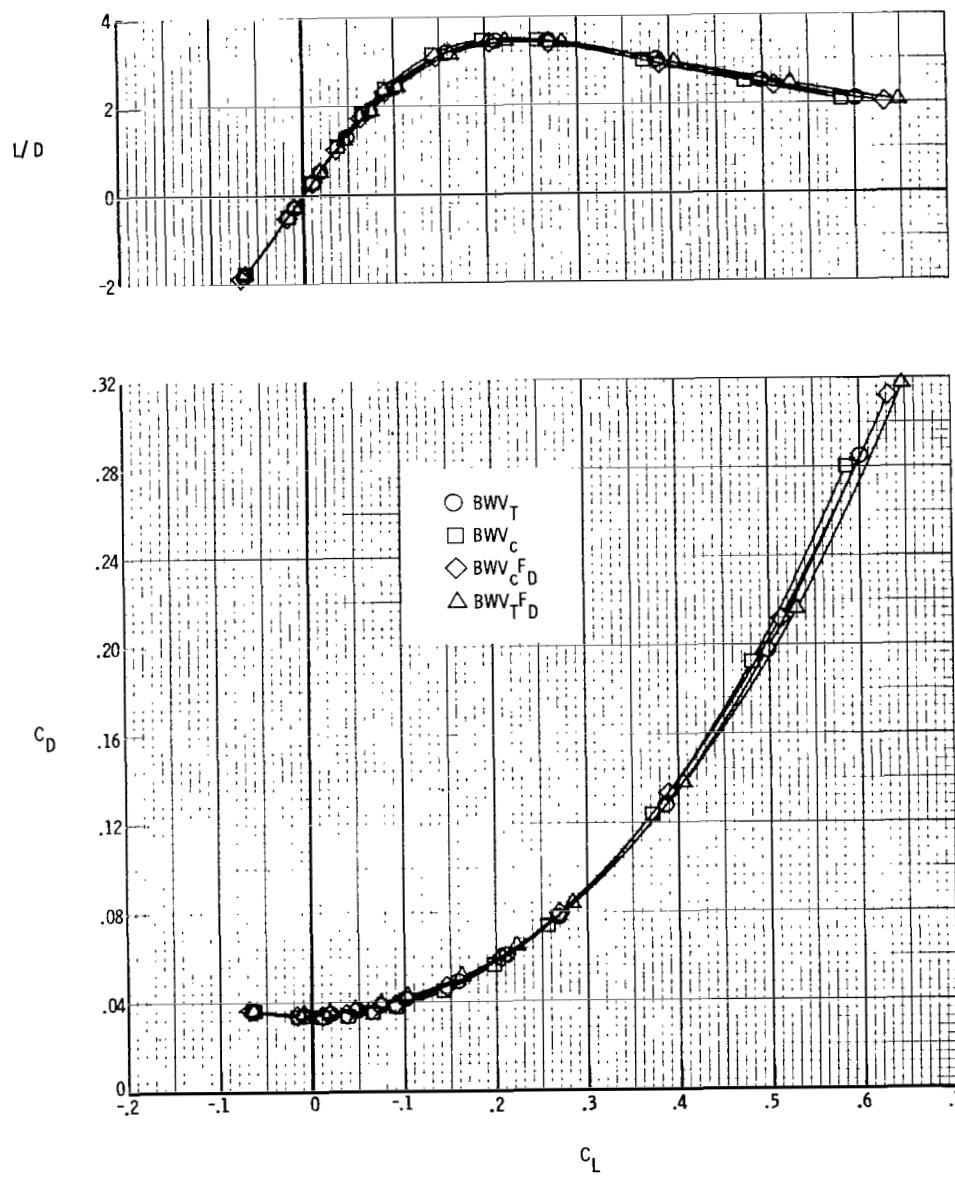
(a) $M = 1.50$. Concluded.

Figure 8.- Continued.



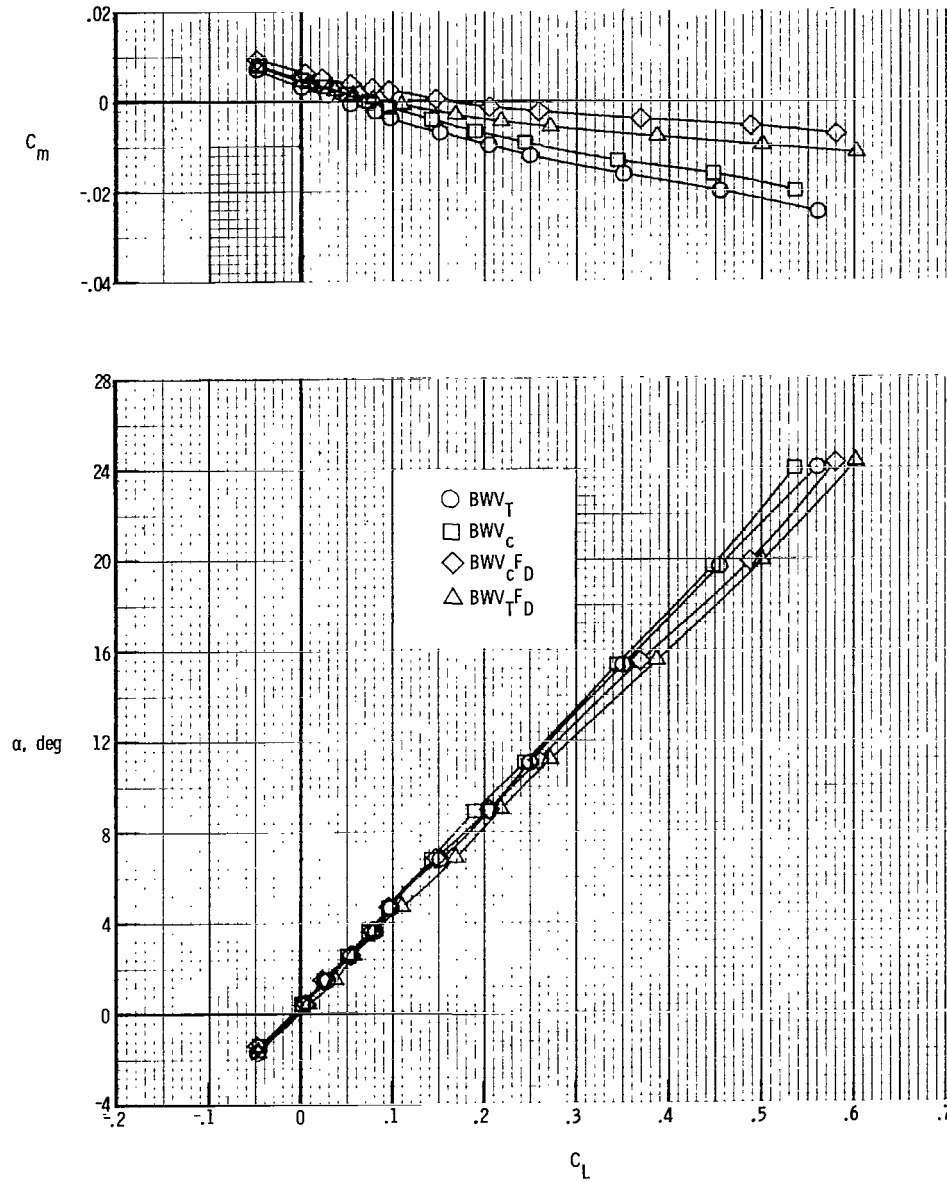
(b) $M = 2.00$.

Figure 8.- Continued.



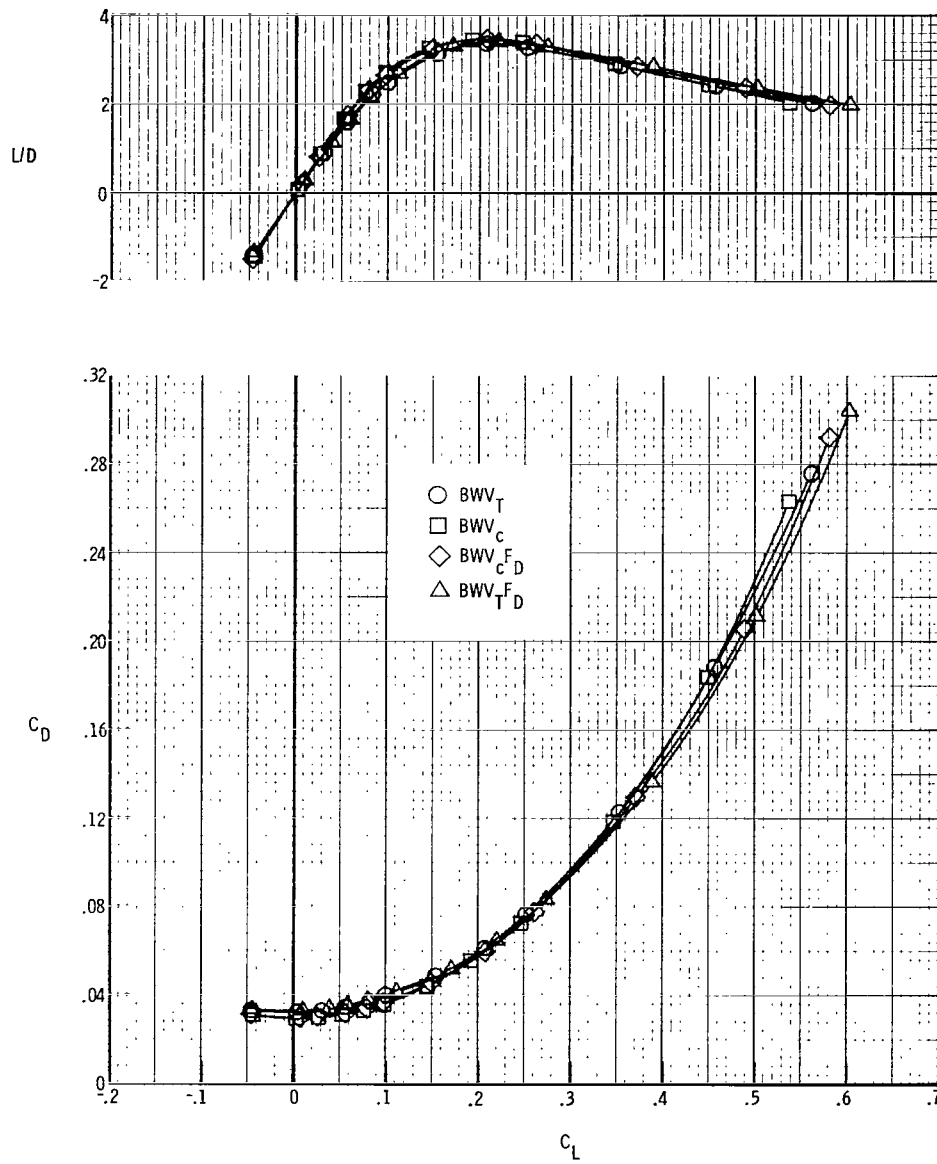
(b) $M = 2.00$. Concluded.

Figure 8.- Continued.



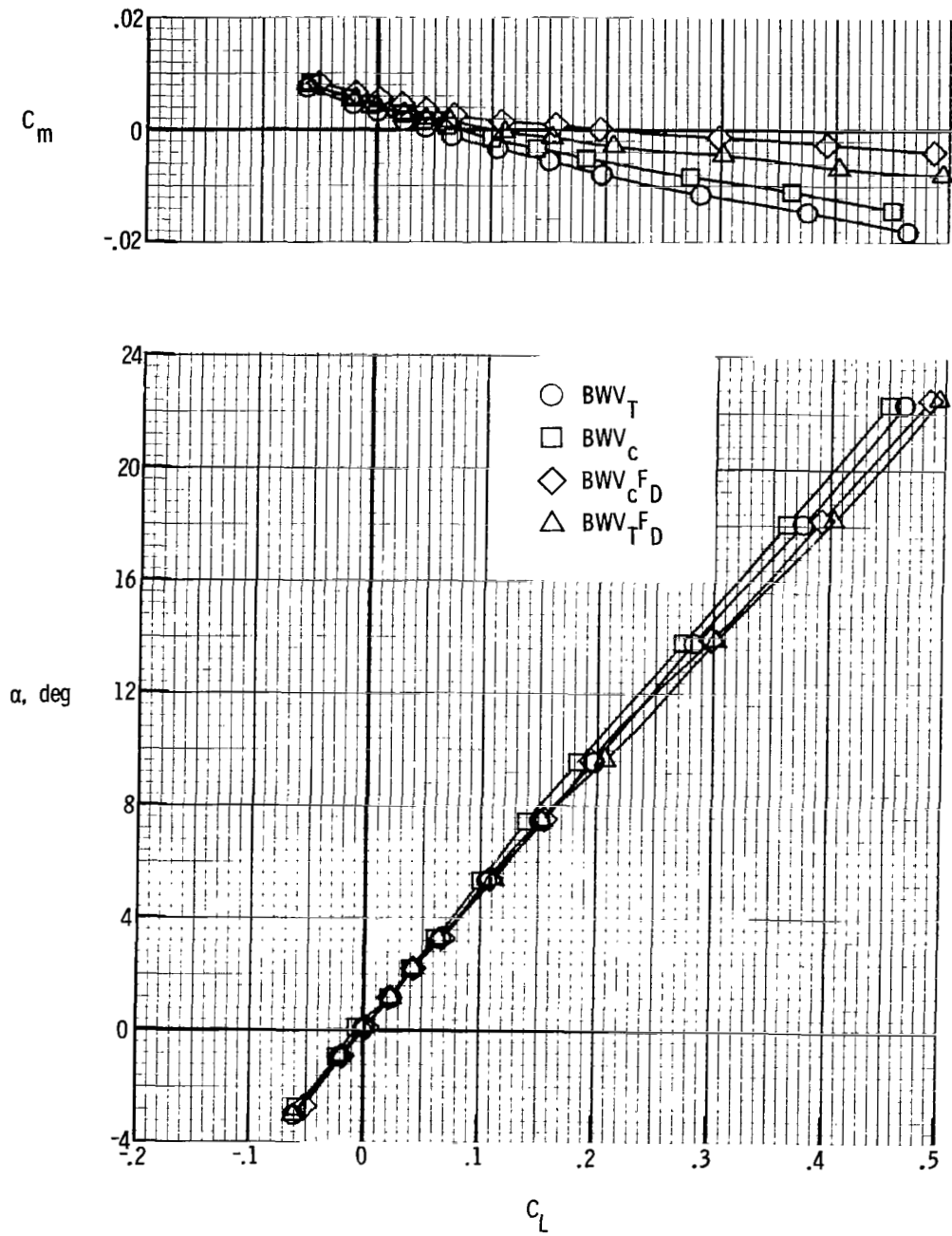
(c) $M = 2.36$.

Figure 8.- Continued.



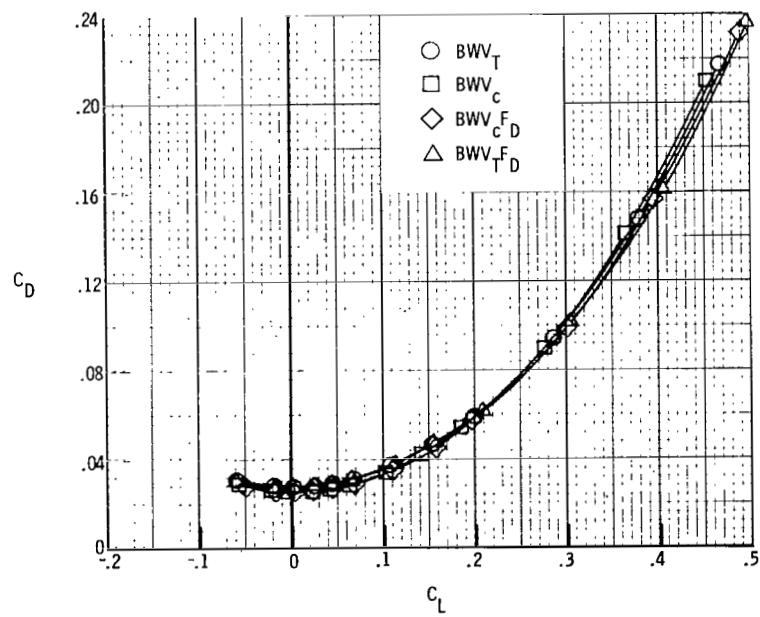
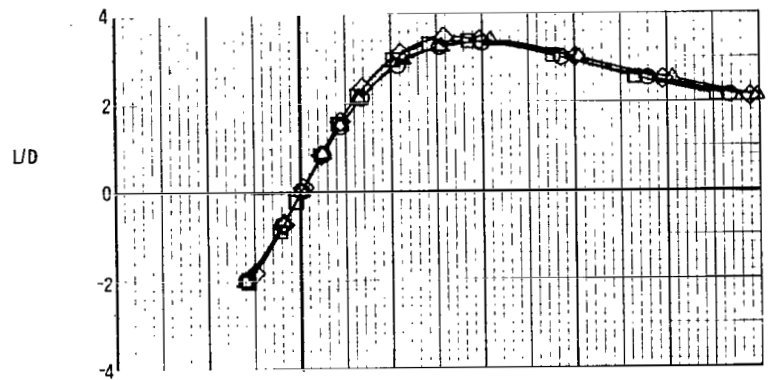
(c) $M = 2.36$. Concluded.

Figure 8.- Continued.



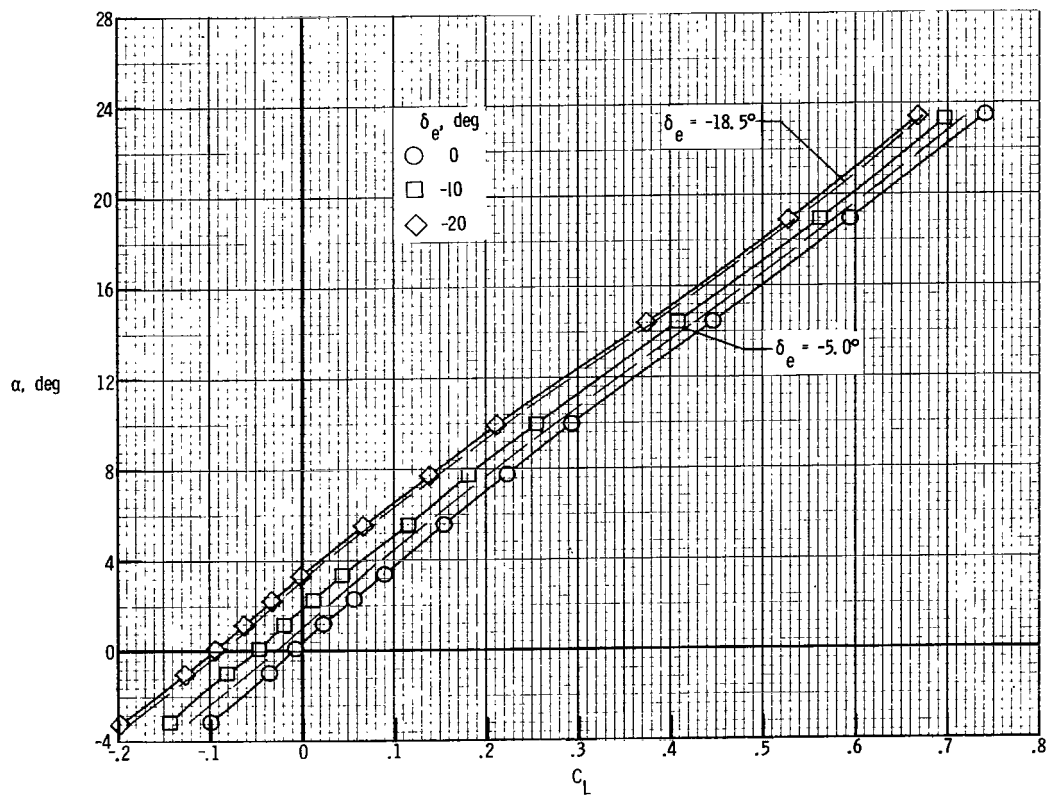
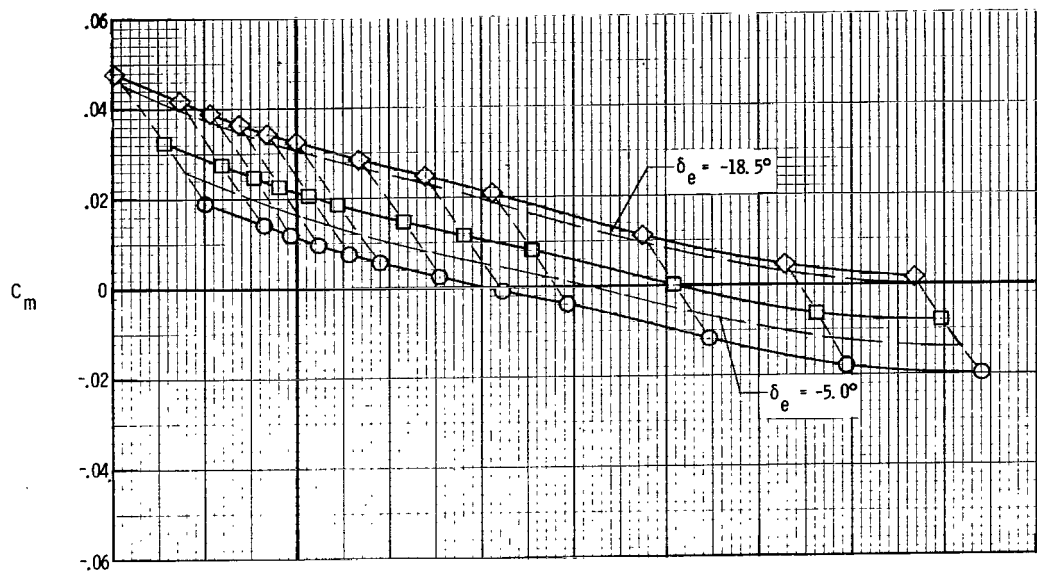
(d) $M = 2.86$.

Figure 8.- Continued.



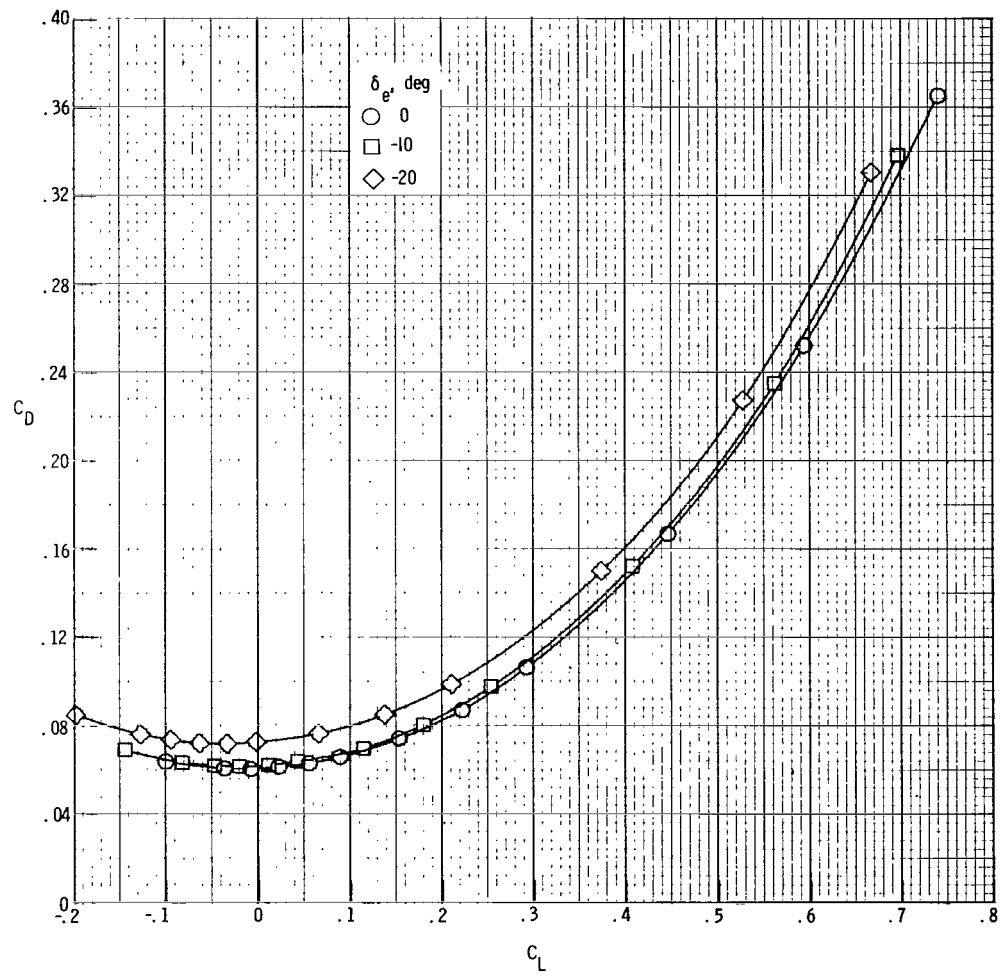
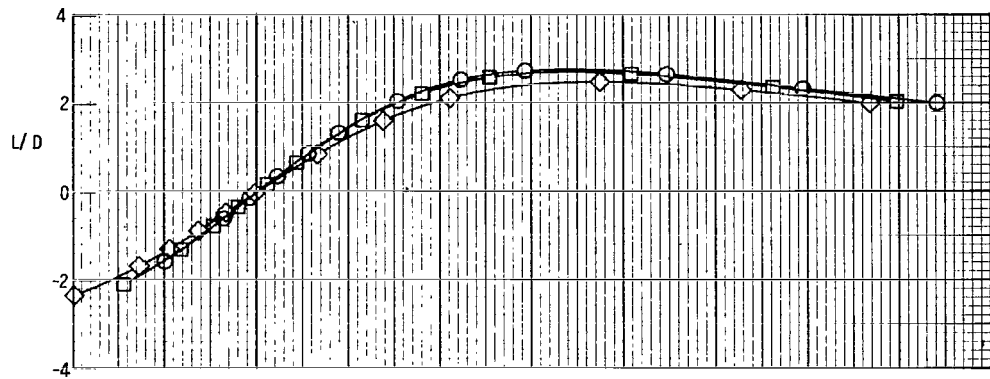
(d) $M = 2.86$. Concluded.

Figure 8.- Concluded.



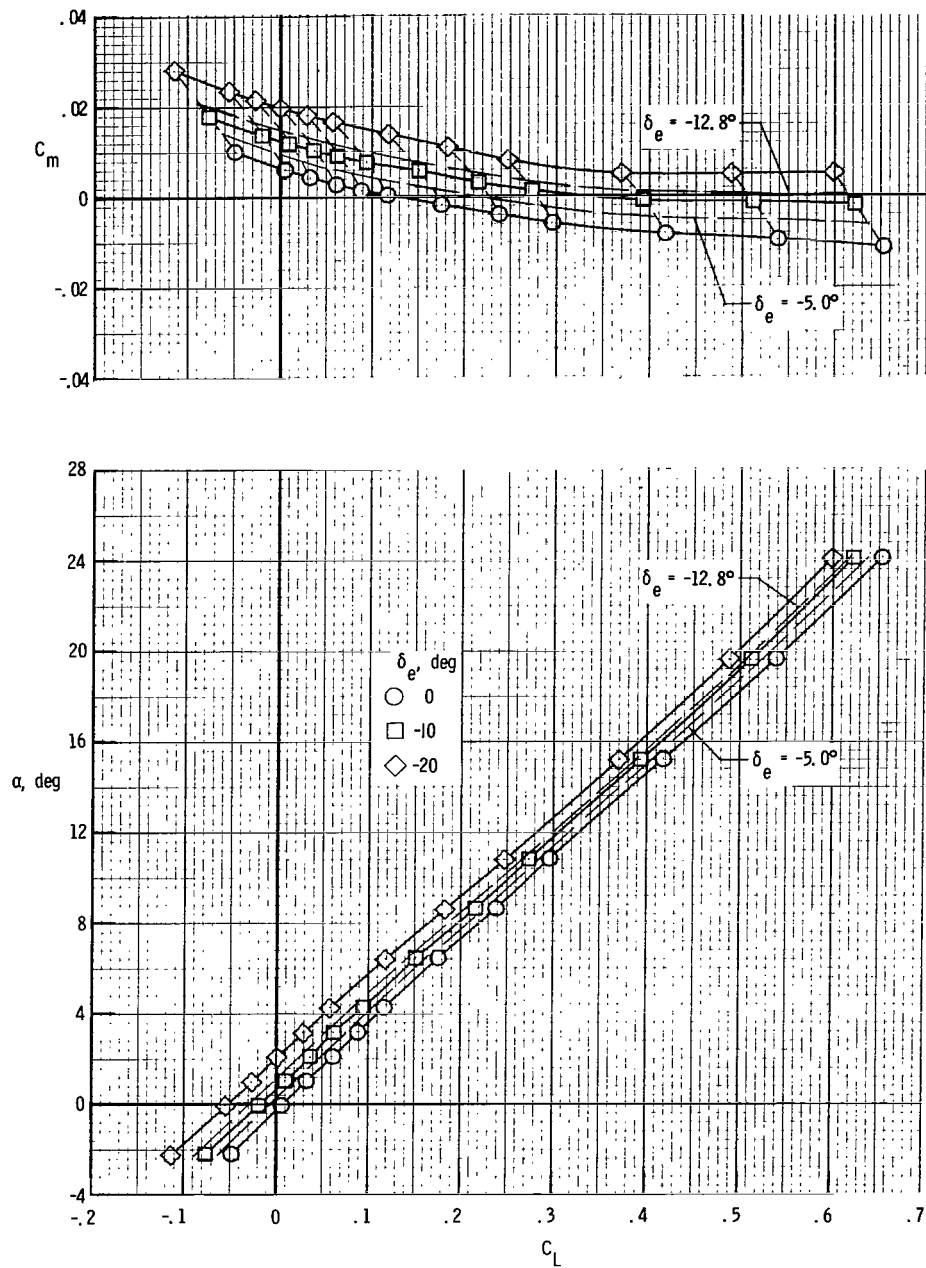
(a) $M = 1.50$.

Figure 9.- Effect of elevon deflection on the longitudinal aerodynamic characteristics of the BWV_TF_DE configuration.



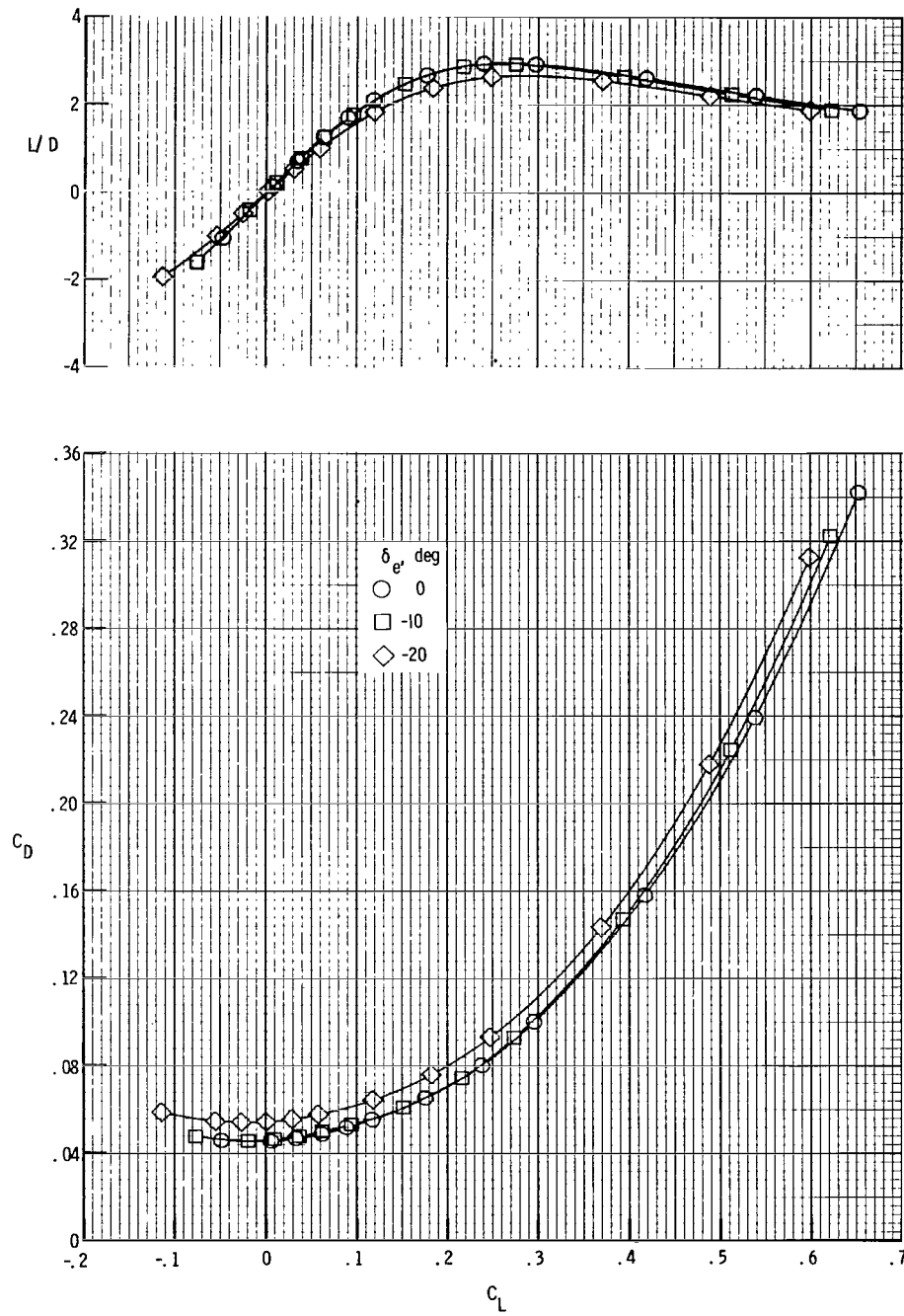
(a) $M = 1.50$. Concluded.

Figure 9.- Continued.



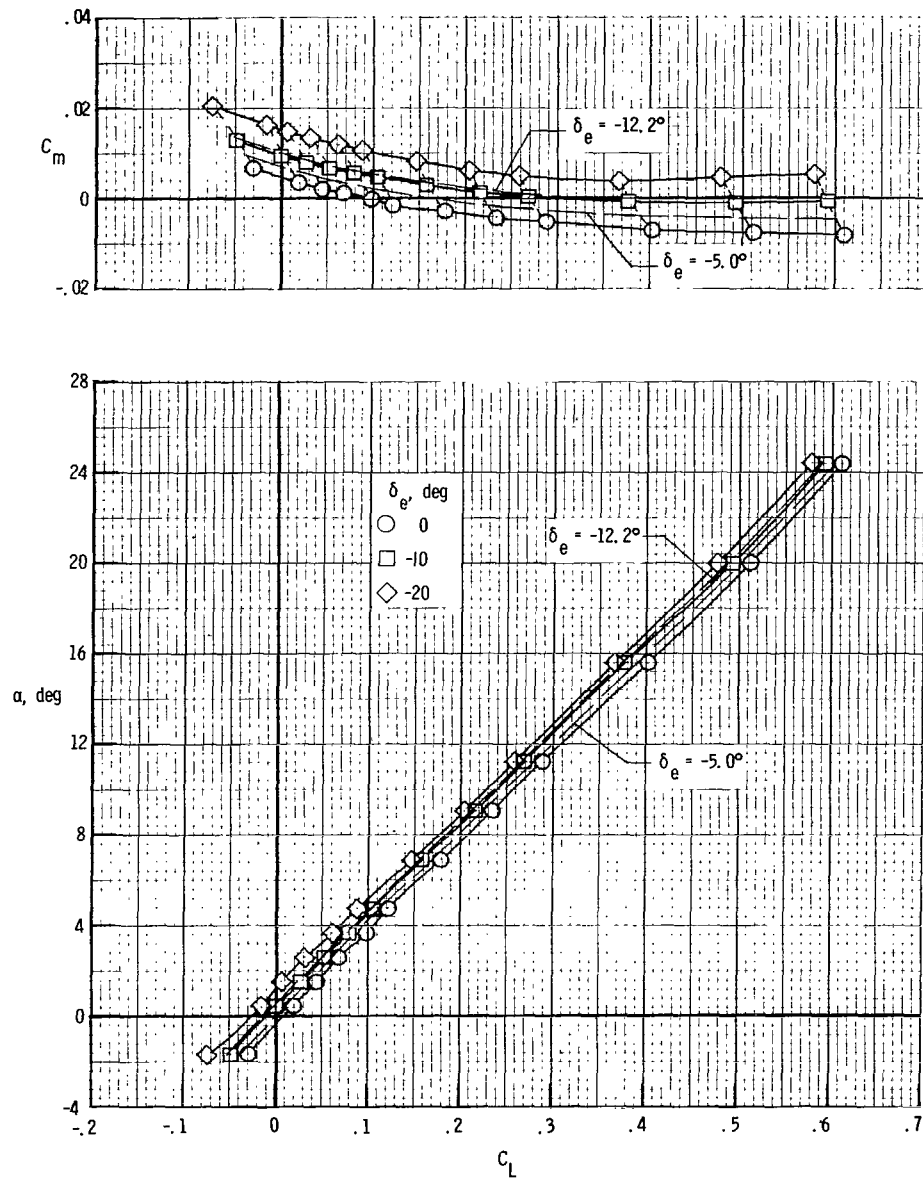
(b) $M = 2.00$.

Figure 9.- Continued.



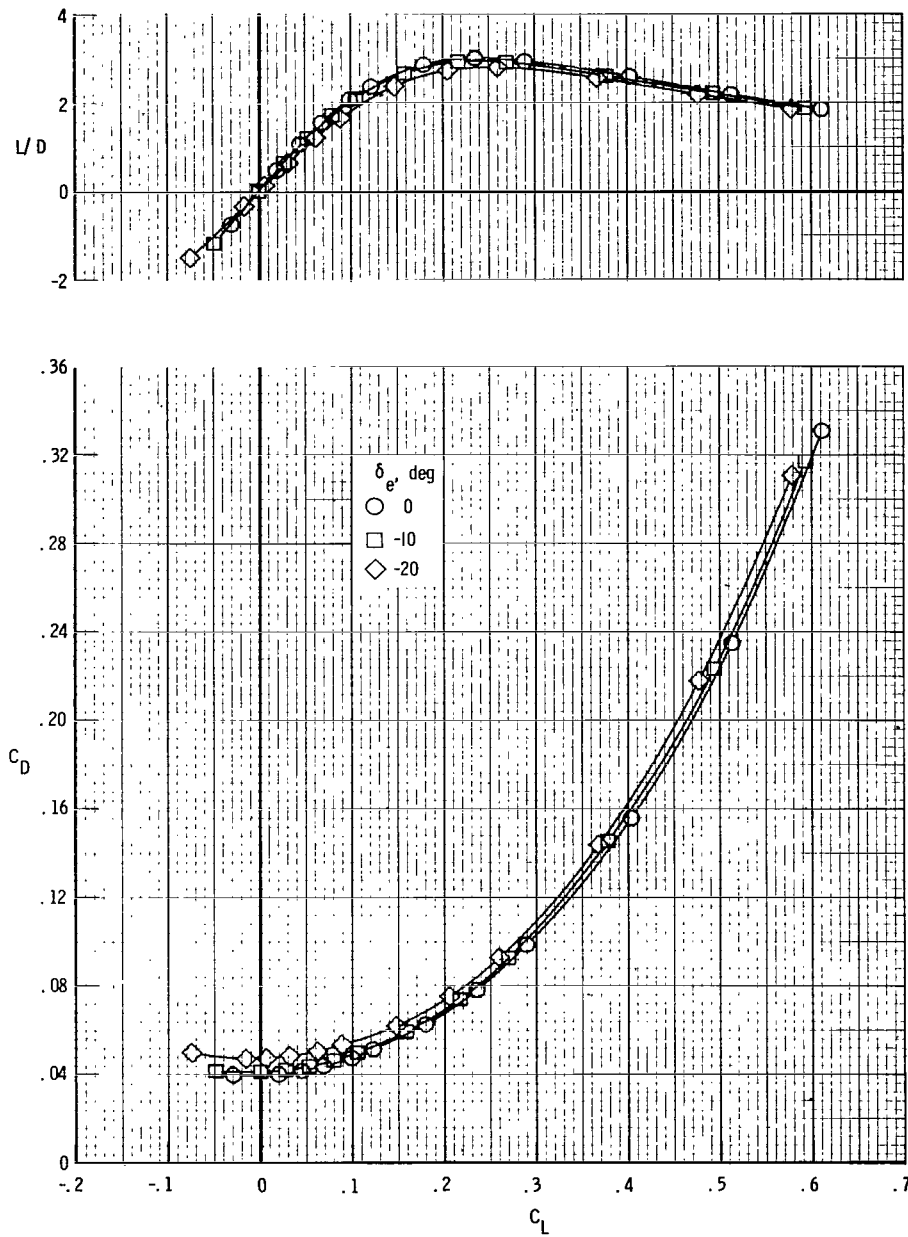
(b) $M = 2.00$. Concluded.

Figure 9.- Continued.



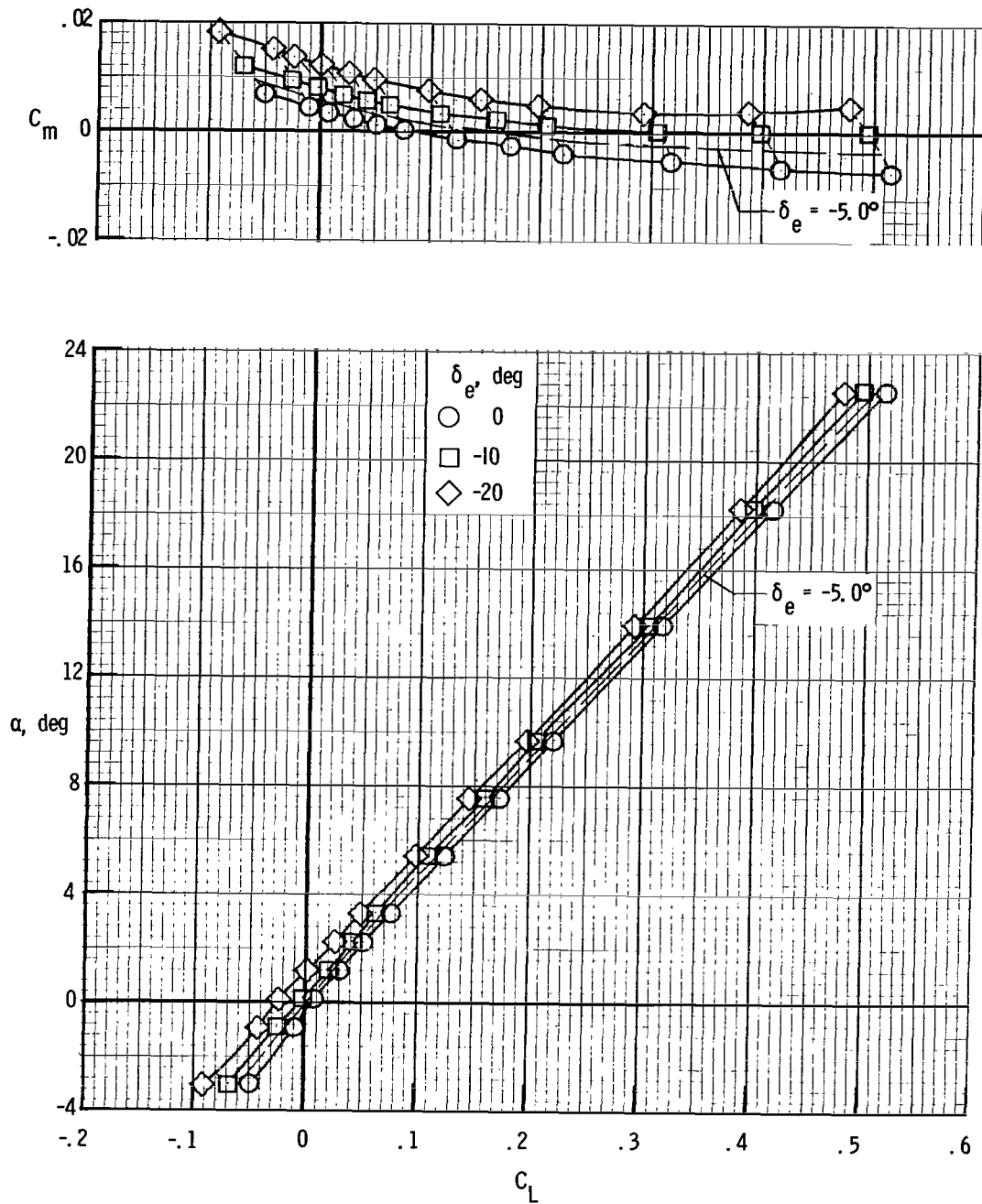
(c) $M = 2.36$.

Figure 9.- Continued.



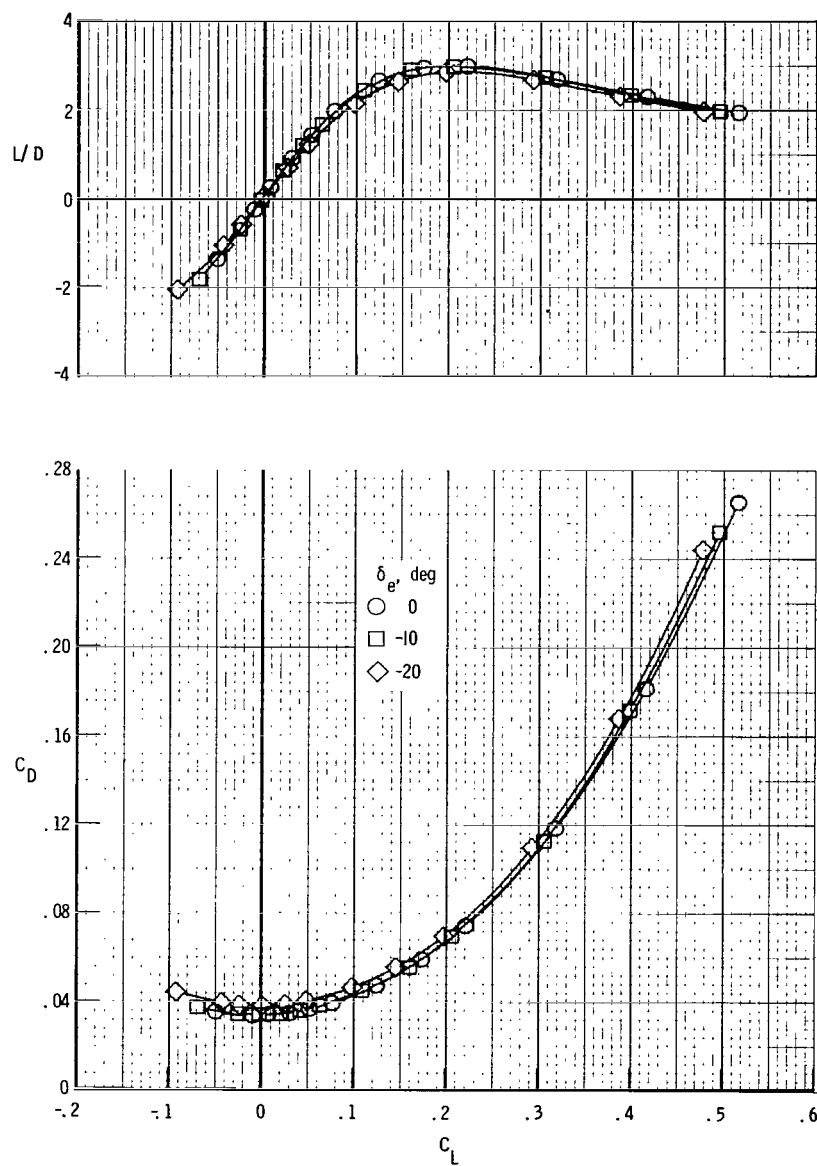
(c) $M = 2.36$. Concluded.

Figure 9.- Continued.



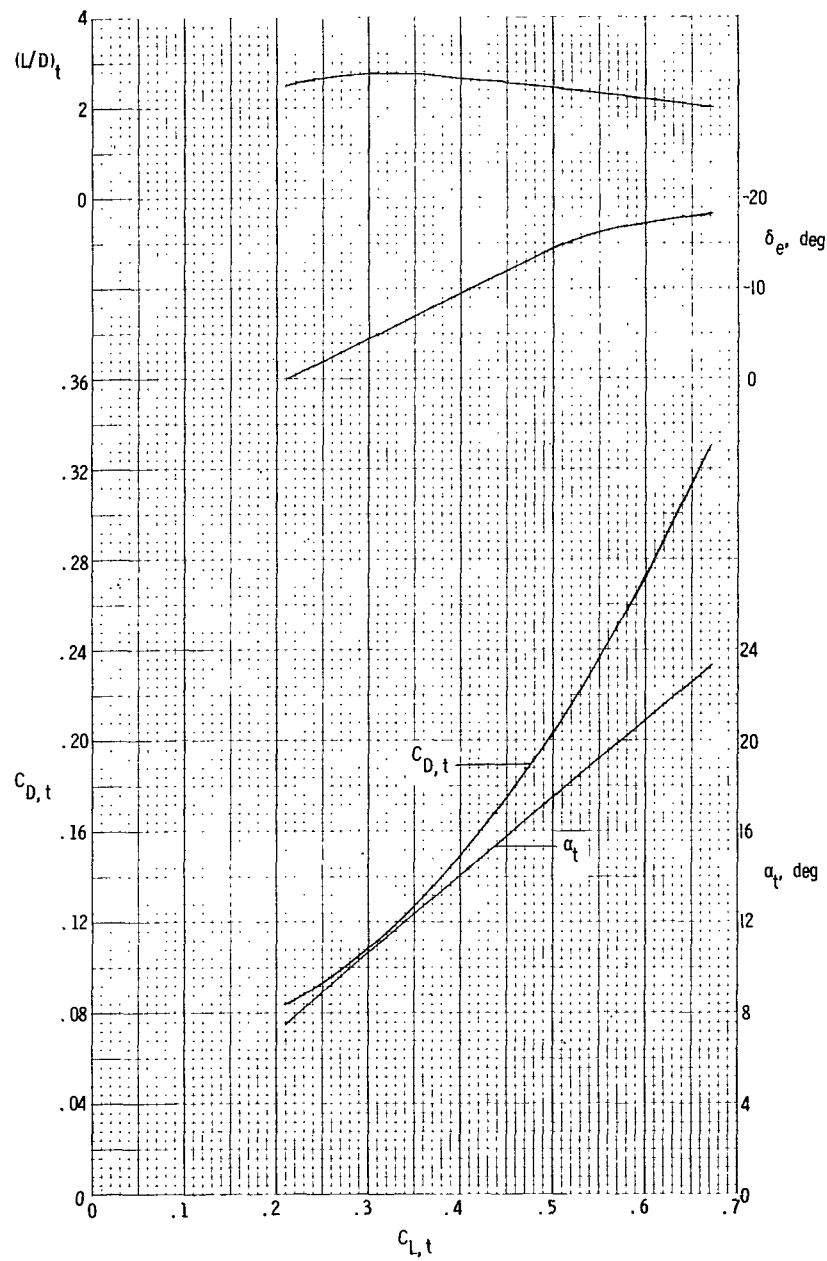
(d) $M = 2.86$.

Figure 9.- Continued.



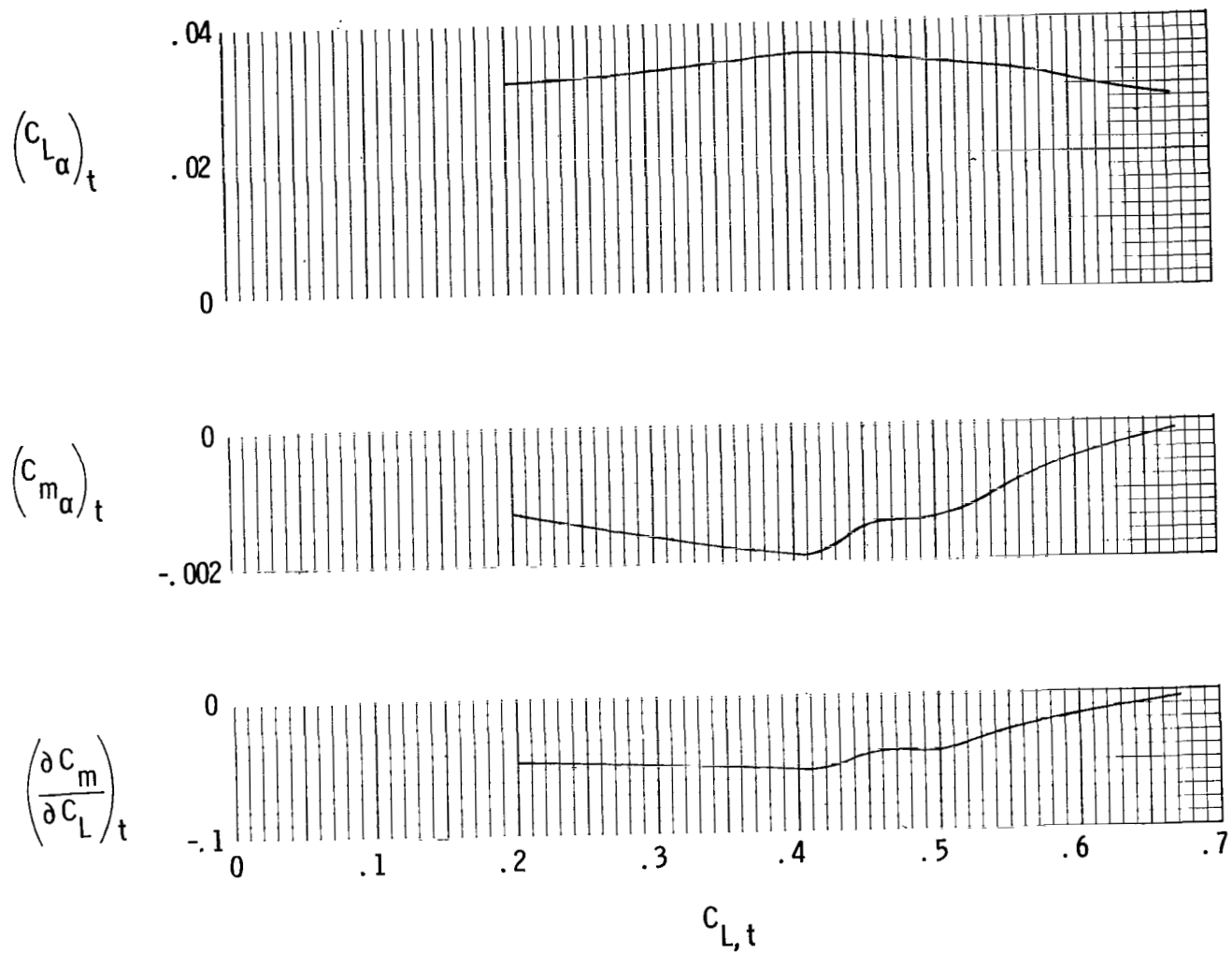
(d) $M = 2.86$. Concluded.

Figure 9.- Concluded.



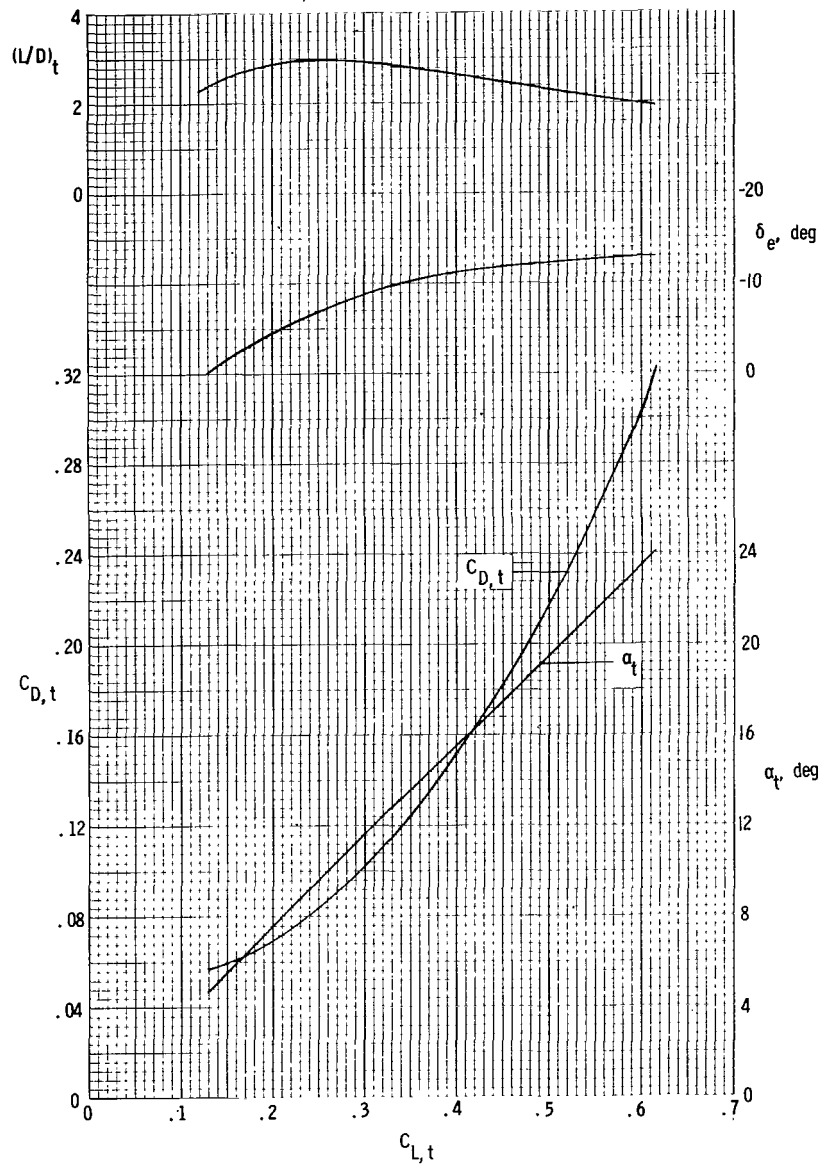
(a) $M = 1.50$.

Figure 10.- Longitudinal aerodynamic characteristics at trim of the BWV_T F_D E configuration.



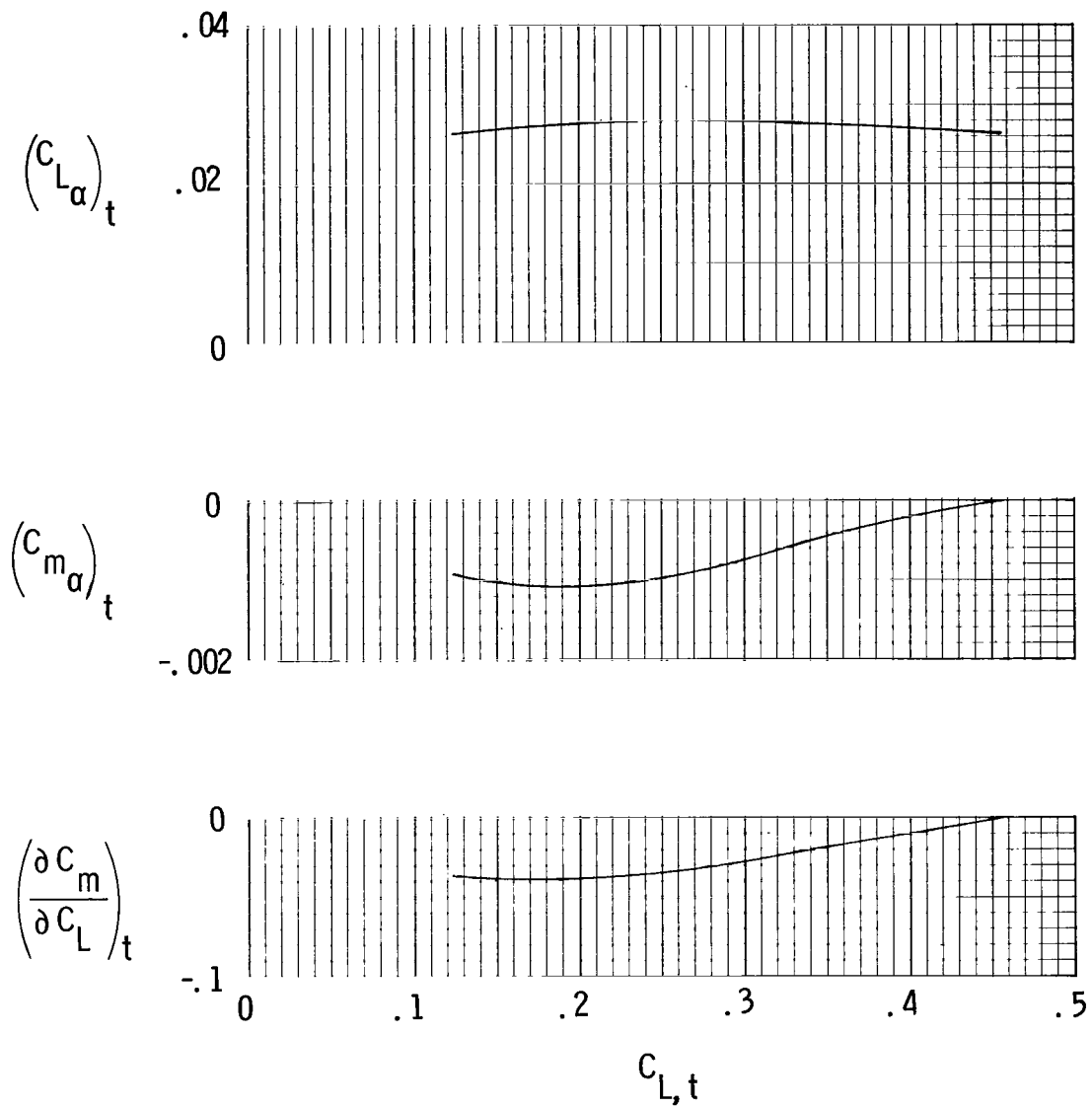
(a) $M = 1.50$. Concluded.

Figure 10.- Continued.



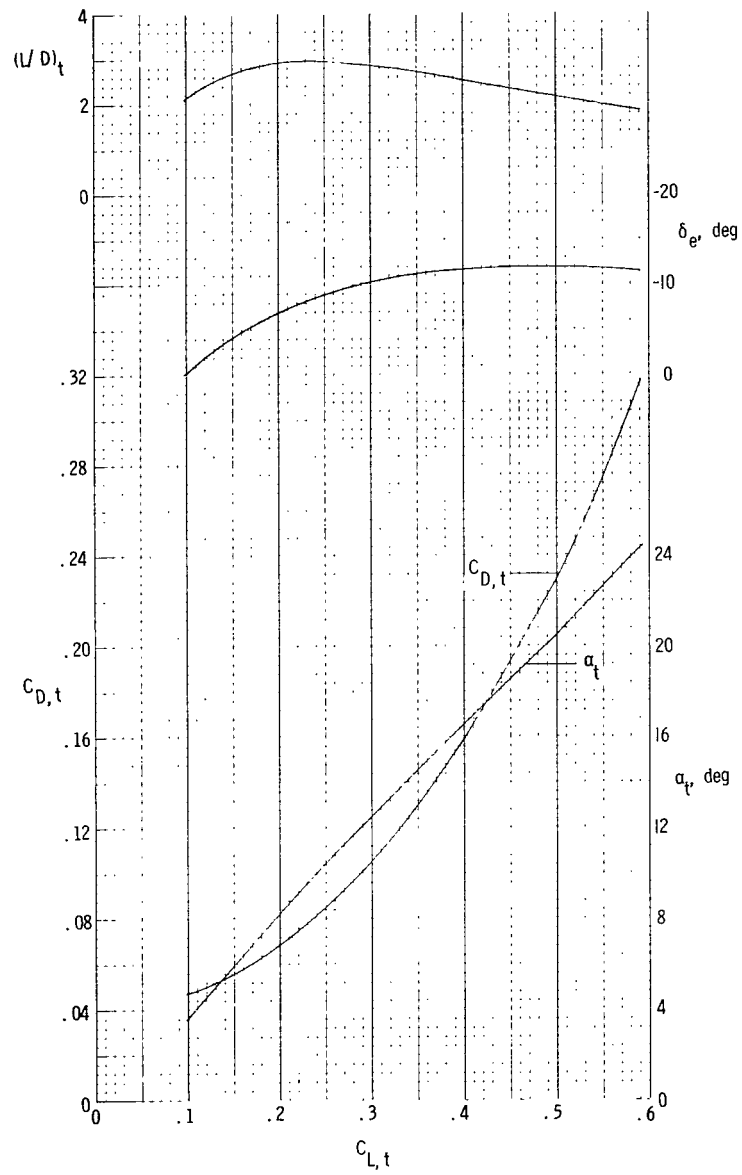
(b) $M = 2.00$.

Figure 10.- Continued.



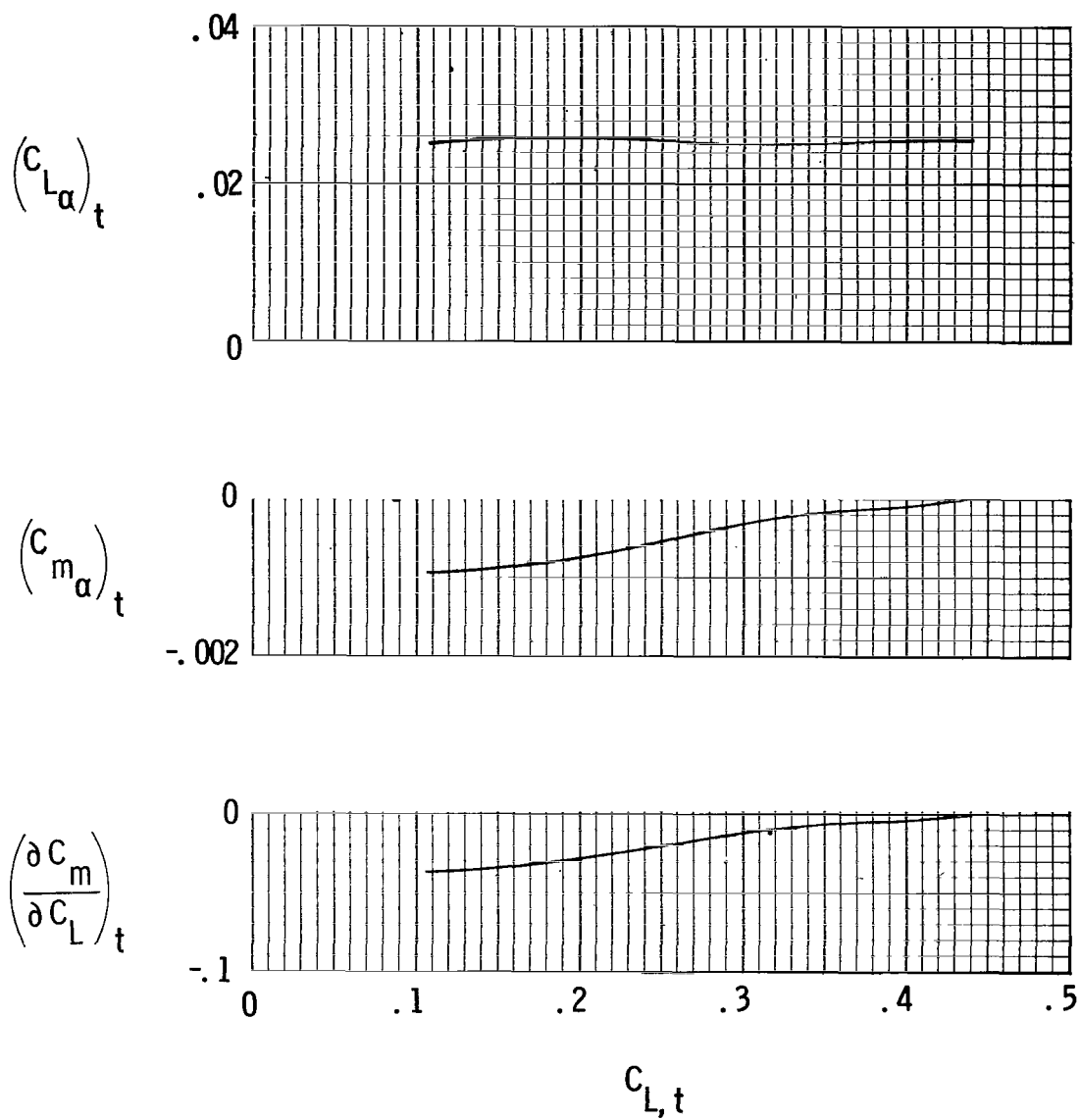
(b) $M = 2.00$. Concluded.

Figure 10.- Continued.



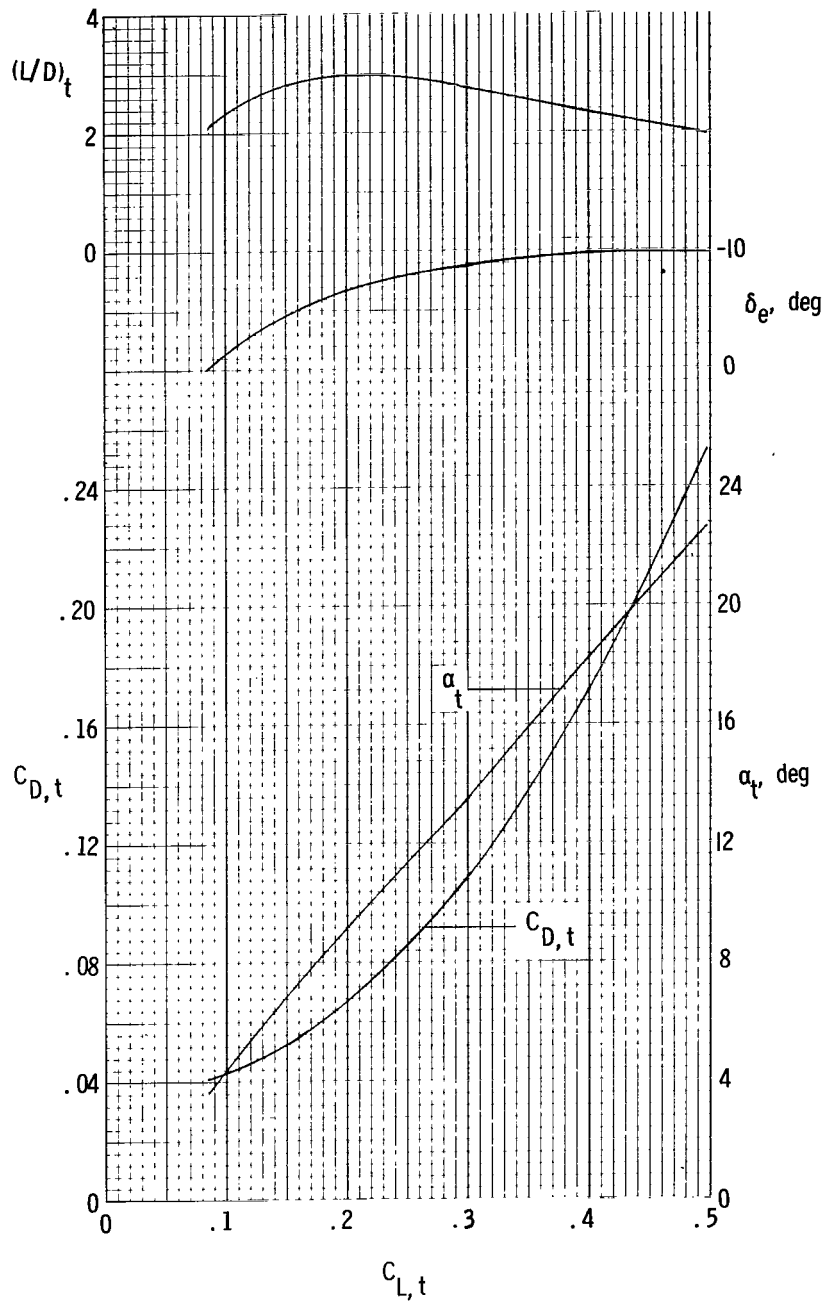
(c) $M = 2.36$.

Figure 10.- Continued.



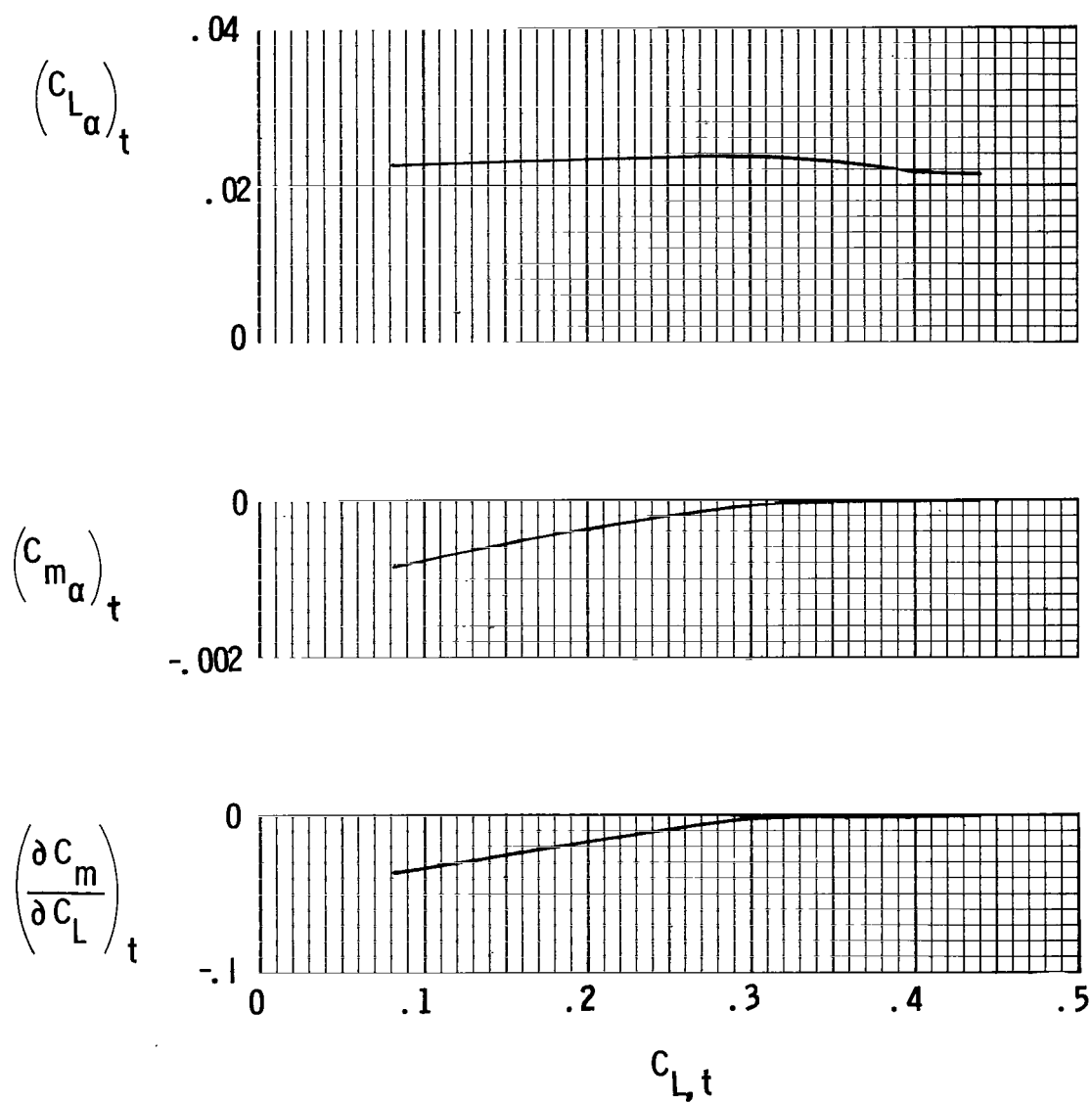
(c) $M = 2.36$. Concluded.

Figure 10.- Continued.



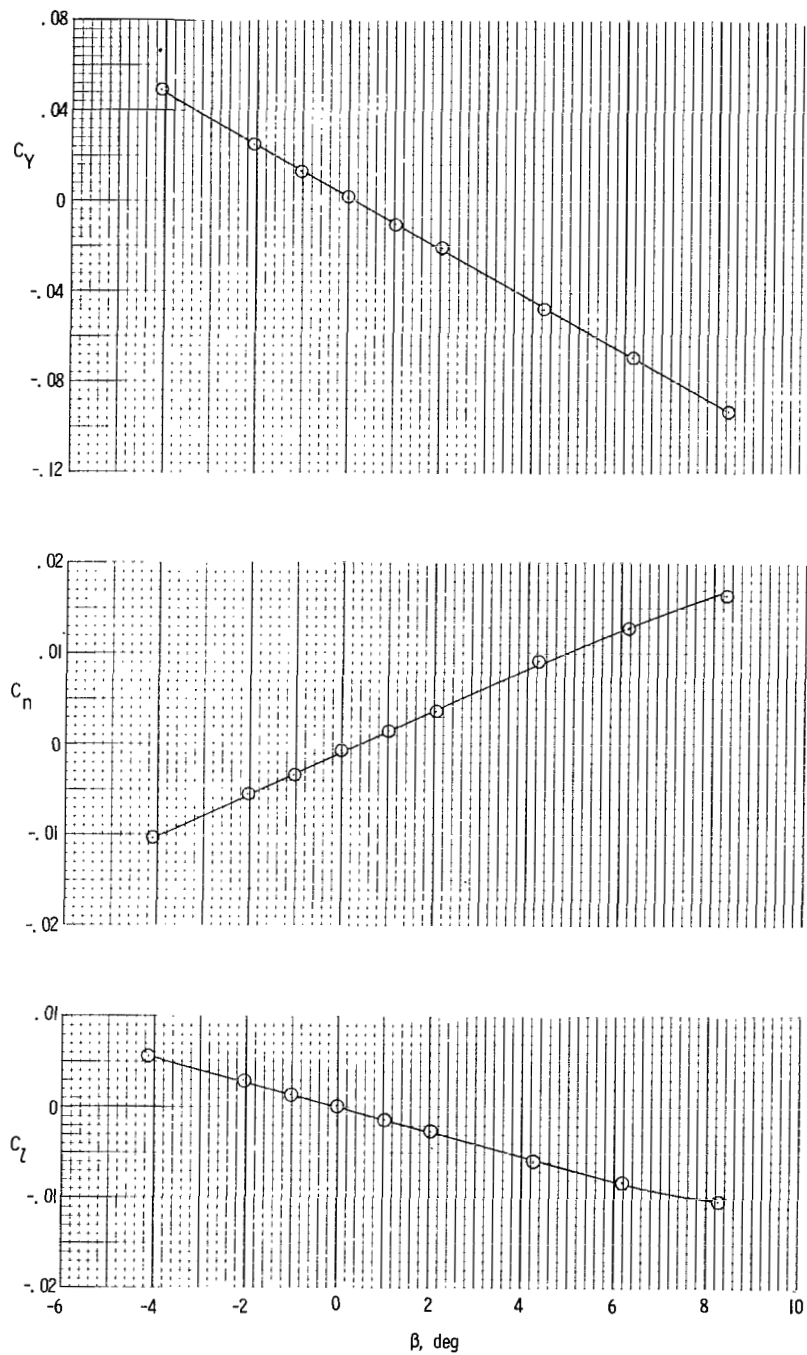
(d) $M = 2.86$.

Figure 10.- Continued.



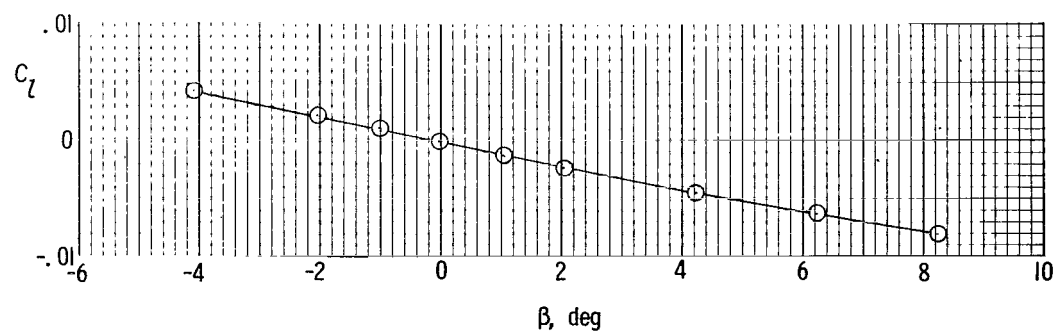
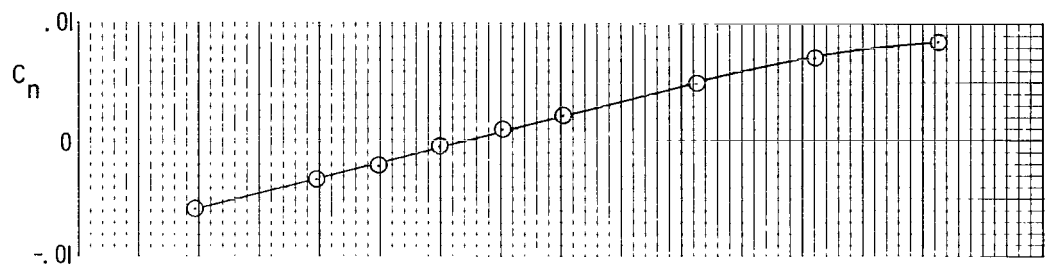
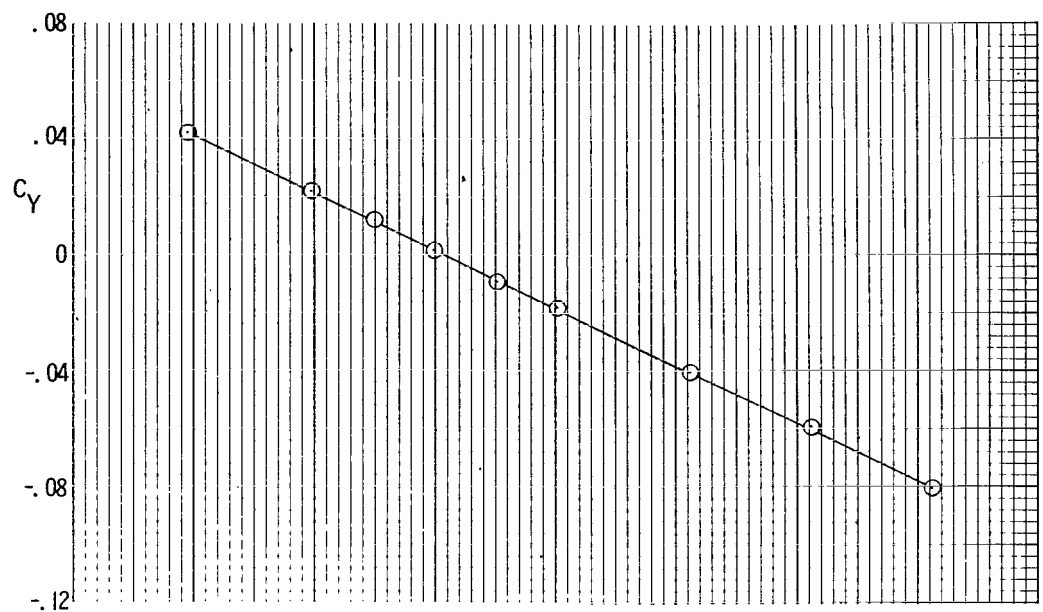
(d) $M = 2.86$. Concluded.

Figure 10.- Concluded.



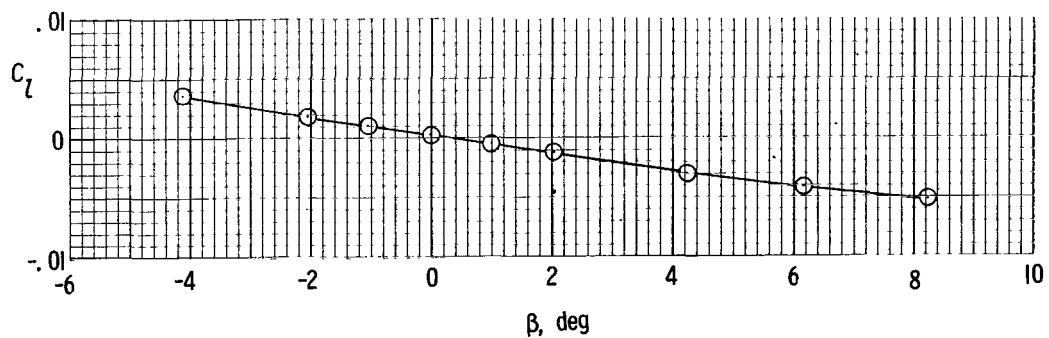
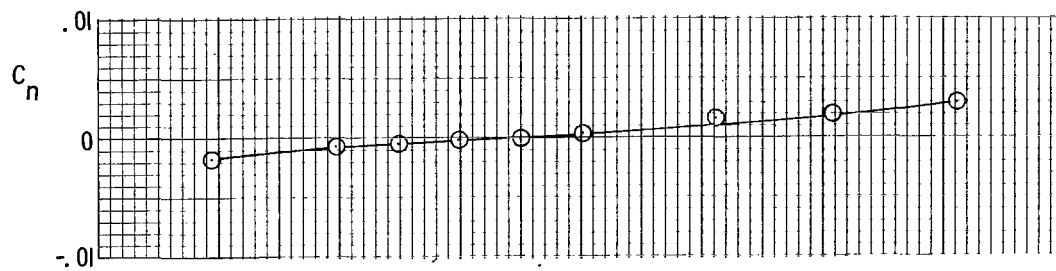
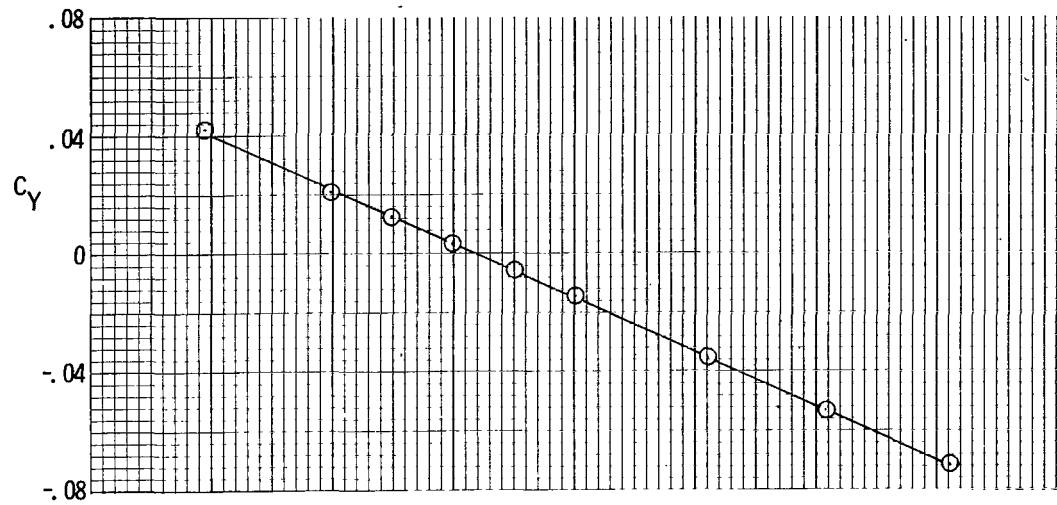
(a) $M = 1.50$.

Figure 11.- Lateral aerodynamic characteristics of the BWV_TF_DE configuration at $\alpha = 0^\circ$.



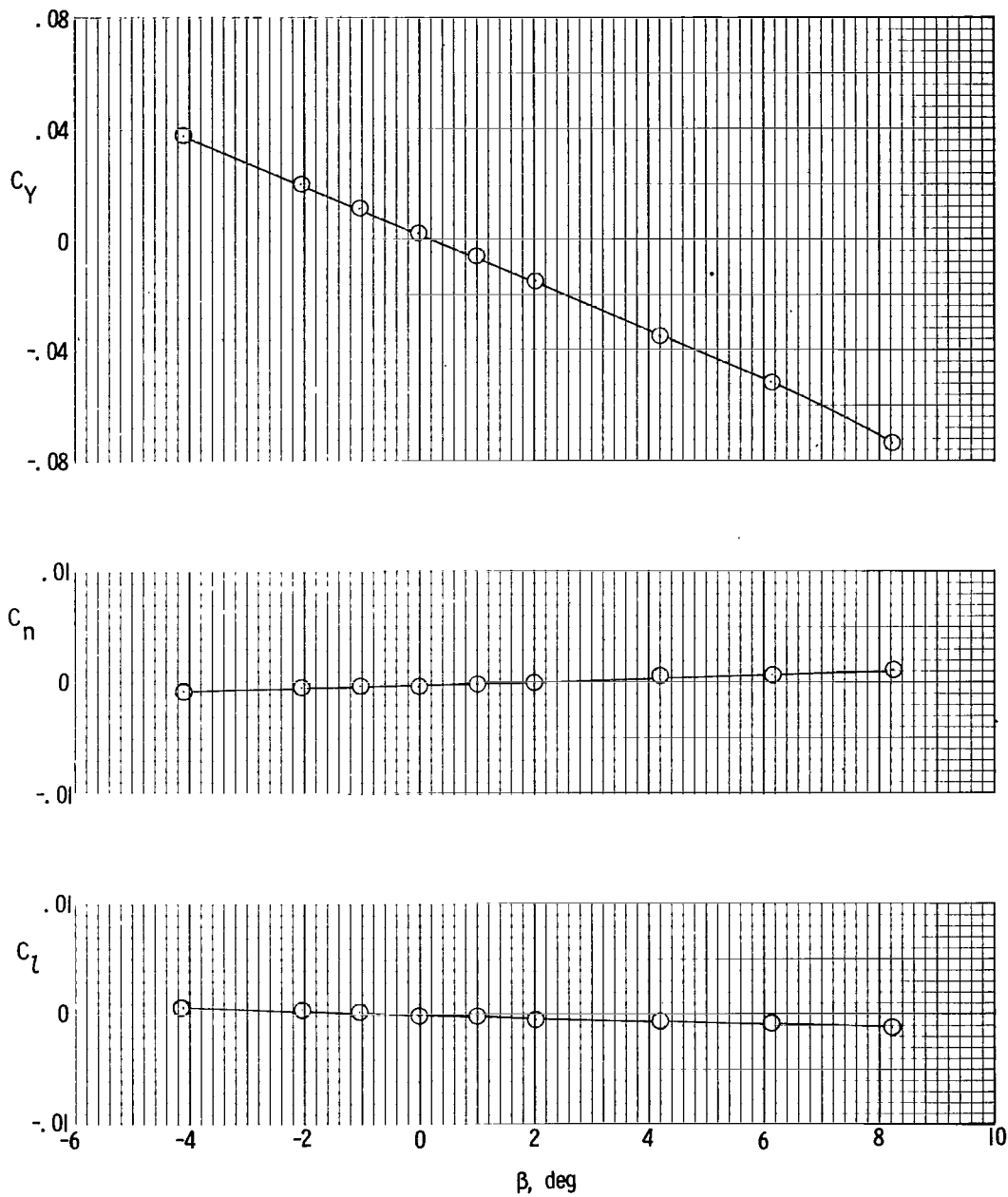
(b) $M = 2.00$.

Figure 11.- Continued.



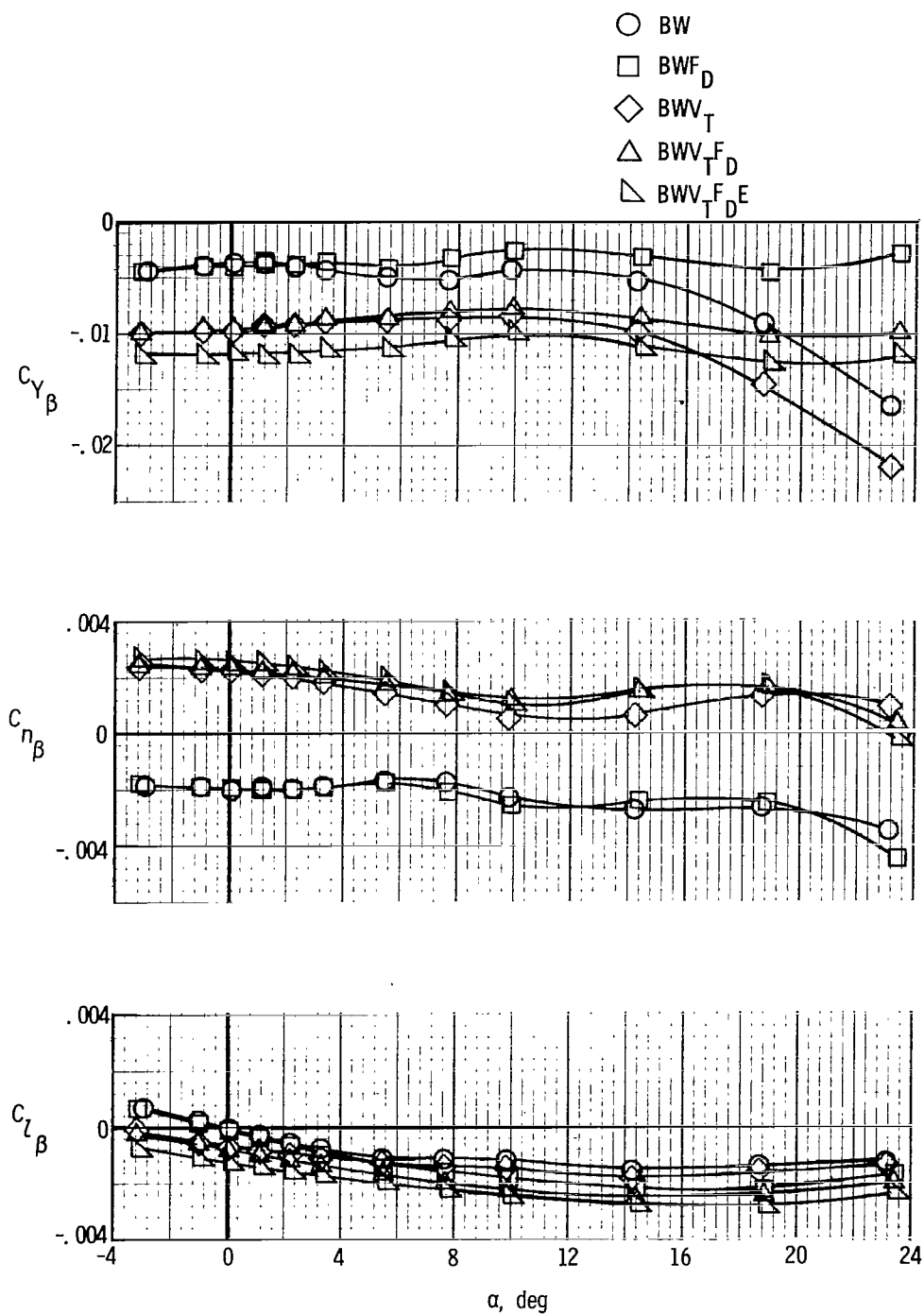
(c) $M = 2.36$.

Figure 11.- Continued.



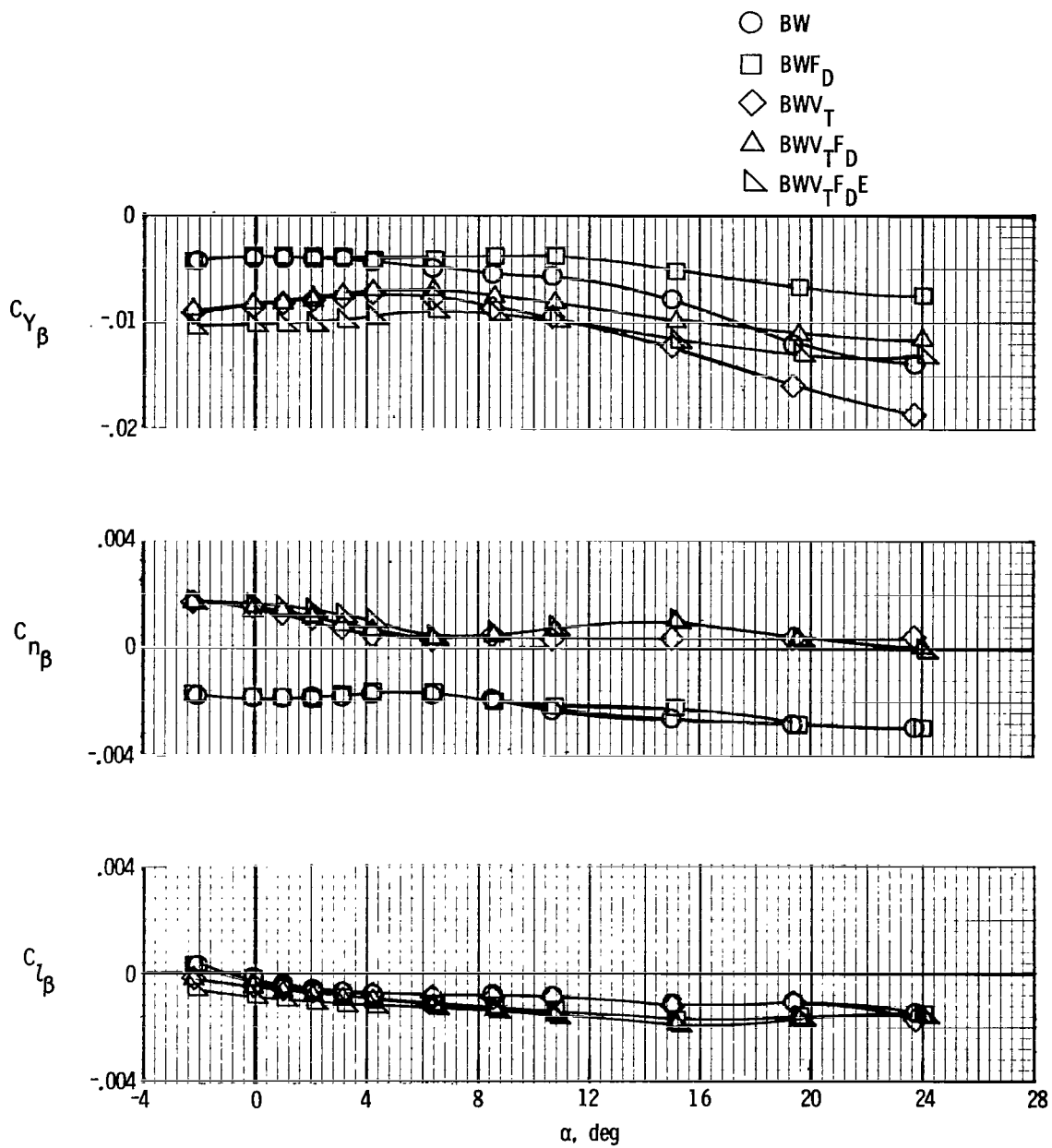
(d) $M = 2.86$.

Figure 11.- Concluded.



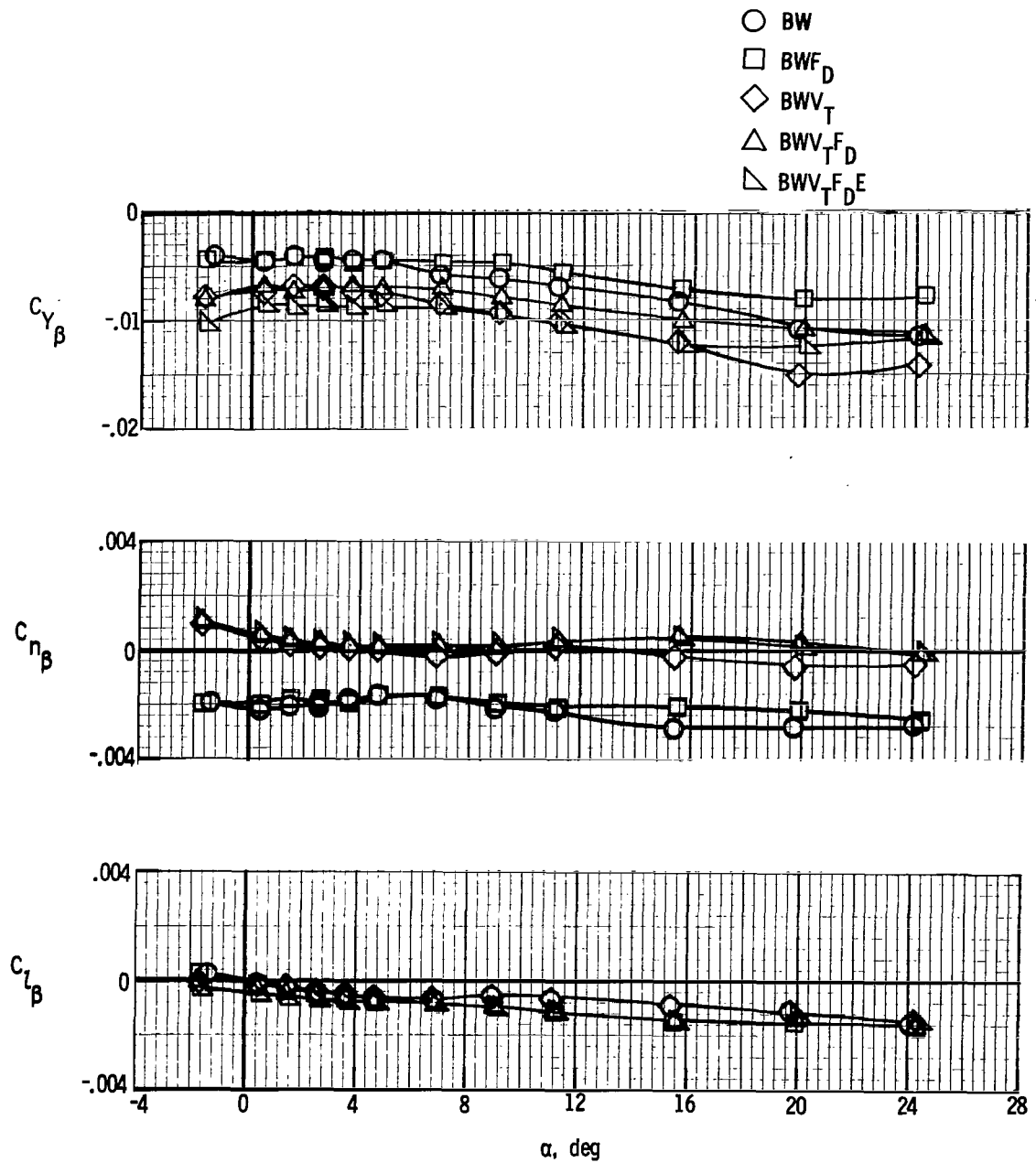
(a) $M = 1.50$.

Figure 12.- Lateral-directional stability characteristics of the body-wing configuration alone and with various forward-delta, tip-fin, and engine components.



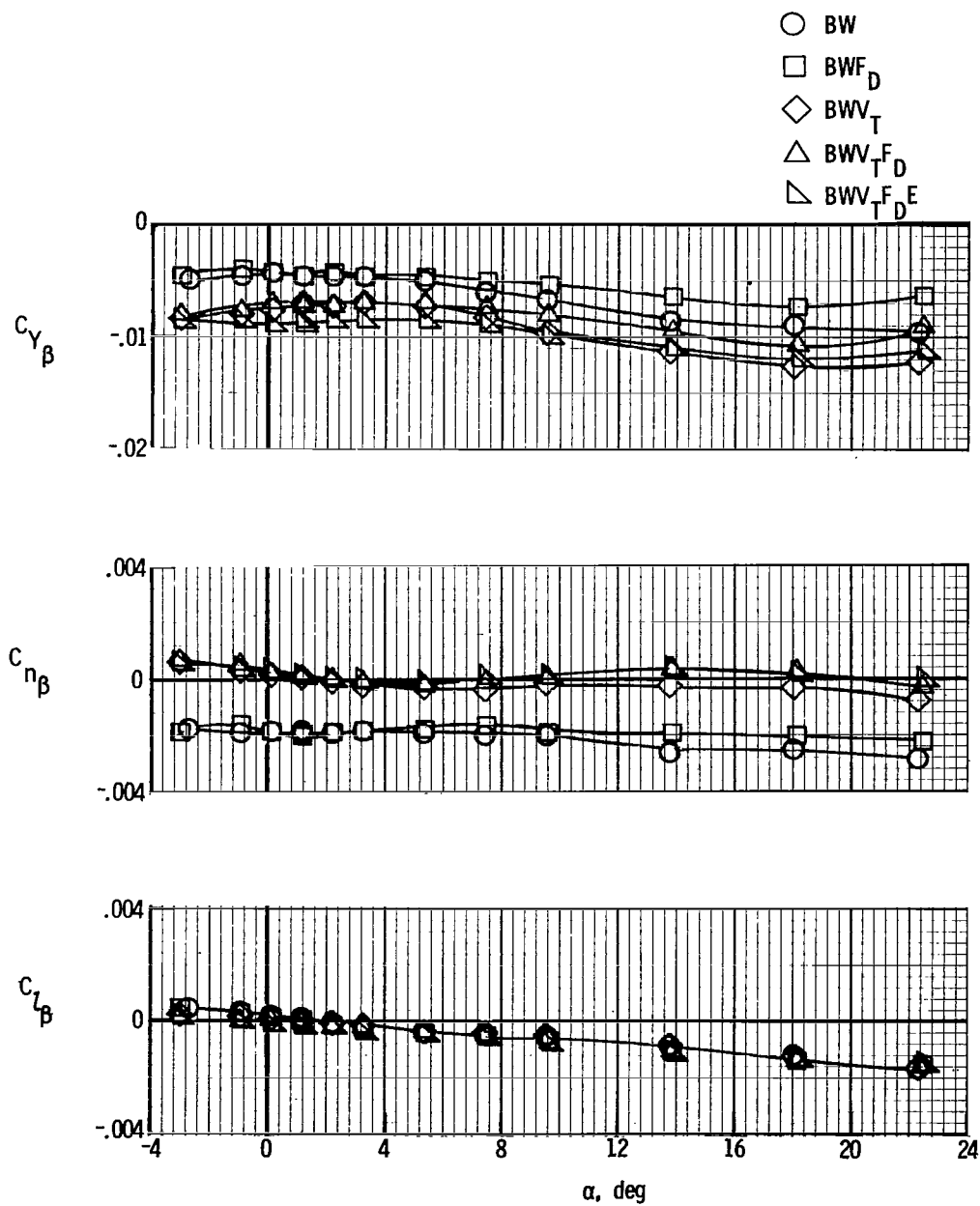
(b) $M = 2.00$.

Figure 12.- Continued.



(c) $M = 2.36$.

Figure 12.- Continued.



(d) $M = 2.86$.

Figure 12.- Concluded.

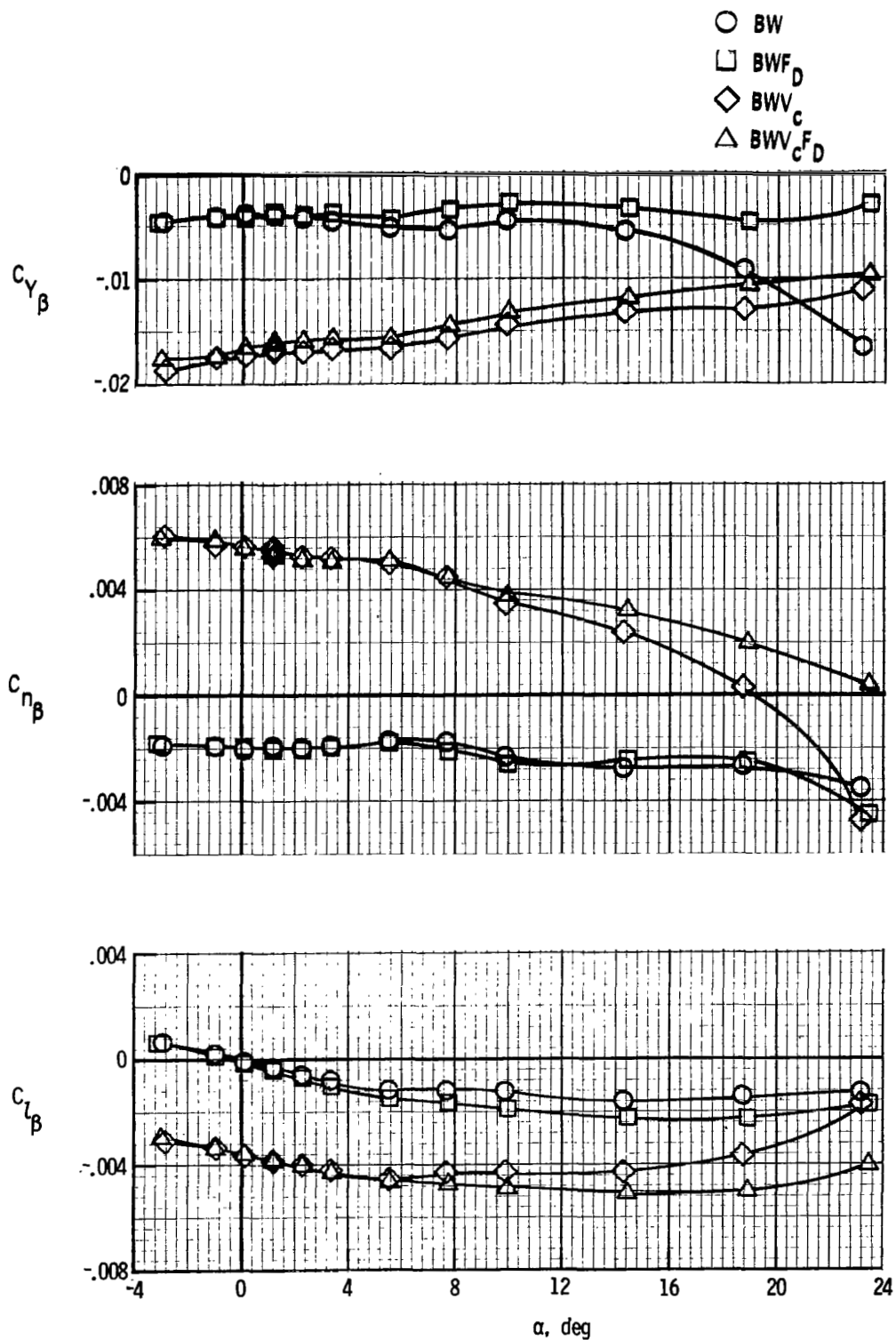
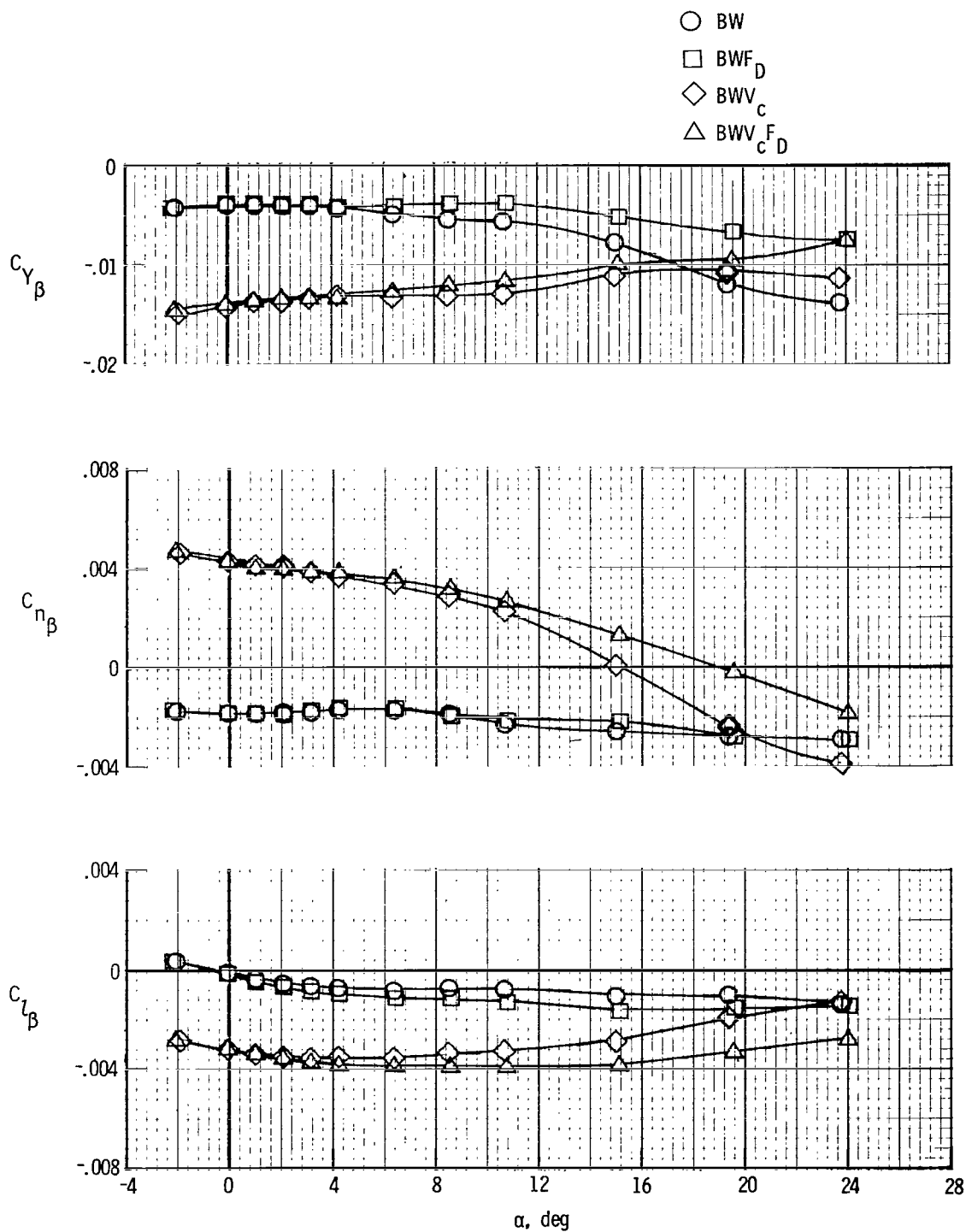
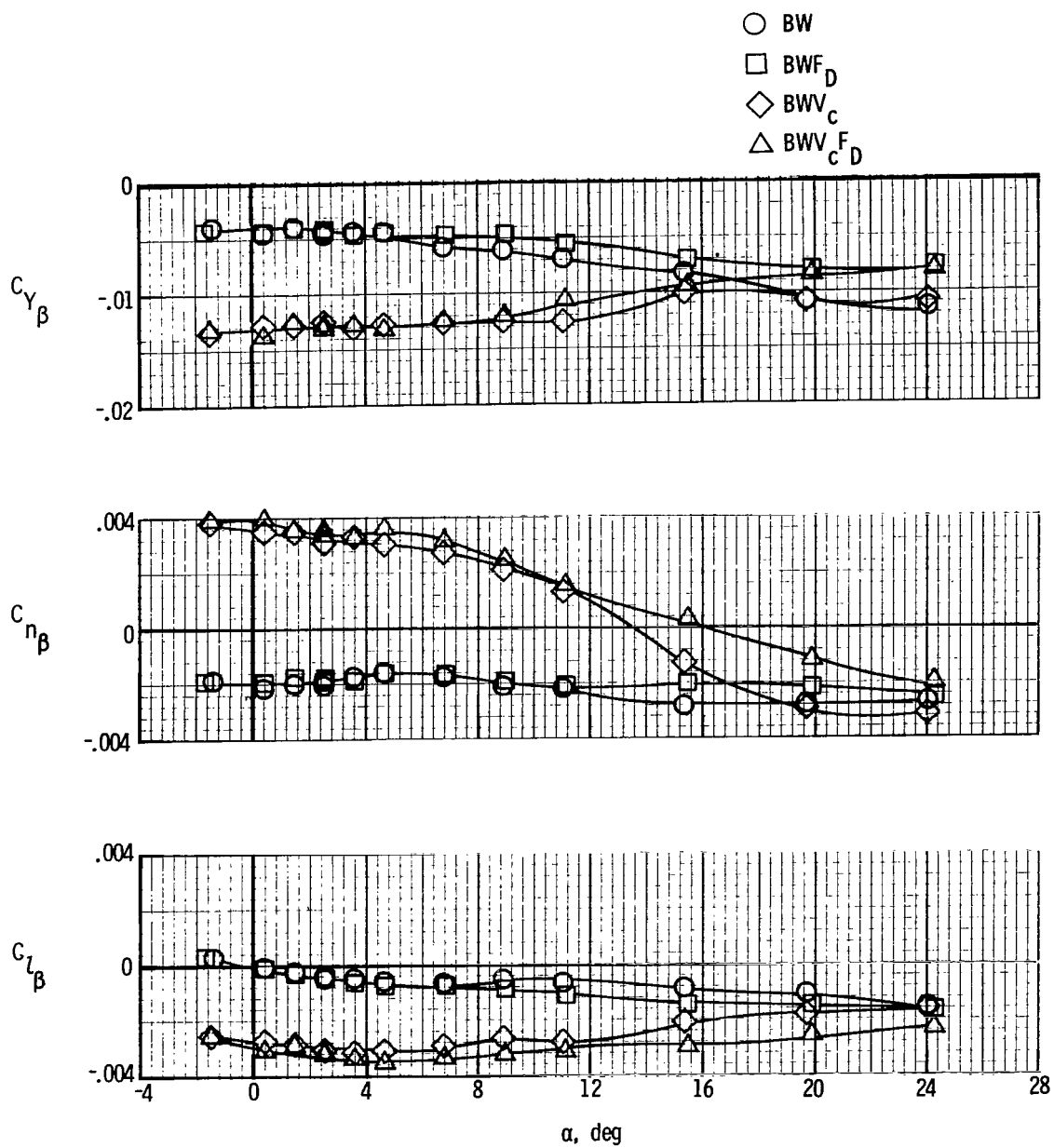


Figure 13.- Lateral-directional stability characteristics of the body-wing configuration alone and with various forward-delta and center-fin components.



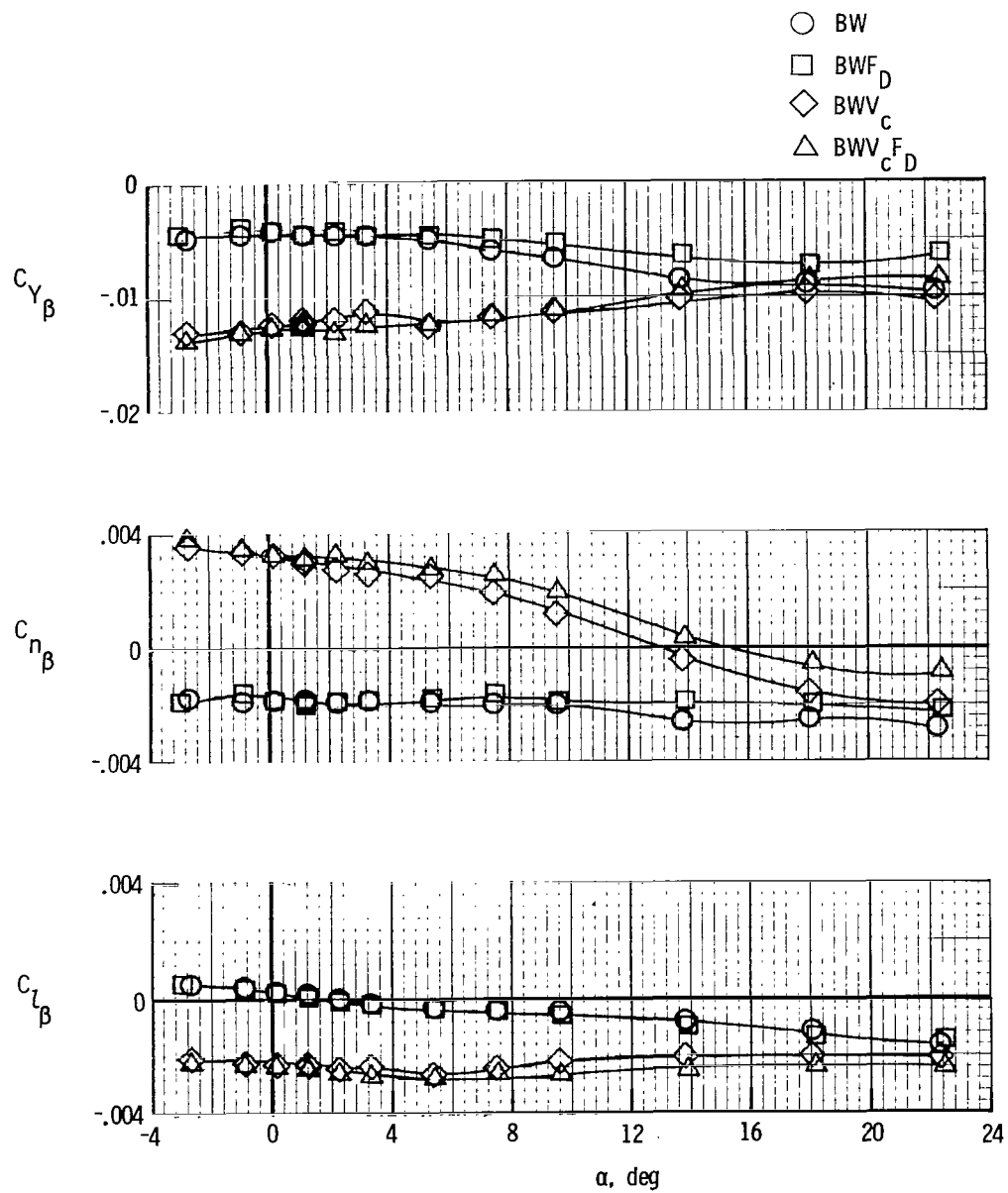
(b) $M = 2.00$.

Figure 13.- Continued.



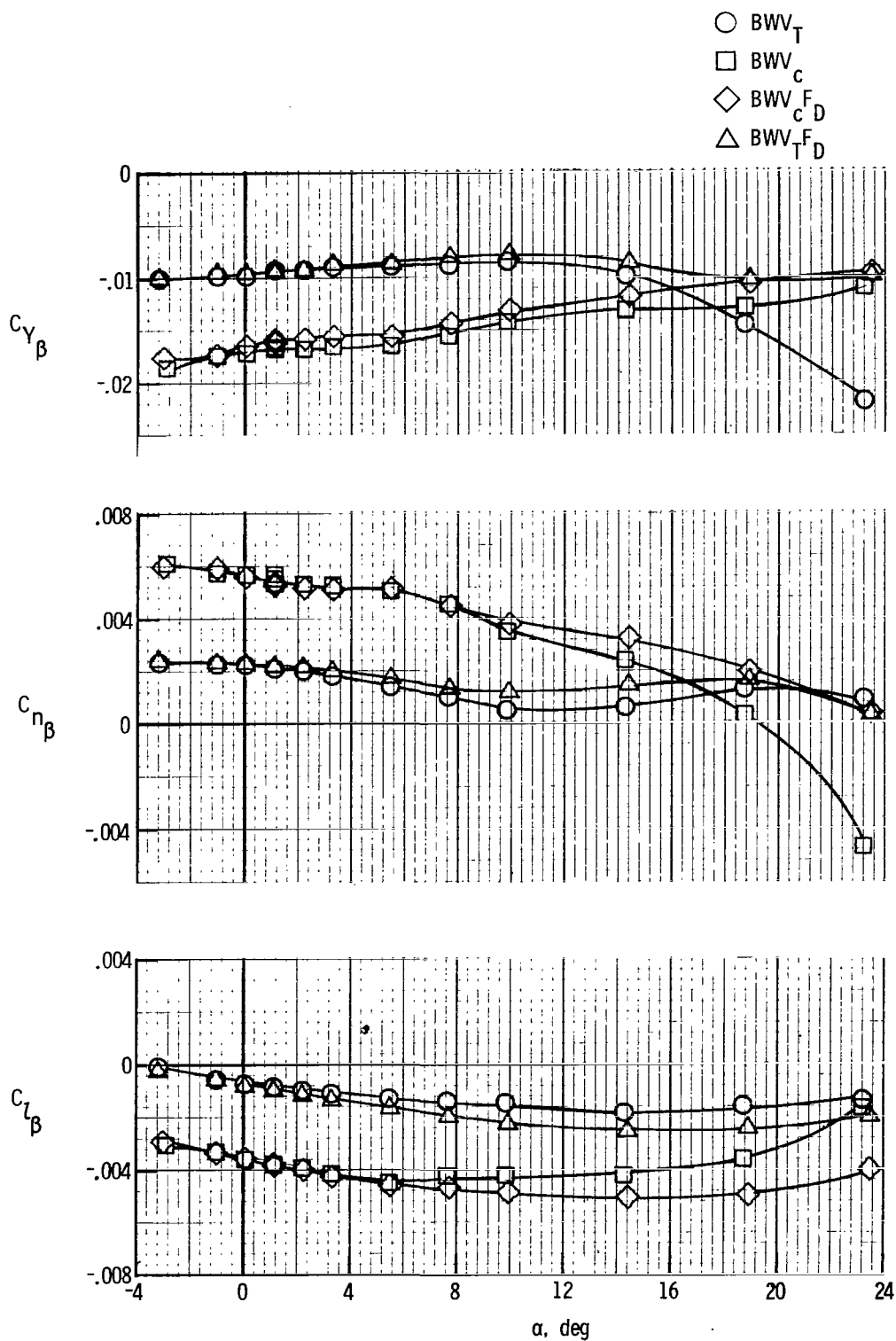
(c) $M = 2.36$.

Figure 13.- Continued.



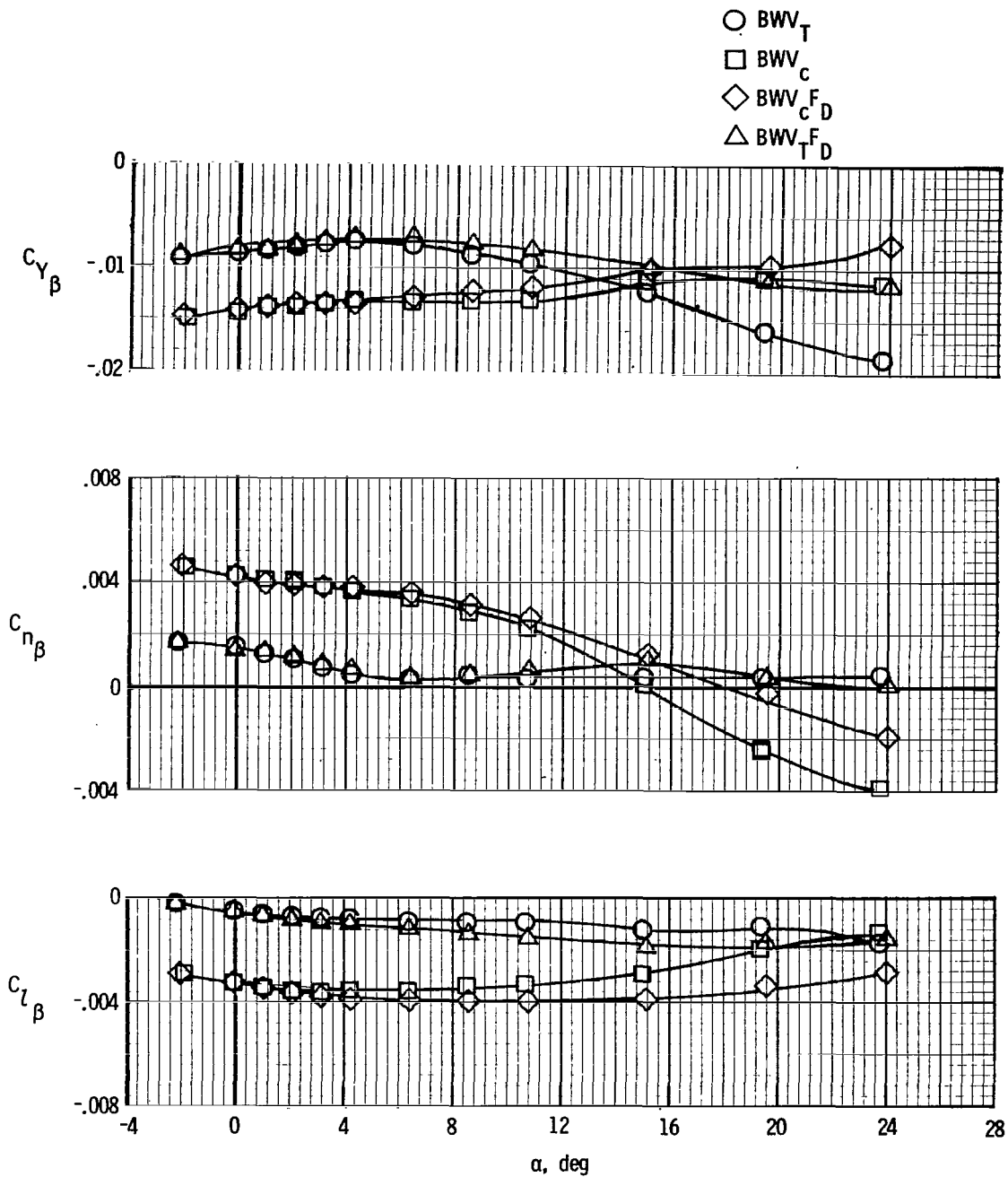
(d) $M = 2.86$.

Figure 13.- Concluded.



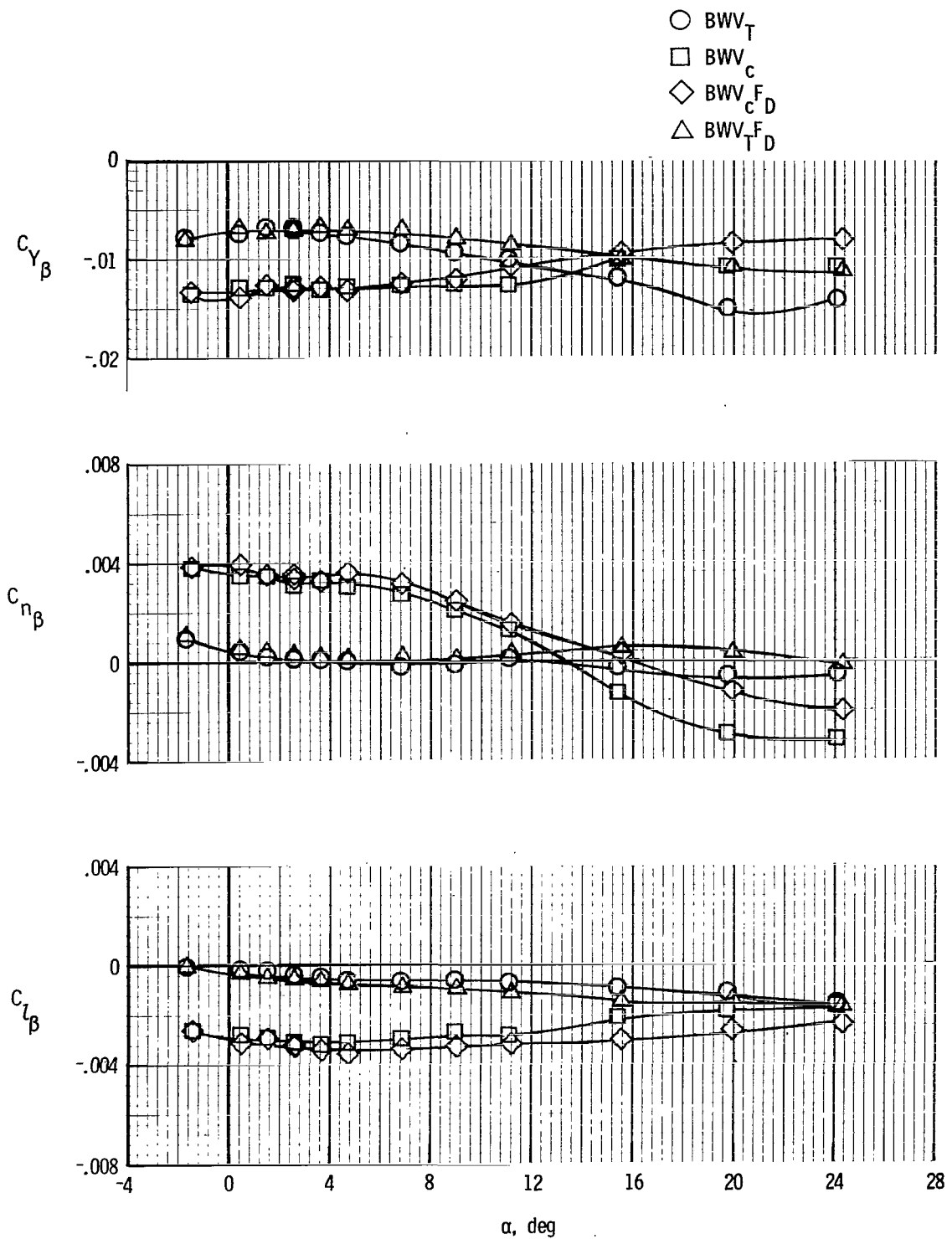
(a) $M = 1.50$.

Figure 14.- Comparison of the lateral-directional stability characteristics of tip-fin and center-fin configurations.



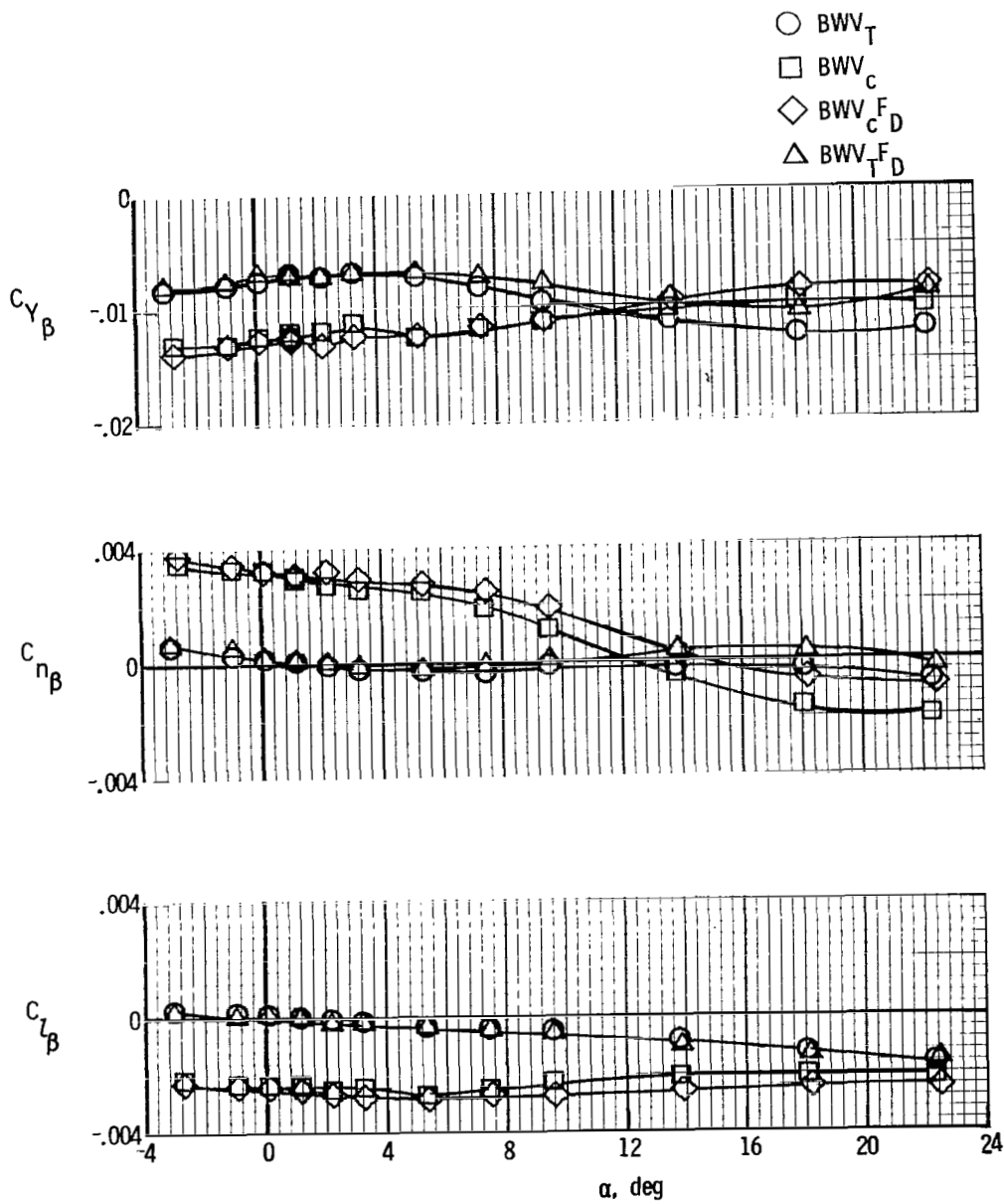
(b) $M = 2.00$.

Figure 14.- Continued.



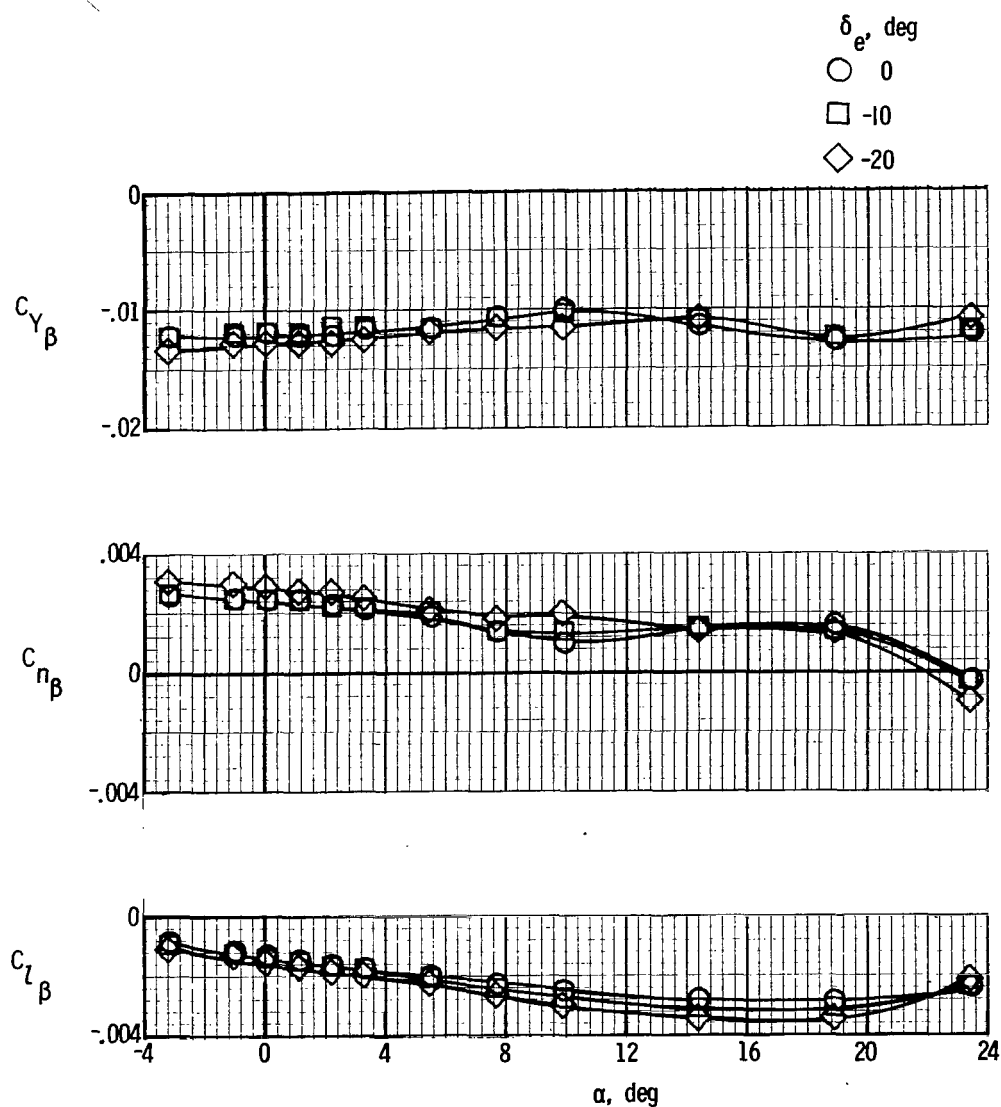
(c) $M = 2.36$.

Figure 14.- Continued.



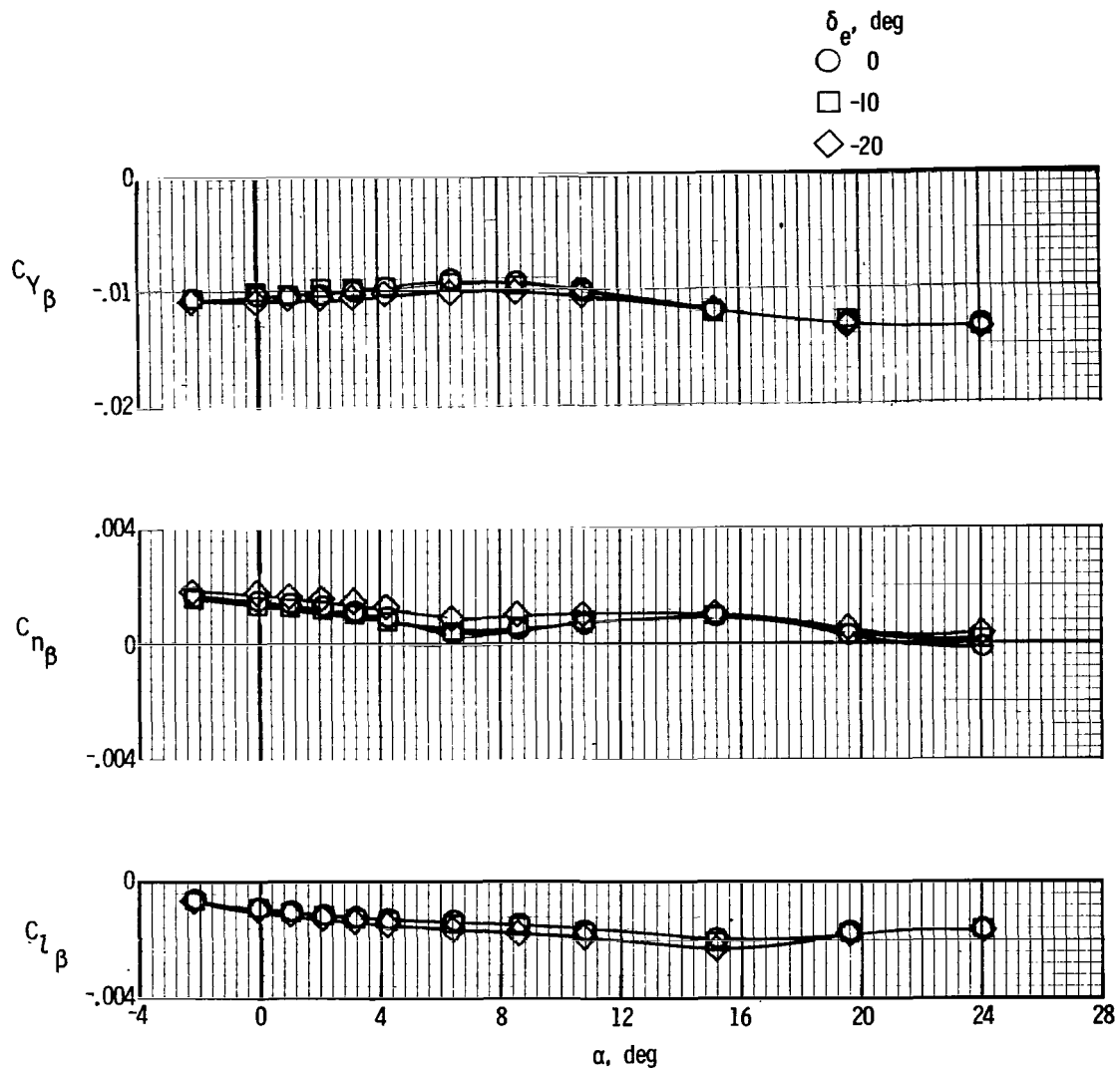
(d) $M = 2.86$.

Figure 14.- Concluded.



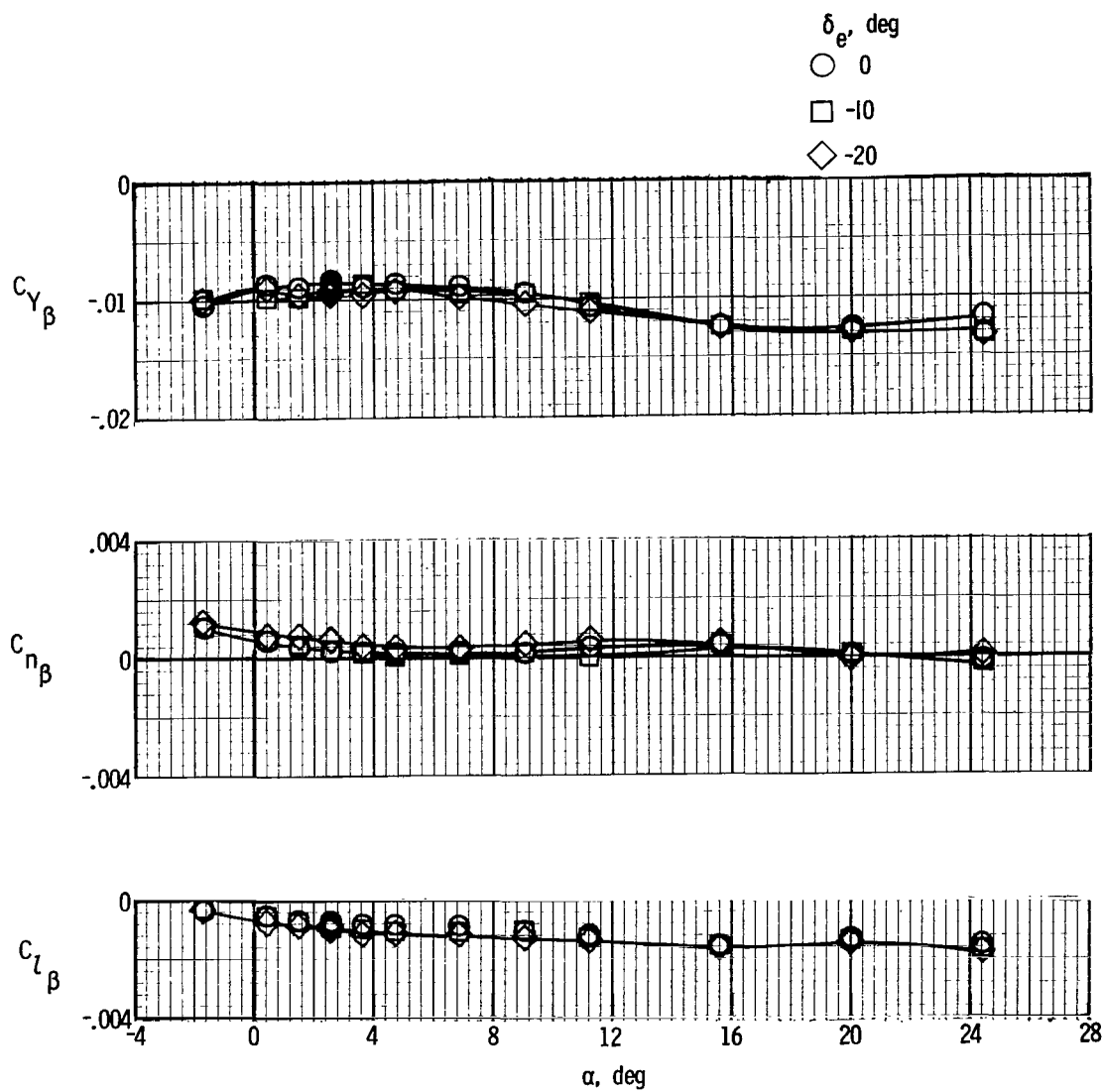
(a) $M = 1.50$.

Figure 15.- Effect of elevon deflection on the lateral-directional stability characteristics of the BWV_T^F_D^E configuration.



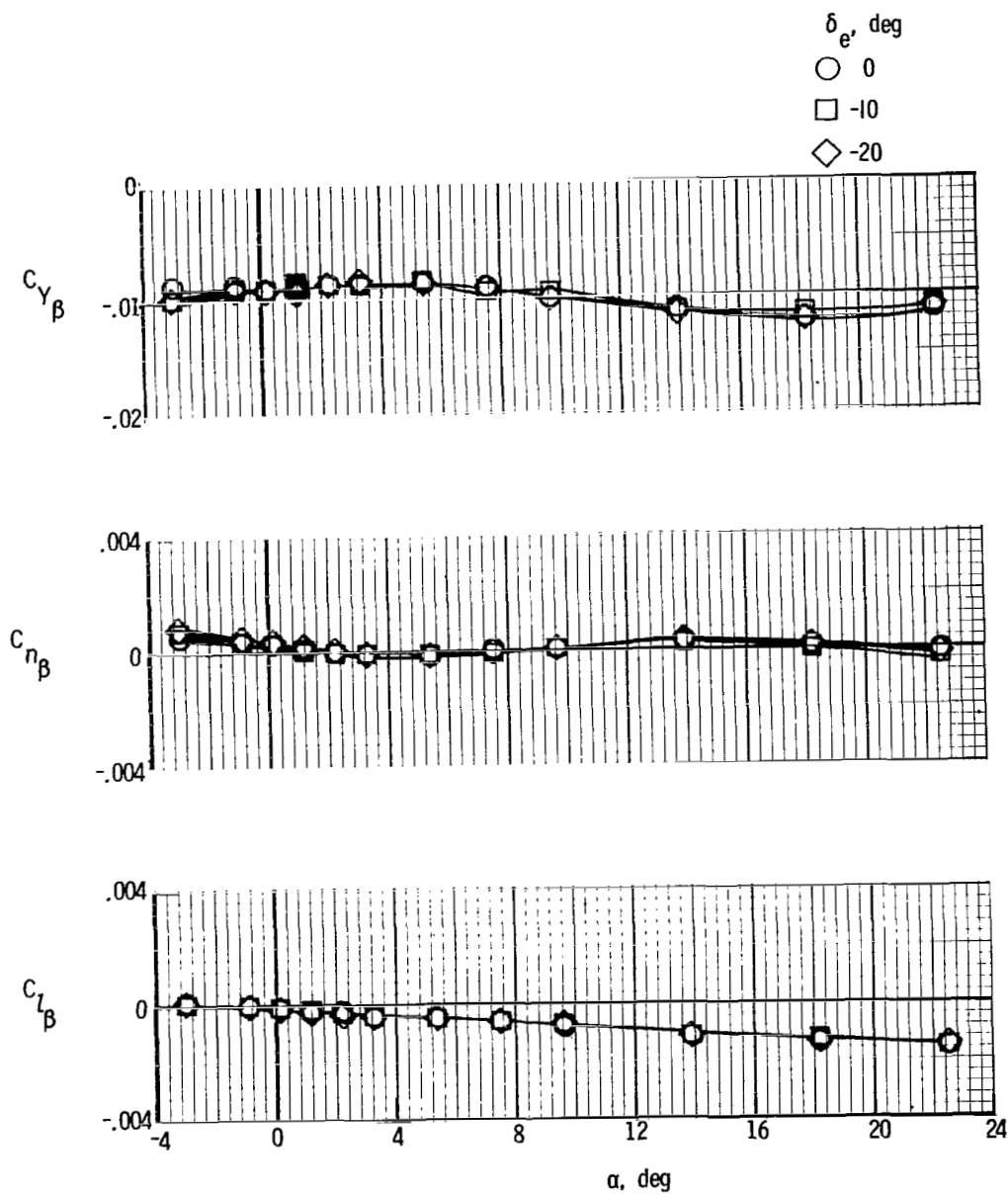
(b) $M = 2.00$.

Figure 15.- Continued.



(c) $M = 2.36$.

Figure 15.- Continued.



(d) $M = 2.86$.

Figure 15.- Concluded.



002 001 01 0 A 751114 500903DS
DEPT OF THE AIR FORCE
AF WEAPONS LABORATORY
ATTN: TECHNICAL LIBRARY (SUL)
KIRTLAND AFB NM 87117

000 000 01 0 A 751114 500903DS

POSTMASTER: If Undeliverable (Section 158
Postal Manual) Do Not Return

"The aeronautical and space activities of the United States shall be conducted so as to contribute . . . to the expansion of human knowledge of phenomena in the atmosphere and space. The Administration shall provide for the widest practicable and appropriate dissemination of information concerning its activities and the results thereof."

—NATIONAL AERONAUTICS AND SPACE ACT OF 1958

NASA SCIENTIFIC AND TECHNICAL PUBLICATIONS

TECHNICAL REPORTS: Scientific and technical information considered important, complete, and a lasting contribution to existing knowledge.

TECHNICAL NOTES: Information less broad in scope but nevertheless of importance as a contribution to existing knowledge.

TECHNICAL MEMORANDUMS: Information receiving limited distribution because of preliminary data, security classification, or other reasons. Also includes conference proceedings with either limited or unlimited distribution.

CONTRACTOR REPORTS: Scientific and technical information generated under a NASA contract or grant and considered an important contribution to existing knowledge.

TECHNICAL TRANSLATIONS: Information published in a foreign language considered to merit NASA distribution in English.

SPECIAL PUBLICATIONS: Information derived from or of value to NASA activities. Publications include final reports of major projects, monographs, data compilations, handbooks, sourcebooks, and special bibliographies.

TECHNOLOGY UTILIZATION PUBLICATIONS: Information on technology used by NASA that may be of particular interest in commercial and other non-aerospace applications. Publications include Tech Briefs, Technology Utilization Reports and Technology Surveys.

Details on the availability of these publications may be obtained from:

SCIENTIFIC AND TECHNICAL INFORMATION OFFICE

NATIONAL AERONAUTICS AND SPACE ADMINISTRATION

Washington, D.C. 20546